

Dissertation zur Erlangung des Doktorgrades
der Fakultät für Chemie und Pharmazie
der Ludwig-Maximilians-Universität München

Separation and Characterization of Subpopulations of Biopharmaceuticals



Robina Mareike Meyer

aus

Hannover, Deutschland

2021

Erklärung

Diese Dissertation wurde im Sinne von §7 der Promotionsordnung vom 28. November 2011 von Prof. Dr. Wolfgang Frieß betreut.

Eidesstattliche Versicherung

Diese Dissertation wurde eigenständig und ohne unerlaubte Hilfe erarbeitet.

München, 20. Oktober 2021

Robina Mareike Meyer

Dissertation eingereicht am: 25. November 2021

1. Gutachterin/Gutachter: Prof. Dr. Wolfgang Frieß

2. Gutachterin/Gutachter: Prof. Dr. Gerhard Winter

Mündliche Prüfung am: 13. Dezember 2021

Acknowledgments

The work for this thesis was conducted between September 2016 and February 2020 at the Department of Chemistry and Pharmacy, Chair of Pharmaceutical Technology and Biopharmacy at the Ludwig-Maximilians University of Munich under the supervision of Prof. Dr. Wolfgang Frieß.

First and foremost, my gratitude goes to Prof. Dr. Wolfgang Frieß for his excellent supervision and scientific guidance, from the initiation of the collaborative project to the submission of the publications.

Likewise, I would like to thank Prof. Dr. Gerhard Winter for taking over the position of the second reviewer, as well as for your inspiring ideas in previous technical discussions. In this context, I would also like to thank Prof. Dr. Olivia Merkel, Dr. Gerhard Simon and Dr. Alexandra Mößlang. A chair does not function without a good soul in the secretariat: many thanks to Sabine Kohler for her warm and always helpful manner.

I am very grateful for the lively technical discussions and fruitful advice from my collaborative partners at Sandoz Biopharmaceuticals. In particular, thanks go to Dr. Lukas Berger, Dr. Stefan Scheler and Dr. Jörg Nerkamp for their commitment. I would also like to thank Anna Sawadzka-Nowicka for her support.

I would also like to thank Amid Gupta and NanoTemper Technologies for the opportunity to perform experiments using the methods and materials provided and for scientific advice.

The best and most profitable experiences during your time as a PhD are gained together with your colleagues. Likewise, failures and low phases are overcome more quickly together. For this I would like to thank my companions in the working groups Frieß, Winter and Merkel. The coffee breaks in the sun, legendary parties and the exchange of experiences have made the PhD life unforgettable.

I would like to make special mention of my lab-mate Ivonne Stelzl. Thanks for the mean laughter, anger management and deciphering hieroglyphics.

Many thanks to the members of all AKs, which I was allowed to get to know in the three and a half years, for the great time and the interesting discussions. Special thanks go to Inas El-Bialy, Martin Domnowski, Natalie Deiringer, Christoph Marschall, Lorenzo Gentiluomo, Aditi Mehta, Tobias Keil, Ute Rockinger, Hristo Svilenov, Andreas Stelzl, Dennis Krieg, Andreas Tosstorff, Julian Gitter, Christian Haase and Imke Leitner.

Thanks also go to my students, whom I had the opportunity to supervise in various internships and practical courses.

I feel infinite gratitude to my parents for their everlasting support, encouragement and love. This thesis is also your credit.

Thank you so much for the tools, the discussions, your empathy and the reassuring hugs you offered me while writing this dissertation, Simon.

Finally, I sincerely thank my friends for their patience and encouragement whenever it was needed. I appreciated this very much.

Contents

Acknowledgements	v
List of Figures	x
List of Tables	xv
1 General Introduction	1
1.1 Subpopulations in Protein Therapeutics	1
1.1.1 Factors Influencing Protein Variant Formation	2
1.2 Heterogeneity in Biopharmaceuticals	2
1.2.1 Charge Variants	3
1.2.2 Hydrophobicity Variants	3
1.2.3 Chemical Changes	3
1.3 Impact of Protein Variants on Product Stability	6
1.4 Aim and Outline of the Thesis	9
Bibliography	11
2 Identification of Monoclonal Antibody Variants Involved in Aggregate Formation – Part 1: Charge Variants	19
2.1 Abstract	20
2.2 Introduction	21
2.3 Materials and Methods	24
2.3.1 mAb Model Protein	24
2.3.2 Separation of Charge Variants	24
2.3.3 Analytical Ion Exchange Chromatography (IEX)	25

2.3.4	Size Exclusion Chromatography (SEC)	25
2.3.5	Dynamic Light Scattering (DLS)	25
2.3.6	Static Light Scattering (SLS)	26
2.3.7	Nano Differential Scanning Fluorimetry (nDSF)	26
2.3.8	Protein Modeling	27
2.3.9	Accelerated Stability Study and Spiking Procedures	27
2.3.10	Visual Inspection	28
2.3.11	Ultraviolet Absorption Spectroscopy at 320nm	28
2.3.12	Fluorescence spectroscopy	28
2.3.13	Subvisible Particle Counting	28
2.3.14	Multi-Angle Light Scattering Coupled Size Exclusion Chromatography (SEC-MALS)	29
2.4	Results and Discussion	30
2.4.1	mAb Charge Variant Separation and Fractionation	30
2.4.2	Aggregation and Degradation Products	32
2.4.3	Conformational Stability and Self-Interaction of mAb Charge Variants	33
2.4.4	Modeling of Charge Variants	36
2.4.5	Forced stability study	38
2.5	Conclusion and Outlook	42
	Bibliography	44
3	Identification of Monoclonal Antibody Variants Involved in Aggregate Formation – Part 2: Hydrophobicity Variants	49
3.1	Abstract	50
3.2	Introduction	51
3.3	Materials and Methods	53
3.3.1	mAb Model Protein	53
3.3.2	Separation of Hydrophobicity Variants	53
3.3.3	Analytical Hydrophobic Interaction Chromatography (HIC)	54
3.3.4	Size Exclusion Chromatography (SEC)	54
3.3.5	Ion Exchange Chromatography (IEX)	55

3.3.6	Dynamic Light Scattering (DLS)	55
3.3.7	Differential Scanning Fluorimetry (nanoDSF)	56
3.3.8	Accelerated Stability Study and Spiking Procedures	57
3.3.9	Visual Inspection	57
3.3.10	Ultraviolet Absorption Spectroscopy at 320nm	57
3.3.11	Fluorescence spectroscopy	58
3.3.12	Subvisible Particle Counting	58
3.3.13	Multi-Angle Light Scattering Coupled Size Exclusion Chromatography (SEC-MALS)	58
3.4	Results and Discussion	60
3.4.1	HIC Method Development	60
3.4.2	mAb Hydrophobicity Variant Separation and Fraction- ation	61
3.4.3	Aggregate and Degradation Product Content of the Fractions	62
3.4.4	Conformational Stability and Self-Interaction Propen- sity of mAb Hydrophobicity Variants	64
3.4.5	Correlation with Charge Variants	67
3.4.6	Accelerated Stability Study	68
3.5	Conclusion and Outlook	73
	Bibliography	74
4	Characterization and Risk Assessment of Charge Variants of Recombinant Human Growth Hormone	79
4.1	Abstract	80
4.2	Introduction	81
4.3	Materials and Methods	83
4.3.1	Materials	83
4.3.2	Strong Cation Exchange Chromatography (SCX)	83
4.3.3	Separation of Charge Variants	83
4.3.4	Size Exclusion Chromatography (SEC)	84
4.3.5	Dynamic Light Scattering (DLS)	84
4.3.6	Static Light Scattering (SLS)	85

4.3.7	Accelerated Stability Study and Spiking Procedures . . .	85
4.3.8	Visual Inspection	86
4.3.9	Ultraviolet Absorption Spectroscopy at 320nm	86
4.3.10	Sub-visible Particle Counting	86
4.4	Results and Discussion	88
4.4.1	rhGH Charge Variant Separation and Fractionation . . .	88
4.4.2	Aggregate and Degradation Product Content of the Fractions	89
4.4.3	Thermal Stability and Self-Interaction of rhGH and the AP2 Charge Variant	91
4.4.4	Stability Study with AP2 Charge Variant	93
4.5	Conclusion and Outlook	96
	Bibliography	97
	Supplementary Data	102
5	I've got you covered: A first step towards a mini-chaperonin for protein variant characterization	105
5.1	Abstract	105
5.2	Introduction	106
5.3	Materials and Methods	108
5.3.1	Materials	108
5.3.2	Plasmid construction	108
5.3.3	Protein expression and purification	108
5.3.4	MicroScale Thermophoresis (MST)	109
5.3.5	Biolayer Interferometry (BLI)	110
5.4	Results and Discussion	111
5.4.1	Mini-chaperonin purification, quantification and iden- tification	111
5.4.2	Functionality of the mini-chaperonin	112
5.5	Conclusion and Outlook	116
	Bibliography	117
6	Final Summary	121

List of Figures

1.1	Overview of factors that induce chemical changes, of the types of changes and the amino acid residues at which these changes occur. The resulting protein heterogeneity can be detected regarding charge and hydrophobicity. Protein heterogeneity in size is not reflected in this overview.	5
2.1	Semi-preparative IEX chromatograms of mAb charge variant separation for a) mAb DS and b) mAb stressed at 40 °C for 16 days.	30
2.2	HMW and LMW content of mAb charge variants for a) mAb DS and b) mAb stored at 40 °C for 16 days.	33
2.3	T _{agg} onset temperatures of charge variants a): of mAb DS by DLS. b): of mAb DS by SLS. c): of mAb stored at 40 °C for 16 days by DLS. d): k _D of SAP11 in comparison to controls by DLS.	34
2.4	T _m onset and scattering onset of charge variants according to DSF from a) mAb DS, b) mAb stored at 40 °C for 16 days and c) time till onset of aggregation in forced degradation study at 67 °C with mAb DS.	36
2.5	Hydrophobic patches (red) and additive aggregation score of naïve mAb (open source sequence) and two charge variants' Fab parts modeled with BioLuminate according to data of the manufacturer.	37
2.6	Visual appearance of mAb variants and spiked DS stressed at 45 °C for 12 weeks.	38

2.7	a) Turbidity at 320 nm compared to a nephelometric standard of mAb variants and spiked DS. b) Unfolding measured by fluorescence of charge variants stored at 45 °C for 12 weeks.	39
2.8	SEC-MALS data of mAb charge variants and spiked DS stored at 45 °C for 12 weeks of a) monomer yield compared to T0 b) amount of HMWS per time point.	40
2.9	Number of particles in mAb variants and spiked DS samples stressed at 45 °C for 12 weeks a) accumulated numbers, b) particles $\geq 1 \mu\text{m}$, c) $\geq 2 \mu\text{m}$, d) $\geq 10 \mu\text{m}$, e) $\geq 25 \mu\text{m}$	41
3.1	Chromatograms of semi-preparative HIC method development. Comparison of the elution enhancers glycerol, arginine, propylene glycol, polyethylene glycol and acetonitrile.	60
3.2	Semi-preparative HIC chromatogram of mAb hydrophobicity variant separation with 6 % of PG in mobile phases for equilibration and elution.	62
3.3	SEC results of separated mAb hydrophobicity variants.	64
3.4	Thermal stability data including SD of mAb hydrophobicity variants with a) T_{agg} onset by DLS, b) T_{m} onset by DSF and c) T_{agg} onset temperature by DSF.	65
3.5	nanoDSF measurements of hydrophobicity variants a) in forced degradation study at 67 °C and b) in stability study in capillaries at 45 °C.	66
3.6	Apparent k_{D} values and SD of mAb hydrophobicity variants at 25 °C.	66
3.7	a) General charge variants content in hydrophobicity variants determined by IEX, b) Specific charge variants of our previous study found in H+3 by IEX. AP = acidic peak; BP = basic peak., c) Charge variant of our previous study with high H+3 content analyzed in HIC.	67
3.8	Visual appearance of mAb DS spiked with hydrophobicity variants stored at 45 °C for 12 weeks.	68

3.9	a) Turbidity at 320 nm. b) Fluorescence at 350/330 nm of mAb DS spiked with hydrophobicity variants.	69
3.10	SEC data of mAb DS spiked with hydrophobicity variants and stressed at 45 °C for 12 weeks of a) monomer yield compared to T0 b) amount of aggregates per time point.	69
3.11	Sub-visible particles found in mAb DS spiked with hydrophobicity variants and stored at 45 °C for 12 weeks a) particles $\geq 1 \mu\text{m}$, b) $\geq 2 \mu\text{m}$, c) $\geq 10 \mu\text{m}$, d) $\geq 25 \mu\text{m}$	70
3.12	Analytical HIC chromatograms of a) mAb DS and b) DS spiked with H+3 stored at 45 °C for 12 weeks.	71
4.1	Semi-preparative AEX chromatogram of rhGH charge variant separation after storage for 5 days at 40 °C with collected fractions marked.	89
4.2	HMW and LMW content of rhGH charge variants in DS stored at 40 °C for 5 days. Error bars indicate SD.	90
4.3	T_{agg} onset temperatures of rhGH stored at 40 °C for 5 days a) by SLS. b) by DLS. Error bars indicate SD.	92
4.4	k_D of charge variants from rhGH stored at 40 °C for 5 days by DLS. Error bars indicate SD.	93
4.5	Turbidity a) in pH 7.0 and b) in pH 5.5 formulations after storage of rhGH protein variants at 40 °C for 6 weeks. The data was normalized to rhGH DS values. Error bars = SD. . .	94
4.6	Particles observed in charge variants from rhGH stored at 40 °C for 6 weeks: a) accumulated numbers at pH 7.0, b) accumulated numbers at pH 5.5. Error bars show SEM.	95
4.7	SEC of a) pH 7.0 and b) pH 5.5 formulations after storage of rhGH protein variants at 40 °C for 6 weeks. The data was normalized to rhGH DS values (= 1). Error bars = SD	103
4.8	Particles observed in charge variants from rhGH stored at 40 °C for 6 weeks: a) particles $\geq 10 \mu\text{m}$ at pH 7.0, b) $\geq 10 \mu\text{m}$ at pH 5.5, c) $\geq 25 \mu\text{m}$ at pH 7.0 and d) $\geq 25 \mu\text{m}$ at pH 5.5. Error bars show SEM.	104

5.1	Monitoring of GroEL-AD purification by SDS PAGE stained with Coomassie blue. Left induced with 1 μ M IPTG, right with 1 mM IPTG.	111
5.2	Gro-EL-AD identified by an anti-His antibody detected by chemiluminescence in western blotting.	112
5.3	MST response of GroEL-AD labeled with NHS with ligands a) rhodanese denatured by temperature or chemical stress b) mAb chemically denatured and c) rhGH and mAb mechanically stressed.	113
5.4	Western Blot with native PAGE of GroEL-AD displayed as a) chemiluminescence and b) inverted.	114

List of Tables

2.1	Area and purity of collected mAb charge variants. n.d. = not determined.	31
3.1	Area and purity of collected mAb hydrophobicity variants. n.d. = not determined.	63
4.1	Relative peak areas in analytical SCX and semi-preparative AEX of rhGH charge variant separation in DS and after storage for 5 days at 40 °C and purity of the collected fractions as determined by analytical SCX. n.d. = not detected.	88
4.2	Visual appearance of rhGH charge variants stored at 40 °C for 6 weeks at pH 7.0 or pH 5.5. clear = no particles or turbidity observed.	102

Chapter 1

General Introduction

1.1 Subpopulations in Protein Therapeutics

Since the first approval of a recombinant protein by the FDA in 1982 the importance of biopharmaceuticals has grown rapidly and enabled the treatment of various indications. In May 2021 the FDA approved the 100th monoclonal antibody product [1]. The market of human biopharmaceuticals is accounted for about a third of pharmaceutical sales, naming over three hundred billion USD. This high proportion is partially based on the high prices of protein therapeutics, which mainly result from high development costs [2]. Due to their highly complex structure and heterogeneity compared to common low molecular weight drugs, the development of protein therapeutics requires a profound analysis of the protein characteristics in order to predict behavior, stability, safety and, consequently, to gain regulatory approval [3].

A major part of the complexity of protein products is due to the fact that they consist not only of the intact protein itself, but also of a variety of slightly altered protein, the subpopulations. The analysis of functionality, stability and aggregation propensity of the subpopulations is vital for product safety and corresponding data are expected from regulatory agencies. This applies equally to originator and biosimilar products [4, 3].

1.1.1 Factors Influencing Protein Variant Formation

Protein subpopulations can derive from several, mostly inevitable conditions affecting the protein:

Post-translational modifications or chemical instabilities that result in the formation or destruction of covalent bonds. They can occur by intra- or extracellular processes during upstream processing, protein recovery and downstream processing [5, 6, 7, 8, 9].

Formulation and surface interactions: The pH of the solution, the type and concentration of salts, excipients and preservatives influence the stability of the protein during manufacturing and storage. Unspecific electrostatic effects or specific charge interactions influence the conformational and colloidal stability [10, 11, 12]. Furthermore, the protein concentration itself has an impact on intra- and inter-molecular interactions. Also interactions with the primary packaging have been reported to induce formation of subpopulations. This involves reactions at the interface to air or the packaging material or its coatings [13].

Physical influences like temperature, agitation, light and pressure have a negative impact on proteins. These stress factors influence protein variants formations at each manufacturing step, during transport, storage and handling by medical professionals and even during application [14, 15].

These influences on the protein are constantly monitored during the development by detailed product characterization. Improvements of the manufacturing processes and on the protein structure are introduced to minimize the presence of protein variants. Also stabilizing excipients are used to avoid the formation and further degradation of protein variants. However, the (re)occurrence of heterogeneity in protein therapeutics is inescapable due to the manifold influences that can easily induce changes in the protein [16, 17].

1.2 Heterogeneity in Biopharmaceuticals

Proteins are build of a library of twenty amino acids that define the chemical function and physicochemical properties of each individual protein. De-

pended on these properties and the type of external influence, the amino acid side chains of a protein can change chemically. These changes result in protein heterogeneity that can be detected as differences in size, charge, hydrophobicity and structure. This thesis focuses on charge and hydrophobicity variants and provides an (non-exhaustive) overview of the underlying chemical changes leading to these protein subpopulations.

1.2.1 Charge Variants

Protein alteration in charge characteristics leads to charge variants which can be distinguished into acidic and basic variants. Compared to the main species, the variants carry more or less surface charge, respectively. The surface charge can be altered directly by a change in the charged residues, e.g. affected by pH or other formulation impacts, or indirectly by chemical changes [18]. These attributes are utilized for variant detection and separation by ion exchange chromatography (IEX), isoelectric focusing (IEF), chromatofocusing or gel electrophoresis [19, 20]. The chemical modifications on which the variant is based can be detected using mass spectrometry (MS) and peptide mapping [21, 22].

1.2.2 Hydrophobicity Variants

Alterations in hydrophobicity arise from amino acids or entire patches with deviating polarity on the protein surface. Thus, there is also a correlation between hydrophobicity and surface charge. Hydrophobicity variants can be separated and detected by hydrophobic interaction chromatography (HIC) or reversed phase chromatography (RPLC) [23]. Coupling of the chromatographic approaches to MS enables further characterization of the variants [22].

1.2.3 Chemical Changes

Deamidation is a very common chemical change, especially observed in recombinant antibodies, that occurs especially at asparagine (Asn) and glycine

(Gly) residues, and in certain proteins in glutamine (Gln) residues. Deamidated variants show a more acidic character. If the neighboring amino acid to Asn is a hydrogen-bond donating residue and the shorter the side chain after the Asn, the more prone for deamidation is the protein at this chain [24, 25]. After deamidation of an Asn residue, the protein may form a succinimide intermediate that subsequently forms an slightly more acidic isoaspartate by hydrolysis. In this process called isomerization, the protein can also undergo structural changes. Alternatively, aspartate is formed. Succinimide is a basic variant and is more hydrophobic than isoaspartate [26, 27, 28]. **Isomerization** can also be observed at trans or cis proline residues.

Oxidation can result in both, acidic or basic variants. After oxidation of a methionine (Met) residue, the size of the molecular weight of the protein is decreases and the side chain of Met becomes more hydrophilic [29]. Oxidized Met residues have also been reported to elute as more basic variants in IEX [30]. The oxidation of tryptophan (Trp) residues also leads to slightly more hydrophilic variants [31].

In presence of a reducing sugar lysine (Lys) loses hydrogen atoms from amino groups while the sugar molecule is attached covalently to the protein. This process is called **glycation**. The positive charge of the amino group is covered by glycation, turning the protein more acidic [32]. Sugars can also bind to the protein via enzymatic reaction in terms of a post-translational modification, the **glycosylation** [33].

A C-terminal lysine can be removed partially and completely in presence of a basic carboxypeptidase. This process is often observed in mAbs. This **C-terminal lysine processing** results in decreased positive charge and size, with varying extend, depending on the number of removed C-terminal lysines. Variants with different numbers of removed lysine can be distinguished in common analytical methods [34]. In case glycine is followed by proline on the C-terminal side, a removal of glycine with subsequent amidation of proline was shown to proceed in mAbs [35]. The obtained variant has a more basic character.

Enzymatic or chemical **cleavage** of peptide bonds is another reason for size and charge heterogeneity, especially in the hinge region of antibodies [14].

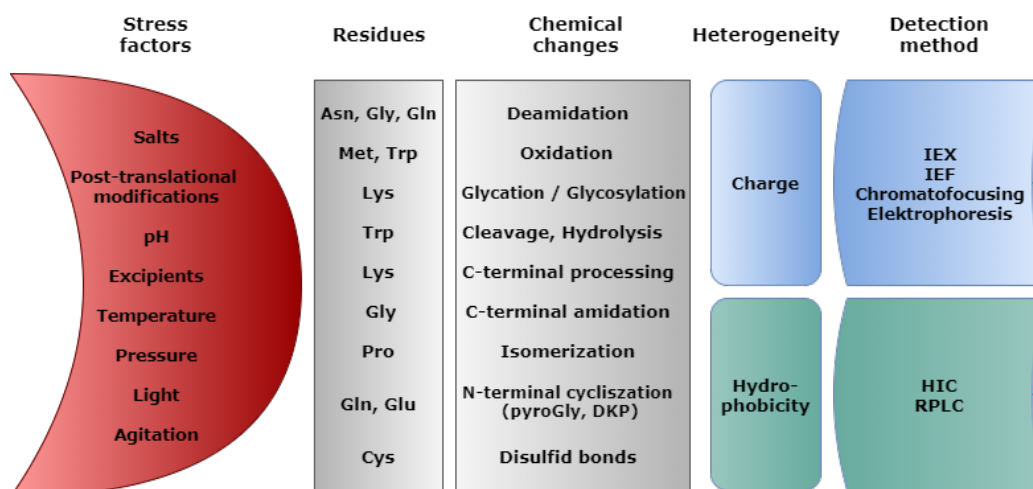


Figure 1.1: Overview of factors that induce chemical changes, of the types of changes and the amino acid residues at which these changes occur. The resulting protein heterogeneity can be detected regarding charge and hydrophobicity. Protein heterogeneity in size is not reflected in this overview.

The hinge region hydrolysis leads to fragmentation at basic pH [36]. Also **hydrolysis** at Trp residues was reported [37].

N-terminal cyclisation of an amine with another carbonyl group can lead to diketopiperazine (DKP) formation. **DKP** is an hydrophobicity variant observed, among others, in hGH [38]. Similarly, **pyroGlu** is formed by a nucleophilic attack of a N-terminal amine on the carbonyl group of a N-terminal glutamine (Glu) or glutamic acid (Gln) residue. The cyclized pyroGlu has basic character [39].

Heterogeneity can also be caused by incomplete **disulfide bonds**. Oxidation of cysteine (Cys) leads to unpaired Cys residues that expose free sulfhydryl groups. This process causes structural changes and increased hydrophobicity [40, 41].

1.3 Impact of Protein Variants on Product Stability

The same factors that influence the formation of protein variants may also lead to protein instability and aggregation. The protein variants as mentioned above may, over time and under already small changes of their environment, lead to misfolding, aggregation or self-interaction [42, 43]. This is due to the low conformational stability of proteins in their native state [44]. The conformational stability of proteins depends on the non-covalent Van der Waals interactions, hydrogen bonds and electrostatic interactions. Furthermore, configurational entropy plays a role in protein stability, as large entropy caused by a high number of buried side chains and certain amino acids, may destabilize proteins [45]. The protein subpopulations that resulted from chemical changes are also altered in the non-covalent forces. Thereby, the thermodynamic parameters of the protein are changed and may favor unfolding, self-interaction of a protein variant or interaction with other variants. All of these behaviors may result in aggregation [46, 47].

In general, protein variants that are more hydrophobic on their surface, e.g. due to partial unfolding or non-polar side chains, show increased intermolecular interactions and, therefore, are more prone for aggregation. The same applies to variants that carry less charge on their surface, as they lack charge - charge repulsion. Furthermore, charge variants with opposite surface charges show attractive forces [48].

The generalized pathway of non-native, irreversible aggregation in biopharmaceuticals proceeds in several steps from reversible conformational changes over conformers with increased aggregation propensity to reversible oligomers and, finally, the assembly to aggregates, which may be soluble or insoluble [49, 50].

Upon injection, misfolded and aggregated protein may be immunogenic and lead to the formation of antibodies which can reduce the efficacy of the therapeutic protein, as well as to severe side effects [51, 52]. Therefore, the aggregation propensity of protein products is thoroughly monitored during development and product life cycle. The probability of aggregation is pre-

dicted by unfolding behavior, protein intrinsic physicochemical parameters or based on sequence and structure of the protein [53, 54]. Considering the high risk posed by aggregates and the enormous effort made to prevent and observe them, it is even more important to know the behavior of protein subpopulations and to identify those variants that tend to aggregate.

1.4 Aim and Outline of the Thesis

The chemical changes that cause heterogeneity in protein therapeutics are well described and monitored during development and manufacturing. Many of these subpopulations were investigated regarding their impact on the therapeutic protein function. Adjustments in processes, formulation and protein engineering are applied to mitigate the number and quantity of protein variants. Yet, the root cause for the formation of protein subpopulations can not be controlled considering the manifold influences that lead to chemical changes [16]. Therefore, it is important to know the impact of each variant on the stability of the protein drug. However, little is known about the impact of each subpopulation on protein stability, self-interaction, interaction with other variants or aggregation propensity.

This thesis aims to separate, characterize and identify potential aggregation prone protein variants. If such variants are identified, further investigations are conducted to determine the influence of the variants on the stability of the therapeutic agent. With this work we aim to develop a tool kit of methods to gain knowledge about aggregation prone variants. A prerequisite for all methods is the maintenance of the intact protein variant in order to avoid any changes that might alter the protein behavior [55]. Our tools include the separation and collection of individual subpopulations in their native state and analytical methods suitable for the limited quantities of sample. In the future, these applications and the knowledge gained from them can be used to remove or stabilize critical variants as a step towards protein therapeutics with increased stability and safety.

The thesis is split into four further chapters, each representing a self-contained contribution to the topic of the thesis and a final chapter summarizing the results.

Chapter 2 focuses on the investigation of stability and aggregation propensity of charge variants of a mAb. Methods to analyze the thermal and colloidal stability are applied as well as molecular modeling and an accelerated stability study.

Chapter 3 investigates the hydrophobicity variants of the mAb. A semi-

preparative HIC without organic solvent is developed in order to separate and collect the hydrophobicity variants in their native states. SEC, DLS and DSF measurements are conducted to determine the stability of hydrophobicity variants. IEX is used to examine a correlation with the charge variants from chapter 2.

Chapter 4 applies the general approach of charge variant investigation (as seen in chapter 2) on a protein of lower molecular weight, naming rhGH. In addition, the impact of formulation conditions on rhGH charge variant stability is considered.

Chapter 5 deals with the setup of a new approach to detect and potentially quantify hydrophobicity in protein variants. A mini-chaperonin derived from Gro-EL is expressed and tested for interaction with protein variants.

Finally, **Chapter 6** will give a short overview on the results and final conclusions of this thesis. This chapter includes a perspective on the future.

Bibliography

- [1] A. Mullard, “FDA approves 100th monoclonal antibody product,” *Nat. Rev. Drug Discov.*, vol. 20, no. 7, pp. 491–495, 2021.
- [2] Z. E. Sauna, H. A. Lagassé, A. Alexaki, V. L. Simhadri, N. H. Katagiri, W. Jankowski, and C. Kimchi-Sarfaty, “Recent advances in (therapeutic protein) drug development,” *F1000Research*, vol. 6, 2017.
- [3] S. A. Berkowitz, J. R. Engen, J. R. Mazzeo, and G. B. Jones, “Analytical tools for characterizing biopharmaceuticals and the implications for biosimilars,” *Nat. Rev. Drug Discov.*, vol. 11, no. 7, pp. 527–540, 2012.
- [4] Y. S. Kim, B. W. Choi, S. W. Yang, S. M. Shin, S. W. Nam, Y. S. Roh, J. Y. Lee, K. J. Lee, Y. J. Kim, J. Y. Kwon, and D. I. Kim, “Biosimilars: Challenges and path forward,” *Biotechnol. Bioprocess Eng.*, vol. 19, no. 5, pp. 755–765, 2014.
- [5] G. W. Notani, A. J. Munro, and P. M. Knopf, “A charge difference between an intracellular and secreted mouse myeloma globulin,” *Biochem. Biophys. Res. Commun.*, vol. 25, no. 4, pp. 395–401, 1966.
- [6] Z. L. Awdeh, B. A. Askonas, and A. R. Williamson, “The homogeneous-gamma-G-immunoglobulin produced by mouse plasmacytoma 5563 and its subsequent heterogeneity in serum.” *Biochem. J.*, vol. 102, no. 2, pp. 548–553, 1967.
- [7] E. Wensch, S. Reiter, S. Hinger, F. Steindl, C. Tauer, A. Jungbauer, H. Katinger, and P. G. Righetti, “Shifts of isoelectric points between cellular and secreted antibodies as revealed by isoelectric focusing and immobilized pH gradients,” *Electrophoresis*, vol. 11, no. 11, pp. 966–969, 1990.
- [8] Y. Mimura, K. Nakamura, T. Tanaka, and M. Fujimoto, “Evidence of intra- and extracellular modifications of monoclonal IgG polypeptide chains generating charge heterogeneity,” *Electrophoresis*, vol. 19, no. 5, pp. 767–775, 1998.

- [9] Y. Yan, H. Wei, Y. Fu, S. Jusuf, M. Zeng, R. Ludwig, S. R. Krystek, G. Chen, L. Tao, and T. K. Das, “Isomerization and Oxidation in the Complementarity-Determining Regions of a Monoclonal Antibody: A Study of the Modification-Structure-Function Correlations by Hydrogen-Deuterium Exchange Mass Spectrometry,” *Anal. Chem.*, vol. 88, no. 4, pp. 2041–2050, 2016.
- [10] B. J. Compton, J. S. Gerald, D. A. Lowe, and R. P. Elander, “Microisoelectric point heterogeneity of a murine monoclonal antibody (L6) originating from cell cultivation conditions,” *Biotechnol. Tech.*, vol. 3, no. 5, pp. 349–354, 1989.
- [11] D. J. Kroon, A. Baldwin-Ferro, and P. Lalan, “Identification of Sites of Degradation in a Therapeutic Monoclonal Antibody by Peptide Mapping,” *Pharm. Res. An Off. J. Am. Assoc. Pharm. Sci.*, vol. 9, no. 11, pp. 1386–1393, 1992.
- [12] E. Sahin, A. O. Grillo, M. D. Perkins, and C. J. Roberts, “Comparative effects of pH and ionic strength on protein-protein interactions, unfolding, and aggregation for IgG1 antibodies,” *J. Pharm. Sci.*, vol. 99, no. 12, pp. 4830–4848, 2010.
- [13] J. S. Bee, T. W. Randolph, J. F. Carpenter, S. M. Bishop, and M. N. Dimitrova, “Effects of surfaces and leachables on the stability of biopharmaceuticals,” *J. Pharm. Sci.*, vol. 100, no. 10, pp. 4158–4170, 2011.
- [14] H. Liu, G. Caza-Bulsecu, D. Faldu, C. Chumsae, and J. Sun, “Heterogeneity of monoclonal antibodies,” pp. 2426–2447, 2008.
- [15] B. A. Kerwin and R. L. Remmele, “Protect from light: Photodegradation and protein biologics,” *J. Pharm. Sci.*, vol. 96, no. 6, pp. 1468–1479, 2007.
- [16] S. Chung, J. Tian, Z. Tan, J. Chen, J. Lee, M. Borys, and Z. J. Li, “Industrial bioprocessing perspectives on managing therapeutic protein charge variant profiles,” pp. 1646–1665, 2018.

-
- [17] M. C. Manning, D. K. Chou, B. M. Murphy, R. W. Payne, and D. S. Katayama, “Stability of protein pharmaceuticals: An update,” *Pharm. Res.*, vol. 27, no. 4, pp. 544–575, 2010.
- [18] J. Vlasak and R. Ionescu, “Heterogeneity of Monoclonal Antibodies Revealed by Charge-Sensitive Methods,” *Curr. Pharm. Biotechnol.*, vol. 9, no. 6, pp. 468–481, 2008.
- [19] J. Kahle and H. Wätzig, “Determination of protein charge variants with (imaged) capillary isoelectric focusing and capillary zone electrophoresis,” *Electrophoresis*, vol. 39, no. 20, pp. 2492–2511, 2018.
- [20] A. Hutanu, S. Kiessig, A. Bathke, R. Ketterer, S. Riner, J. Olaf Stracke, M. Wild, and B. Moritz, “Application of affinity capillary electrophoresis for charge heterogeneity profiling of biopharmaceuticals,” *Electrophoresis*, vol. 40, no. 22, pp. 3014–3022, 2019.
- [21] I. A. Kaltashov, C. E. Bobst, R. R. Abzalimov, G. Wang, B. Baykal, and S. Wang, “Advances and challenges in analytical characterization of biotechnology products: Mass spectrometry-based approaches to study properties and behavior of protein therapeutics,” *Biotechnol. Adv.*, vol. 30, no. 1, pp. 210–222, 2012.
- [22] F. Füssl, L. Strasser, S. Cari, and J. Bones, “Native LC–MS for capturing quality attributes of biopharmaceuticals on the intact protein level,” *Curr. Opin. Biotechnol.*, vol. 71, pp. 32–40, 2021.
- [23] M. Haverick, S. Mengisen, M. Shameem, and A. Ambrogelly, “Separation of mAbs molecular variants by analytical hydrophobic interaction chromatography HPLC: Overview and applications,” pp. 852–858, 2014.
- [24] N. E. Robinson, “Protein deamidation,” *Proc. Natl. Acad. Sci. U. S. A.*, vol. 99, no. 8, pp. 5283–5288, 2002.
- [25] D. Gervais, “Protein deamidation in biopharmaceutical manufacture: Understanding, control and impact,” *J. Chem. Technol. Biotechnol.*, vol. 91, no. 3, pp. 569–575, 2016.

- [26] J. Cacia, R. Keck, L. G. Presta, and J. Frenz, "Isomerization of an aspartic acid residue in the complementarity-determining regions of a recombinant antibody to human IgE: Identification and effect on binding affinity," *Biochemistry*, vol. 35, no. 6, pp. 1897–1903, 1996.
- [27] A. A. Wakankar, R. T. Borchardt, C. Eigenbrot, S. Shia, Y. J. Wang, S. J. Shire, and J. L. Liu, "Aspartate isomerization in the complementarity-determining regions of two closely related monoclonal antibodies," *Biochemistry*, vol. 46, no. 6, pp. 1534–1544, 2007.
- [28] R. J. Harris, B. Kabakoff, F. D. Macchi, F. J. Shen, M. Kwong, J. D. Andya, S. J. Shire, N. Bjork, K. Totpal, and A. B. Chen, "Identification of multiple sources of charge heterogeneity in a recombinant antibody," *J. Chromatogr. B Biomed. Sci. Appl.*, vol. 752, no. 2, pp. 233–245, 2001.
- [29] X. M. Lam, J. Y. Yang, and J. L. Cleland, "Antioxidants for prevention of methionine oxidation in recombinant monoclonal antibody HER2," *J. Pharm. Sci.*, vol. 86, no. 11, pp. 1250–1255, 1997.
- [30] C. Chumsae, G. Gaza-Bulsecu, J. Sun, and H. Liu, "Comparison of methionine oxidation in thermal stability and chemically stressed samples of a fully human monoclonal antibody," *J. Chromatogr. B Anal. Technol. Biomed. Life Sci.*, vol. 850, no. 1-2, pp. 285–294, 2007.
- [31] J. Yang, S. Wang, J. Liu, and A. Raghani, "Determination of tryptophan oxidation of monoclonal antibody by reversed phase high performance liquid chromatography," *J. Chromatogr. A*, vol. 1156, no. 1-2 SPEC. ISS., pp. 174–182, 2007.
- [32] S. Arena, A. M. Salzano, G. Renzone, C. D'Ambrosio, and A. Scaloni, "Non-enzymatic glycation and glycoxidation protein products in foods and diseases: An interconnected, complex scenario fully open to innovative proteomic studies," *Mass Spectrom. Rev.*, vol. 33, no. 1, pp. 49–77, 2014.
- [33] F. Higel, A. Seidl, F. Sörgel, and W. Friess, "N-glycosylation heterogeneity and the influence on structure, function and pharmacokinetics

- of monoclonal antibodies and Fc fusion proteins,” *Eur. J. Pharm. Biopharm.*, vol. 100, pp. 94–100, 2016.
- [34] R. J. Harris, “Processing of C-terminal lysine and arginine residues of proteins isolated from mammalian cell culture,” *J. Chromatogr. A*, vol. 705, no. 1, pp. 129–134, 1995.
- [35] K. A. Johnson, K. Paisley-Flango, B. S. Tangarone, T. J. Porter, and J. C. Rouse, “Cation exchange-HPLC and mass spectrometry reveal C-terminal amidation of an IgG1 heavy chain,” *Anal. Biochem.*, vol. 360, no. 1, pp. 75–83, 2007.
- [36] A. J. Cordoba, B. J. Shyong, D. Breen, and R. J. Harris, “Non-enzymatic hinge region fragmentation of antibodies in solution,” *J. Chromatogr. B Anal. Technol. Biomed. Life Sci.*, vol. 818, no. 2, pp. 115–121, 2005.
- [37] D. M. Luykx, M. G. Casteleijn, W. Jiskoot, J. Westdijk, and P. M. Jongen, “Physicochemical studies on the stability of influenza haemagglutinin in vaccine bulk material,” *Eur. J. Pharm. Sci.*, vol. 23, no. 1, pp. 65–75, 2004.
- [38] J. Battersby, W. Hancock, E. Canova-Davis, J. Oeswein, and B. O’Connor, “Diketopiperazine formation and N-terminal degradation in recombinant human growth hormone,” *Int. J. Pept. Protein Res.*, vol. 44, no. 3, pp. 215–222, jan 2009.
- [39] M. Messer, “Enzymatic cyclization of L-glutamine and L-glutaminy peptides,” *Nature*, vol. 197, no. 4874, p. 1299, 1963.
- [40] R. J. Harris, “Heterogeneity of recombinant antibodies: Linking structure to function,” *Dev. Biol. (Basel)*, vol. 122, pp. 117–127, 2005.
- [41] W. B. Chaderjian, E. T. Chin, R. J. Harris, and T. M. Etcheverry, “Effect of copper sulfate on performance of a serum-free CHO cell culture process and the level of free thiol in the recombinant antibody expressed,” *Biotechnol. Prog.*, vol. 21, no. 2, pp. 550–553, 2005.

- [42] H.-C. Mahler, W. Friess, U. Grauschopf, and S. Kiese, “Protein aggregation: pathways, induction factors and analysis.” *J. Pharm. Sci.*, vol. 98, no. 9, pp. 2909–34, 2009.
- [43] Q. Luo, M. K. Joubert, R. Stevenson, R. R. Ketchem, L. O. Narhi, and J. Wypych, “Chemical modifications in therapeutic protein aggregates generated under different stress conditions,” *J. Biol. Chem.*, vol. 286, no. 28, pp. 25 134–25 144, 2011.
- [44] E. Y. Chi, S. Krishnan, T. W. Randolph, and J. F. Carpenter, “Physical stability of proteins in aqueous solution: Mechanism and driving forces in nonnative protein aggregation,” pp. 1325–1336, 2003.
- [45] K. P. Murphy, “Noncovalent forces important to the conformational stability of protein structures.” in *Protein Stab. Fold.*, B. Shirley, Ed. Totowa, New Jersey: Humana Press, 1995, vol. 40, pp. 1–34.
- [46] D. B. Volkin, H. Mach, and C. R. Middaugh, “Degradative Covalent Reactions Important to Protein Stability,” *Appl. Biochem. Biotechnol. - Part B Mol. Biotechnol.*, vol. 8, no. 2, pp. 105–122, 1997.
- [47] E. Freire, “The thermodynamic linkage between protein structure, stability, and function.” in *Protein Struct. Stability, Fold.*, K. Murphy, Ed. Totowa, New Jersey: Humana Press, 2001, vol. 168, pp. 37–68.
- [48] C. J. Roberts, “Therapeutic protein aggregation: Mechanisms, design, and control,” *Trends Biotechnol.*, vol. 32, no. 7, pp. 372–380, 2014.
- [49] —, “Nonnative protein aggregation: Pathways, kinetics, and stability prediction,” in *Misbehaving Proteins Protein (Mis)Folding, Aggregation, Stab.*, R. M. Murphy and A. M. Tsai, Eds. Springer, 2006, pp. 17–46.
- [50] D. Pfister, L. Nicoud, and M. Morbidelli, *Continuous Biopharmaceutical Processes: Chromatography, Bioconjugation, and Protein Stability*. Cambridge University Press, 2018.

-
- [51] C. Maas, S. Hermeling, B. Bouma, W. Jiskoot, and M. F. Gebbink, “A role for protein misfolding in immunogenicity of biopharmaceuticals,” *J. Biol. Chem.*, vol. 282, no. 4, pp. 2229–2236, jan 2007.
- [52] M. Sauerborn, V. Brinks, W. Jiskoot, and H. Schellekens, “Immunological mechanism underlying the immune response to recombinant human protein therapeutics,” *Trends Pharmacol. Sci.*, vol. 31, no. 2, pp. 53–59, feb 2010.
- [53] Z. Hamrang, N. J. Rattray, and A. Pluen, “Proteins behaving badly: Emerging technologies in profiling biopharmaceutical aggregation,” *Trends Biotechnol.*, vol. 31, no. 8, pp. 448–458, 2013.
- [54] M. Shah, “Commentary: New perspectives on protein aggregation during Biopharmaceutical development,” pp. 1–6, 2018.
- [55] A. Staub, D. Guillarme, J. Schappler, J. L. Veuthey, and S. Rudaz, “Intact protein analysis in the biopharmaceutical field,” *J. Pharm. Biomed. Anal.*, vol. 55, no. 4, pp. 810–822, 2011.

Chapter 2

Identification of Monoclonal Antibody Variants Involved in Aggregate Formation – Part 1: Charge Variants

The following chapter was published in the European Journal of Pharmaceutics and Biopharmaceutics 2020, Vol. 158.

Authors

Robina Mareike Meyer ¹, Lukas Berger ², Joerg Nerkamp ², Stefan Scheler ²,
Sebastian Nehring ², Wolfgang Friess ¹

¹: Ludwig-Maximilians University Munich, Germany

²: Sandoz Biopharmaceuticals, Langkampfen, Austria

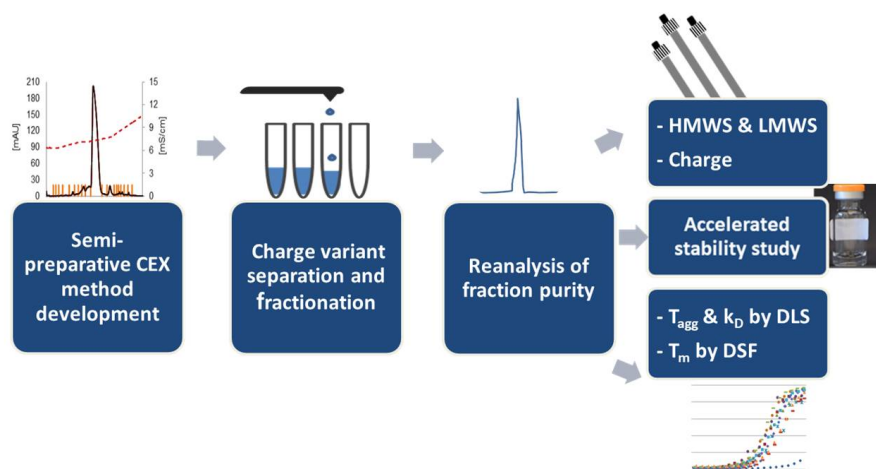
Keywords

mAb charge variants; protein aggregation; protein stability; FPLC; light scattering; differential scanning fluorimetry

2.1 Abstract

Biopharmaceutical products contain conformational and chemical variants, that are typically well characterized regarding identity and activity. However, little is known about their self-interaction propensity and tendency to unfold, which are critical characteristics for drug stability and safety. This study aimed to separate and compare charge variants of a monoclonal antibody (mAb) and to identify aggregation prone species. We show a semi-preparative cation exchange method, that we developed to separate the individual acidic and basic variants from the naïve mAb. Additionally, we demonstrate, that the yield and purity of the fractionated charge species, extracted by that method, were sufficient for subsequent analysis of aggregate content, conformation stability and self-interaction. Our analysis revealed a differently behaving acidic variant and confirmed its increased aggregation propensity by molecular modeling. During a stability study, the potentially aggregation prone charge variant posed a limited risk to the drug substance (DS). We are the first to look at the stability of single charge variants of biopharmaceuticals, and thus present manufacturers and regulatory authorities with a method to enhance drug safety.

Graphical Abstract



2.2 Introduction

The growing market of biopharmaceuticals underlines the success of therapeutic proteins during the last two decades. Rigid purification of the drug substance during downstream processing ensures the efficacy and safety of these drugs. Still, drug substance and drug product contain multiple protein species [1]. This micro-heterogeneity originates from degradation or modification in the amino acid sequence caused by stress during production steps, handling or storage [2]. As a result, altered protein species are formed by different mechanisms that include deamidation, oxidation and fragmentation. For example, the hydrolytic reaction of asparagine or glutamine deamidation and isomerization in alternative reactions leads to changes of the protein backbone and conversion of charge distribution. If these changes occur in the complementarity-determining region of a mAb, they could have a negative impact on stability and binding affinity [3, 4]. Additionally, the clipping of amino acids and post-translational glycosylation can change the charge of the protein [5]. In general, the kind of modification that led to the respective charged species determines the impact of charge variants on the properties of therapeutic proteins [6]. In case of alterations leading to a changed charge distribution on the surface, charge variants with altered isoelectric points can be found. These variants are characteristic constituents of a biopharmaceutical product and should not be mistaken with impurities [7]. Instead, charge variants are characterized by manufacturers as quality parameters. However, the quality assessments so far do not involve the analysis of behavior and stability of charge variants. Indeed, this is of importance, as the electrostatic surface charge has a high influence on molecular interactions of proteins. In case of varying charge distribution, intermolecular attractions could occur due to the interaction of protein surfaces with positive and negative potential [8]. The resulting association of single proteins to larger protein molecules is one of several pathways of aggregate formation [9] and was shown in literature for a variety of proteins [10, 11, 12, 13]. Consequently, charge variants can pose a potential risk of self-association and aggregate formation, that might lead to the induction of immunogenicity and reduction of

biologic activity of a drug. A lot of effort is put into the detection of the resulting soluble and insoluble aggregates as well as particles in the visible and sub-visible range [9, 14]. Therefore, it would be beneficial to gain deeper knowledge about the behavior of charge species by variants separation and characterization in order to reduce the risk of potentially aggregation prone species.

In related literature, Hintersteiner et al. separated acidic, basic and main species of a variety of antibodies by cation exchange chromatography. The assessment of these variants by differential scanning calorimetry revealed no differences in conformational stability, whereas varying affinity to Fc-domain binding surface receptors was found [15]. In other studies, different mAb charge variants were separated and collected to characterize their target binding, bioavailability or *in vivo* activity [16, 17]. An effect on *in vitro* or *in vivo* potency was not found. None of the studies focused on aggregation of the different charge species.

Sule et al. analyzed the impact of acidic variant pools generated via modulating bioreactor batch time on aggregation of an high concentration antibody formulation. Here, the acidic pools had a similar colloidal or conformational stability relative to main species and aggregation was not increased [18]. All of the mentioned studies have in common, that acidic and basic variants of the respective proteins were pooled for analysis. To the best of our knowledge, no work has yet been published, that separated and characterized *single* charge variants of a mAb in order to find aggregation prone species.

With this paper we propose a first step to close this gap by developing a method to separate single charge variants by cation exchange chromatography in a semi-preparative scale and applying this method successfully. Our method involved a step wise salt-gradient and a pH-gradient in order to achieve the highest resolution possible [19]. The collected charge variants were characterized regarding purity and aggregate content. Charge variants collected in sufficient concentrations were selected for further analysis. The conformational and colloidal stabilities of these variants were assessed using dynamic and static light scattering as well as differential scanning fluorime-

try. Furthermore, we repeated this process using thermally stressed mAb DS as the thermal stress is an established approach to simulate the aging process and amplify the charge variant populations [20]. For deeper understanding and to underline our results, we calculated the aggregation score of a potentially aggregation prone variant by molecular modeling. Additionally, we applied a forced stability study at 45 °C for 12 weeks to test the aggregation behavior of potentially aggregation prone species both pristine and in mixtures with DS.

The results reveal the possibility of detecting single charge variants with decreased stability and increased aggregation propensity. The knowledge of aggregation prone species at an early stage of development could enable optimal purification and removal of such species and thus lower costs and improve quality of biopharmaceuticals. Improved stability may allow lower cost of goods by avoiding lyophilization, since the drug substance per se shows better resistance against aggregation. Alternatively, stabilizing additives in liquid formulation could be used to reduce the impact of an aggregation prone variant.

Our contributions are:

- the development of an ion exchange method to separate and collect single charge variants
- the restatement, that aggregate formation in antibody formulations can specifically involve certain aggregation prone subpopulations
- the identification of a potentially aggregation prone acidic variant of a mAb
- and a risk assessment in terms of an accelerated stability study of charge variants spiked into DS.

2.3 Materials and Methods

2.3.1 mAb Model Protein

The drug substance (DS) of a therapeutic IgG1 model monoclonal antibody (mAb) was provided by Sandoz Biopharmaceuticals, Schafftenau, Austria. It was produced in CHO cells and formulated in a 50 mM sodium phosphate buffer at pH 6.2 with a concentration of 55 mg/ml and an extinction coefficient of 1.7 ml g⁻¹ cm⁻¹ at 280 nm. In order to generate higher amounts of charge variants, the DS was stored at 40 °C for 16 days.

2.3.2 Separation of Charge Variants

Charge variant fractions of the mAb DS were collected with a GE ÄKTA purifier FPLC system (GE Healthcare, Uppsala, Sweden) equipped with a 9 x 250 mm ProPac WCX-10 column (Thermo Scientific, Wilmington, Delaware, USA). MAb DS was diluted in equilibration buffer (25 mM sodium phosphate buffer pH 6.2) to a concentration of 5 mg/ml and loaded onto the column with a flow rate of 1.2 ml/min. Charge variants were eluted with a stepwise salt gradient from zero to 125 mM sodium chloride and a pH gradient from pH 6.20 to 6.39. During elution, fractions of 1.2 ml volume were collected in 15 ml polypropylene (PP) tubes by a Frac-920 fraction collector (GE Healthcare). Unicorn 5.31 Software (GE Healthcare) was used for programming and evaluation of the method. In several separation cycles, fractions containing single variants were saved and pooled in order to collect sufficient material for further analysis. To ensure the validity of our process, all fractions collected were reunited as control sample and the same analytical process was performed. All fractions were concentrated in VivaSpin 20 centrifugation filter units with 30.000 Da MWCO (Sartorius Stedim Biotech, Göttingen, Germany) and buffer was exchanged to 10 mM sodium phosphate pH 6.2. The final concentrations were determined via the extinction coefficient using a Nanodrop 2000 photometer (Thermo Scientific). The fractions were stored at 4 °C - 6 °C.

2.3.3 Analytical Ion Exchange Chromatography (IEX)

Pooled charge variants were analyzed for purity by cation exchange (CEX) with a 3 x 250 mm ProPac WCX-10 column (Thermo Scientific) connected to an Agilent 1200 HPLC system (Agilent Technologies, Santa Clara, California, USA). All samples were diluted in equilibration buffer to a concentration of 1.15 mg/ml. 30 μ g of each sample were injected onto the column with a flow rate of 1 ml/min. The equilibration and elution conditions were equivalent to those utilized during charge variant separation (see 2.2). The eluted sample was detected by UV absorption at 280nm and chromatograms were analyzed with ChemStation B.02.01-SR2 (Agilent Technologies) regarding retention time and area under the curve (AUC). All chromatograms were corrected by subtraction of a chromatogram of a buffer injection.

2.3.4 Size Exclusion Chromatography (SEC)

SEC was run on an Agilent 1200 series HPLC system (Agilent Technologies). 30 μ g per sample were injected onto a Tosoh TSKgel G2000SWXL column (7.8 x 300 mm, Tosoh Bioscience, Stuttgart, Germany) using a mobile phase of 25 mM sodium phosphate pH 6.2 with 125 mM sodium chloride at a flow rate of 0.5 ml/min. Chromatograms were analyzed with ChemStation software version B.02.01-SR2 (Agilent Technologies) regarding retention time and area under the curve (AUC) after UV detection at 280 nm.

2.3.5 Dynamic Light Scattering (DLS)

DLS analysis was conducted with a DynaPro Plate Reader II (Wyatt Technologies, Dernbach, Germany). Samples and dilution buffer (10 mM sodium phosphate pH 6.2) were filtered with a 0.2 μ m regenerated cellulose filter (Sartorius, Göttingen, Germany) prior to dilution. After dilution, each sample was centrifuged at 10 000 rpm for 10 min to remove any insoluble particles and the supernatant was used for analysis. 5.5 μ l of sample solutions were transferred into 1536-well-plates (Aurora, Whitefish, MT, USA) in triplicates and centrifuged at 2000 rpm for two minutes in order to remove trapped air

from the plate bottom. Wells were sealed with a drop of silicone oil and again centrifuged at 2000 rpm for one minute. Aggregation onset temperatures (T_{agg} onset) were measured in triplicates at 1.5 mg/ml with a temperature ramp from 25 °C to 70 °C and a ramp rate of 0.143 °C/min. The standard deviation was depicted in error bars. Diffusion interaction parameters (k_D) were determined by measuring diffusion coefficients (D) at 25 °C using six protein concentrations between 1 mg/ml and 4 mg/ml. Each well was analyzed with five acquisitions and an acquisition time of 5s. The control of the instrument and data acquisition were executed with Dynamics 7.6 software (Wyatt Technologies). The diffusion interaction parameter was calculated as linear fit of D versus protein concentration to obtain the diffusion coefficient at infinite dilution D_0 . After normalizing D by D_0 , the slope of the linear fit corresponds to the interaction parameter k_D [21].

2.3.6 Static Light Scattering (SLS)

Colloidal stability and aggregation of charge variants and controls were also studied by static light scattering (SLS) analysis using an Avacta Optim 1000 fluorescence and light scattering analyzer (Avacta Analytical Ltd., Wetherby, UK). Samples of 1.5 mg/mL were centrifuged at 10 000 rpm for 10 min to remove any insoluble particles and the supernatant was used for analysis. Optim specific microcuvette arrays were loaded with 9 μL protein solution. SLS intensities at 266 nm were measured as a function of temperature in the range of 25 °C to 70 °C at a ramp rate of 0.143 °C/min. T_{agg} was evaluated for 90° light scattering by Optim Analysis software V2.0.4 (Avacta Analytical). Standard deviations were depicted in error bars.

2.3.7 Nano Differential Scanning Fluorimetry (nDSF)

Thermal unfolding in terms of the increase in intrinsic fluorescence intensity was detected as the ratio of fluorescence at 350 to 330 nm with the Prometheus NT.48 differential scanning fluorimeter (NanoTemper Technologies, Munich, Germany). Samples were filled in triplicates in standard nDSF™ grade capillaries and excited at 280 nm. A temperature ramp of

1 °C/min from 25 to 80 °C was applied. Aggregation was detected by reflection intensity referred to as scattering. Protein melting temperatures (T_m) were determined with the PR.ThermControl software V2.1 (NanoTemper Technologies, Munich, Germany) from the maximum of the first derivatives of the thermal unfolding curves. Forced degradation studies were performed isothermal at 67 °C for 12 h. The scattering onset in dependence on time was determined with the PR.TimeControl software V1.0.2 (NanoTemper Technologies, Munich, Germany). Standard deviations of all nDSF measurements were depicted in error bars.

2.3.8 Protein Modeling

Homology modeling based on the published mAb structure provided by DrugBank Version 5.0. Three dimensional structures of Fab parts of the variants were adapted with BioLuminate (Schroedinger LLC, New York, USA) according to characterization data from the supplier. Protein surface analysis was carried out and the additive aggregation score (Aggscore) of variants was calculated as a prediction of aggregation prone regions based on the presence of hydrophobic surface patches [22]. The energetic stability of the obtained folding shapes was predicted mathematically.

2.3.9 Accelerated Stability Study and Spiking Procedures

The charge variants, controls, buffer and DS were sterile filtered with a 0.22 μm polyethersulfone filter (VWR International, Radnor, PA), diluted with 50 mM sodium phosphate to a concentration of 1.5 mg/ml and filled into pre-sterilized DIN2R glass type I vials (MGlass AG, Germany) in duplicates. Additionally, these samples were added to sterile and filtrated but otherwise untreated DS in a concentration of 10 % (v/v) to obtain spiked samples of 1.5 mg/ml. The vials with a total fill volume of 0.5 ml were crimped with rubber stoppers (West Pharmaceutical Services, USA) and stored at 45 °C until the time point of analysis.

2.3.10 Visual Inspection

Vials were gently swirled and the presence of visible particles was assessed visually in accordance with Ph.Eur. chapter 2.9.20. Each vial was observed for at least 5 s in front of a white plate as well as in front of a black plate. The occurrence of particles and turbidity was recorded.

2.3.11 Ultraviolet Absorption Spectroscopy at 320nm

Turbidity was measured with an Agilent 8453 UV-Vis Spectrophotometer (Agilent Technologies, Santa Clara, California, USA) and a Quartz SUPRASIL® Type ultramicro cuvette (Hellma Analytics, Müllheim, Germany) with a path length of 10 mm. 70 μl of sample were analyzed at 320 nm wavelength. The instrument was calibrated with seven dilutions of TURB 4000 NTU Formazin (Sigma-Aldrich) as nephelometric standard. The results are presented in nephelometric turbidity units (NTU), correspondingly.

2.3.12 Fluorescence spectroscopy

Intrinsic fluorescence emission was measured with a FLUOstar Omega Star plate reader (BMG Labtech, Ortenberg, Germany). 35 μl of each vial were filled in a 384-well plate (Corning Life Science, Tewksbury, MA, USA) with transparent flat bottom. The samples were excited at 280 nm and emission at 330 nm and 350 nm was measured.

2.3.13 Subvisible Particle Counting

The FlowCam 8100 (Fluid Imaging Technologies, Scarborough, ME, USA) was used for counting of sub-visible particles. Protein samples were diluted 1:1 with formulation buffer. 150 μl sample were analyzed with 10 \times magnification at 0.150 ml/min flow rate and 29 frames per second frame rate. A segmentation threshold of 13.0 for dark pixels and 10.0 for light pixels was applied. After each measurement, the flow cell was rinsed with highly purified water (HPW). Sub-visible particles bigger than or equal to 1, 2, 10, and

25 mm were evaluated with VisualSpreadsheet software Version 4.7.6 (Fluid Imaging Technologies) and are presented as counts per mL.

2.3.14 Multi-Angle Light Scattering Coupled Size Exclusion Chromatography (SEC-MALS)

An Dionex UltiMate 3000 HPLC system (Thermo Fisher Scientific, CA, USA) with an UltiMate 3000 VWD multiple wavelength detector (Thermo Fisher Scientific) and a DAWN HELEOS multiangle light scattering (MALS) detector (Wyatt Technology, Santa Barbara, USA) were used for the SEC-MALS measurements. Sample elution was monitored at 280 nm. 30 μg per sample were injected onto a Tosoh TSKgel G3000SWXL column (7.8×300 mm, Tosoh Bioscience, Stuttgart, Germany). A mobile phase of 25 mM sodium phosphate pH 6.2 with 125 mM sodium chloride was used at a flow rate of 0.5 ml/min. Chromatograms were acquired and analyzed using the Chromeleon CDS Software Version 7.2.7.10369 (Thermo Scientific). A buffer injection signal was subtracted as blank. MALS data collection and processing were performed using the ASTRA software, Version 7.1 (Wyatt Technology).

2.4 Results and Discussion

2.4.1 mAb Charge Variant Separation and Fractionation

Beside the naïve species (main species), the semi-preparative separation of mAb charge variants rendered 13 acidic (AP) and eight basic peaks (BP) (Figure 2.1a, Table 2.1). The most prominent peaks ($Area \geq 0.5\%$) were collected in sufficient amounts for further analysis.

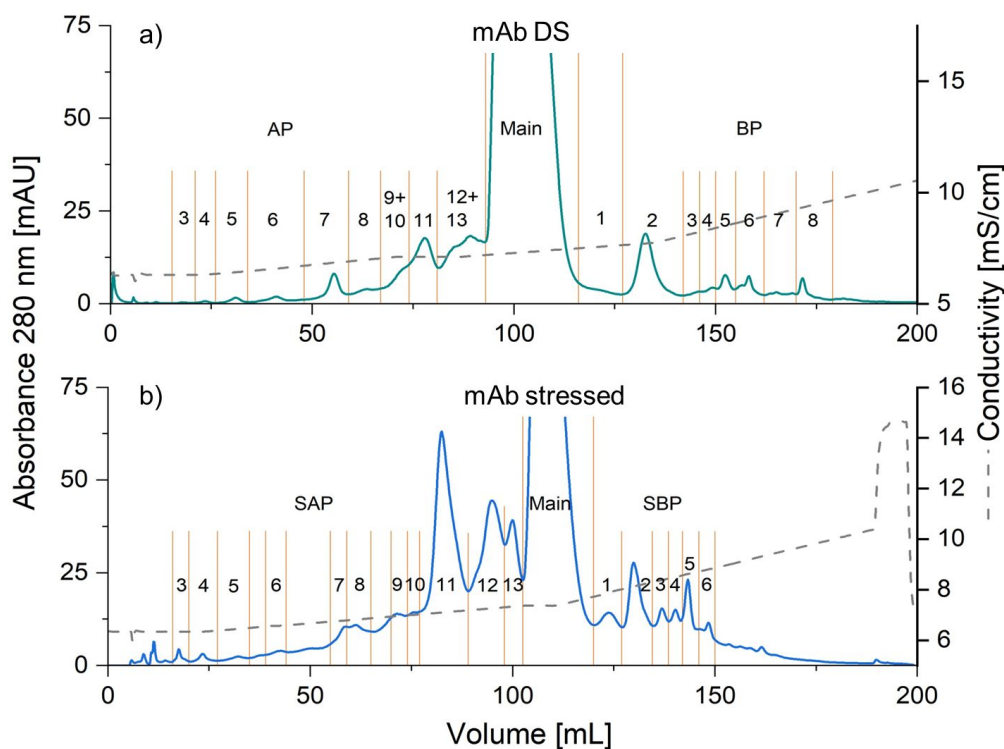


Figure 2.1: Semi-preparative IEX chromatograms of mAb charge variant separation for a) mAb DS and b) mAb stressed at 40 °C for 16 days.

After temperature stress at 40 °C for 16 days, the peak areas increased and the peak pattern changed slightly as the number of acidic species increased (Figure 2.1b, Table 2.1). The storage of mAb DS at elevated temperatures led to the desired amplification of modification processes. Some prominent

mAb peaks could be separated more clearly after storage at 40 °C and the stress storage enabled the separation of single charge variants in increased amounts. It is important to keep in mind, that single peaks may contain more than one mAb form showing very similar electrostatic interactions with the CEX column. Nevertheless, here, we consider each collected peak as a charge species, demonstrating similar charge distribution on the surface.

mAb DS				Stressed mAb			
Peak	Area [%]	Purity [%]	Contains	Peak	Area [%]	Purity [%]	Contains
				SAP7	0.7	74	21 % SAP 8
AP8	0.7	54		SAP8	0.8	86	
AP9+10	1.7	34		SAP9	0.7	95	
AP11	3.4	75		SAP10	0.2	86	
AP12+13	5.7	73		SAP11	12.6	95	
Main	78.8	94		SAP12	6.0	92	
				SAP13	2.8	98	
				Main	67.2	98	
				SBP1	0.8	82	
BP2	3.7	89	4 % Main	SBP2	3.7	n.d.	
BP3-7	-	59	35 % Main				
BP3	0.5	n.d.		SBP3	0.9	43	25 % Main 18 % SAP11
BP4	0.5	n.d.		SBP 4	0.7	45	23 % Main 6 % SAP11 10 % SAP13
BP5	0.8	n.d.		SBP5	1.4	29	40 % Main 5 % SAP11
BP6	1.0	n.d.		SBP6	0.3	42	50 % Main
BP7	0.7	n.d.					
BP8	0.7	n.d.					
Control	100	n.d.		stressed Control	100	n.d	

Table 2.1: Area and purity of collected mAb charge variants. n.d. = not determined.

Despite a flattened gradient during critical peak elution, not all variants could be distinctly separated from each other, i.e., by baseline separation. Nevertheless, reanalysis of the collected and concentrated fractions by analytical chromatography confirmed reasonable purity of most of the collected

variants (Table 2.1). The purity, especially of the acidic variants, improved during collection of temperature stressed DS variants. Impurities were generally caused by the presence of neighboring peaks. Interestingly, basic species contained high amounts of naïve protein and the species of the stressed acidic peak 11 (SAP11), despite of being well separated from these mentioned peaks. Aggregates are known to elute as basic species in IEX [23]. The observation of main and acidic species eluting within basic variants led us to the hypothesis of aggregates build of main species and SAP11. Since these variants can be found separately in basic fractions, this aggregation is thought to be at least partially reversible.

2.4.2 Aggregation and Degradation Products

In order to characterize the presence of aggregates in the different fractions, size exclusion chromatography was conducted by injection of same concentrations of each enriched variant. Under non-stressed conditions, basic charge species contained higher amounts of aggregates compared to acidic species (Figure 2.2a). The amounts of aggregates in terms of high molecular weight (HMW) species found in BP7 and BP8 were noticeably high with 23 % and 73 %, respectively. However, both species were found with a relative peak area of 0.7 % in mAb DS (Table 2.1). Calculating the total amount of aggregates of these species nearly summed up to the total amount of aggregates found in mAb DS. Therefore, almost all soluble aggregates of mAb DS were eluting in two basic species.

As expected, after the application of thermal stress, the amount of aggregates and fragments (low molecular weight (LMW) species) increased (Figure 2.2b). Temperature stress can generate chemical modifications like asparagine deamidation, clippings and conformational changes [24] and some of these changes may be involved in aggregate formation [25]. Nonetheless, these effects are likely to reflect the general behavior of mAb DS.

Again, aggregates eluted mainly in basic species. This was especially true for those basic fractions containing high amounts of main and SAP11 species. Thereby, SEC data underlined our hypothesis of partially reversible

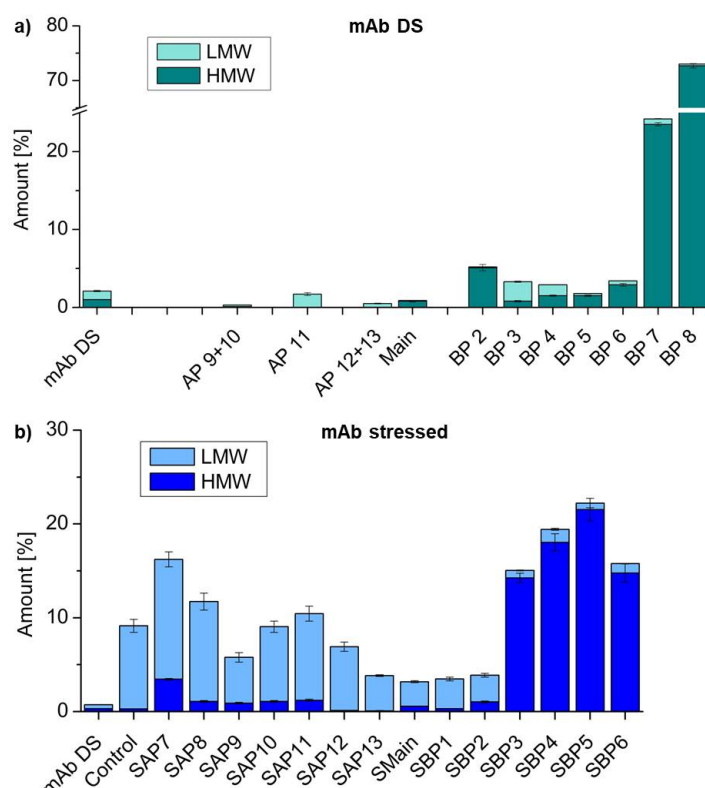


Figure 2.2: HMW and LMW content of mAb charge variants for a) mAb DS and b) mAb stored at 40 °C for 16 days.

aggregate formation. At this point, it is not possible to conclude at which process step the separation of the previously mixed basic species occurred.

2.4.3 Conformational Stability and Self-Interaction of mAb Charge Variants

Single charge variants were further analyzed regarding their propensity to unfold and to aggregate. The aggregation onset temperature in DS formulation at pH 6.2, determined by DLS, did not differ between the charge variants (Figure 2.3a). Although AP11 showed the tendency to earlier aggregation, the T_{agg} value was within the error bars of the naïve protein and control sample, which resembles all fractions collected after IEX separation. At pH 7.2, closer to the mAb's isoelectric point, AP11 showed a lower T_{agg} compared

2. Identification of Monoclonal Antibody Variants Involved in Aggregate Formation – Part 1: Charge Variants

34

to other species. This indicates a decreased conformational stability of this variant, while it does not behave differently at the pH of DS formulation. It is well known that the formulation pH has a substantial impact on protein stability. Here, the pH shift underlined the fragility of SAP11. Since we aimed to understand aggregation propensity in DS formulation, we maintained measurement conditions at pH 6.2.

To confirm T_{agg} results, the samples were also measured by SLS. T_{agg} values obtained by SLS were lower but correlated with the DLS results (Figure 2.3b). The T_{agg} of AP11 was decreased compared to other fractions. This effect was more pronounced in SLS in comparison to DLS data. DLS measurements of charge variants of stressed mAb revealed a decreased T_{agg} in DS formulation for SAP11, the corresponding variant of AP11 (Figure 2.3c). Overall, (S)AP11 proved to be less stable under thermal stress conditions than the other variants.

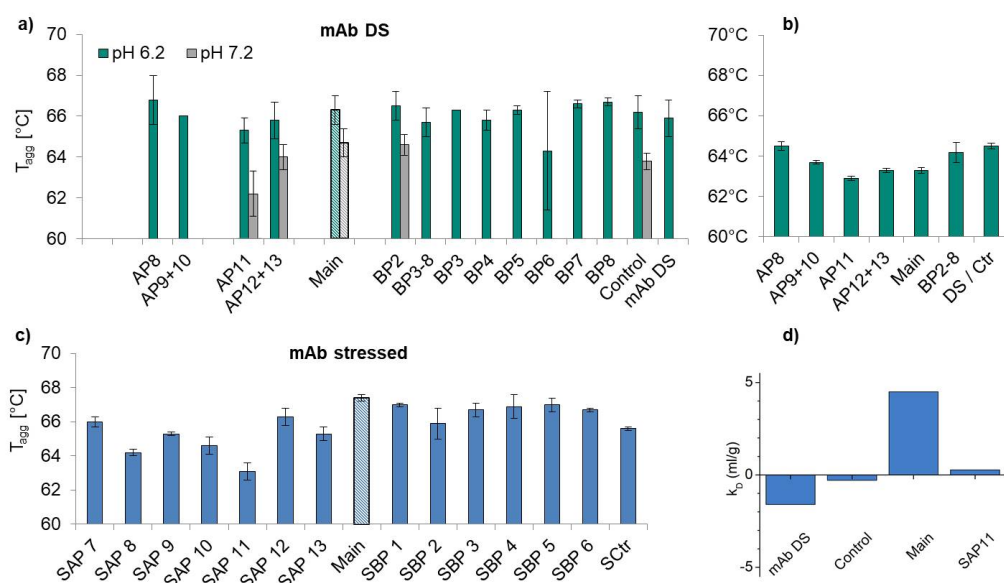


Figure 2.3: T_{agg} onset temperatures of charge variants a): of mAb DS by DLS. b): of mAb DS by SLS. c): of mAb stored at 40 °C for 16 days by DLS. d): k_D of SAP11 in comparison to controls by DLS.

The self-interaction propensity of SAP11 was assessed with the help of the diffusion interaction parameter by DLS and compared to the naïve species

and controls. The k_D values were between -5 and +5 ml/g for all samples (Figure 2.3d). Lehermayr et al. described a linear correlation of k_D from DLS measurements and the second virial coefficient A_2 for mAbs in order to indicate colloidal stability [26]. Connolly et al. and Menzen et al. confirmed this correlation [27, 28]. According to the calculations of Menzen et al., a k_D of -6.29 ml/g is the inflection point, where the corresponding thermodynamic interaction parameter A_2^* changes from net attraction to net repulsion. Thus, all tested samples showed slightly repulsive forces. By implication, self-interaction of SAP11 was not the driving force for aggregate formation. This finding was consistent with the low amount of aggregates found in the SAP11 fraction. Examples in literature state, that colloidal stability is not always a predictor for aggregation propensity, especially if electrostatic interactions are low [29, 30]. This observation is another hint, that (S)AP11 may interact with other species in DS solution in order to form aggregates.

nDSF measurements were performed in order to further elucidate potential differences in the unfolding and aggregation behavior of the mAb charge species. In accordance to the light scattering results, AP11 and SAP11 showed a lower T_m onset as well, indicating an earlier unfolding (Figure 2.4a and b). Also scattering, due to the formation of aggregates, was observed at slightly lower temperatures compared to other species. To further investigate the conformational stability of mAb charge variants, a forced degradation study at 67 °C was set up with selected variants. AP11 was clearly the first variant to start unfolding during this isothermal measurement, indicating that a higher fraction of unfolded protein was present at the tested temperature (Figure 2.4c).

Overall, our results demonstrate that charge variation has an effect on the conformational stability. The measurements at higher temperatures confirmed a lower conformational stability of (S)AP11 compared to other samples. Upon unfolding of this variant, the hydrophobicity increases and leads to immediately following aggregation.

At room temperature, (S)AP11 is present as naïve, folded species. Under these conditions, it appears as if aggregation also occurs with other mAb

2. Identification of Monoclonal Antibody Variants Involved in 36 Aggregate Formation – Part 1: Charge Variants

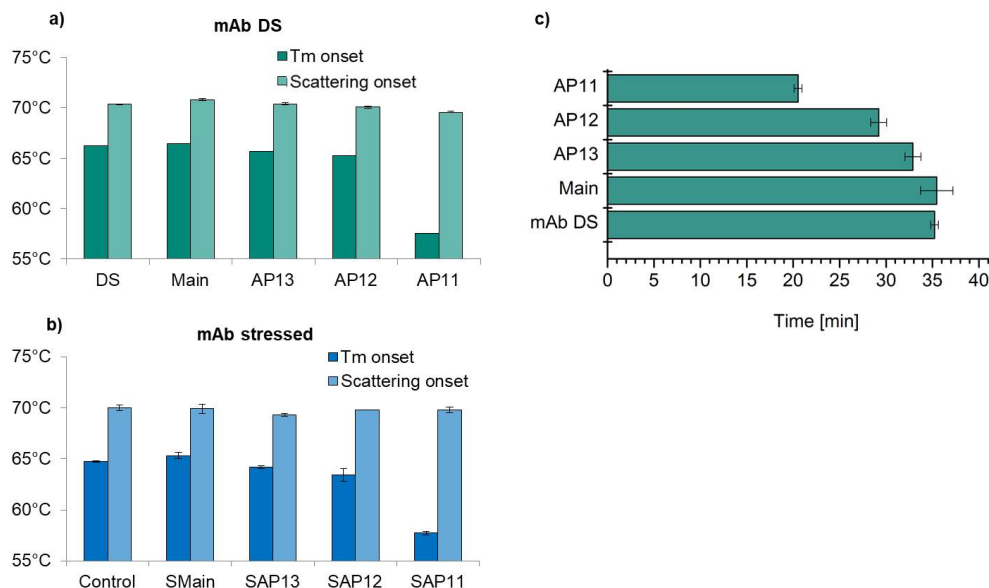


Figure 2.4: T_m onset and scattering onset of charge variants according to DSF from a) mAb DS, b) mAb stored at 40 °C for 16 days and c) time till onset of aggregation in forced degradation study at 67 °C with mAb DS.

variants. Thereby, the decreased stability of this acidic species may influence aggregate formation of the whole DS.

2.4.4 Modeling of Charge Variants

To gain a better understanding of the potentially aggregation prone species, we had a look on proposed hydrophobic patches of charge variants by molecular modeling with Schroedinger's BioLuminate. The open source sequence of the naïve mAb was changed according to alterations in the amino acid sequence of the Fab part based on LC-MS and peptide mapping data of the manufacturer. In their data AP12+13 were consolidated as one peak based on less high chromatographical resolution. The Fc part was neglected as it was not subject to alterations. According to mathematical prediction, the applied changes in the amino acid sequences did not cause different folding shapes of the charge variants. All structures were energetically stable. This calculation serves as a plausibility check of the inserted changes.

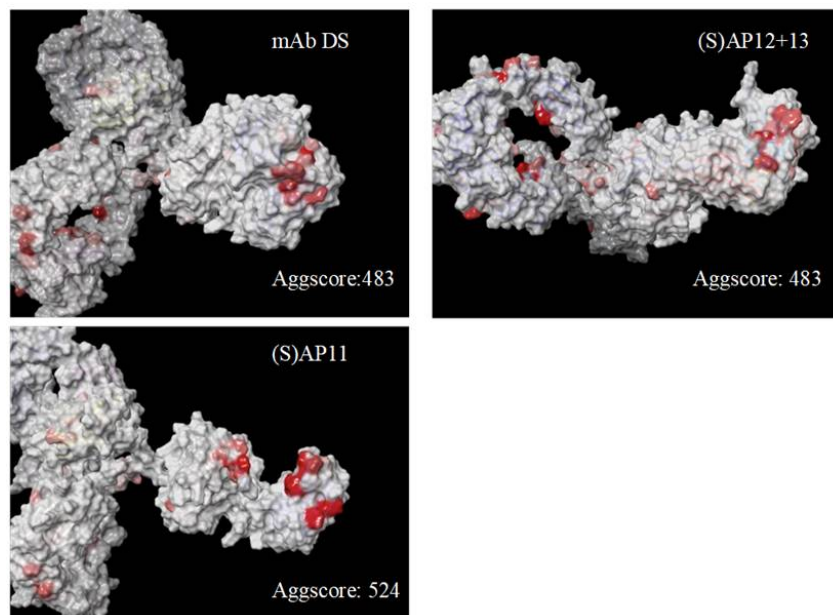


Figure 2.5: Hydrophobic patches (red) and additive aggregation score of naïve mAb (open source sequence) and two charge variants' Fab parts modeled with BioLuminate according to data of the manufacturer.

While the Aggscore of the naïve mAb and (S)AP12+13 were identical, we obtained an increased Aggscore of (S)AP11 due to more surface-exposed hydrophobic patches (Figure 2.5). These patches were caused by the clipping of amino acids and can act as structural hotspots for aggregation.

The interaction of hydrophobic patches leads to noncovalent aggregates [9]. Thereby, the increased surface hydrophobicity calculated by this model can explain the observed interaction of (S)AP11 in its native state with other species. In contrast attractive self-interaction of (S)AP11 at room temperature is not increased. This is potentially due to electrostatic repulsion, either due to the low concentration condition during k_D measurements or due to the effect of the Fc part, which is not considered in the Aggscore calculations. (S)AP12+13 and the naïve species, which behave similar in the stability indicating thermal methods also show similar Aggscore.

2.4.5 Forced stability study

The behavior of SAP11 and its impact on the DS were analyzed in a stability study at 45 °C for 12 weeks. This study was conducted with SAP11 alone and spiked in DS. Several control samples and SAP12 spiked in DS were used for comparison.

Over time, cloudiness and large particles formed. The visual appearance was ranked according to Figure 2.6. Charge variants followed the trend of the main species or the control samples.

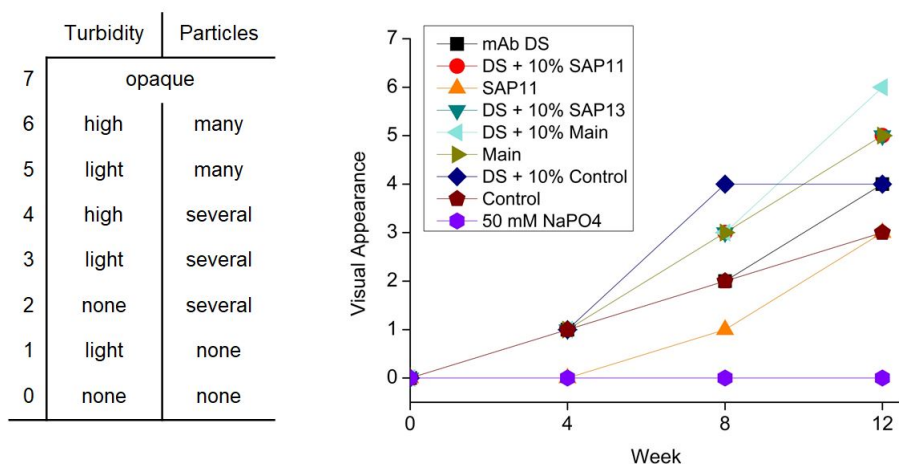


Figure 2.6: Visual appearance of mAb variants and spiked DS stressed at 45 °C for 12 weeks.

In order to underline the visual observations, a turbidity measurement of the charge variants was performed. An increase in turbidity was observed after 12-weeks. All samples behaved similar to the DS (Figure 2.7a). This data is in accordance with the visual appearance.

The conformational stability was determined fluorimetrically. The strongest increase in fluorescence over time was observed in pure SAP11 with a low fluorescence at T0 and a slightly higher value after 12 weeks, compared to other charge variants. At the time points 4 and 8 weeks, however, the fluorescence of SAP11 was comparable with other variants and DS.

SEC-MALS analysis was conducted to compare soluble aggregation and degradation of the variants. The loss of monomeric species in all charge

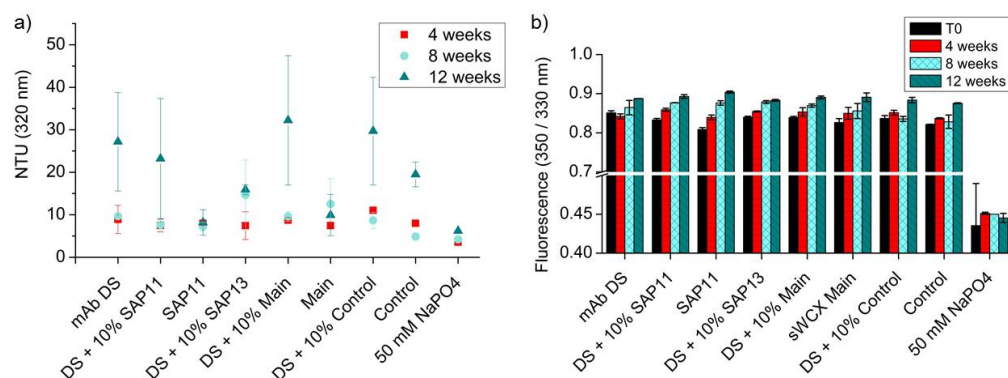


Figure 2.7: a) Turbidity at 320 nm compared to a nephelometric standard of mAb variants and spiked DS. b) Unfolding measured by fluorescence of charge variants stored at 45 °C for 12 weeks.

variants after 4 weeks was similar to that of the respective main species and controls. After 12 weeks, the monomer content decreased to an average of 85% in all samples (Figure 2.8a). The strongest loss in monomer content compared to T0 was found in SAP11. This was not due to soluble aggregate formation, but due to an increase in the amount of fragments. A fragment appearing as main peak shoulder with a size of 140 kDa was found in relatively high amounts of 3-4 % in all variants. SAP11 contained 5 % of this peak, most likely reflecting a hinge degradation product with full target binding functionality.

The content of HMWS of pure and spiked charge variant samples were below the content of the control at any time point (Figure 2.8b). According to their molecular weight, aggregates mainly consisted of dimers of intact monomer. After 12 weeks, also peaks of multimeric aggregates were detectable. No additional aggregates were formed by SAP11 or by spiking it into DS. Therefore, our hypothesis of reversible aggregate formation of SAP11 with itself or with other species was not confirmed.

Sub-visible particles were analyzed to characterize the insoluble aggregate content in the mAb charge variants and spiked DS in number and size. A strong increase in total number of particles was observed after 8 and 12 weeks (Figure 2.9a). This was mainly due to particles smaller than 2 μm . The monomer yield in SEC remained constant at these time points, indicating

2. Identification of Monoclonal Antibody Variants Involved in Aggregate Formation – Part 1: Charge Variants

40

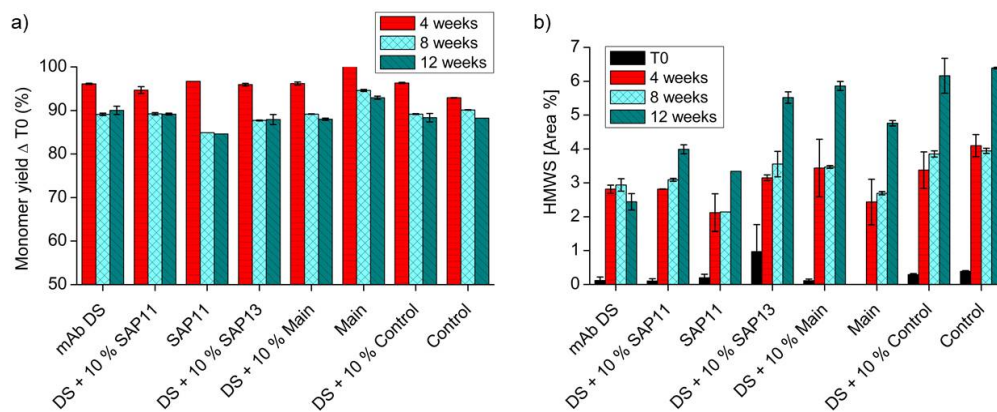


Figure 2.8: SEC-MALS data of mAb charge variants and spiked DS stored at 45 °C for 12 weeks of a) monomer yield compared to T0 b) amount of HMWS per time point.

agglomeration of soluble aggregates toward above the solubility limit, leading to the higher number of particles found in FlowCam measurements. Particles of $\geq 25 \mu\text{m}$ decreased in number between 8 weeks and 12 weeks (Figure 2.9e). This can be explained by a conglomeration to bigger particles, which were found as visible particles and increased turbidity after 12 weeks.

Overall, the investigated variants showed similar aggregation behavior. Under the applied conditions, SAP11 did show enhanced aggregate formation and did not induce aggregate formation with other species in the DS. Despite its aggregation propensity, it poses limited risk to the overall DS stability. Other stress conditions or a long term stability study at 4 °C - 6 °C might provide more pronounced differences in aggregation behavior. Nevertheless, the results of this stability study present a general assessment of the acidic charge species at being not critical in terms of product stability.

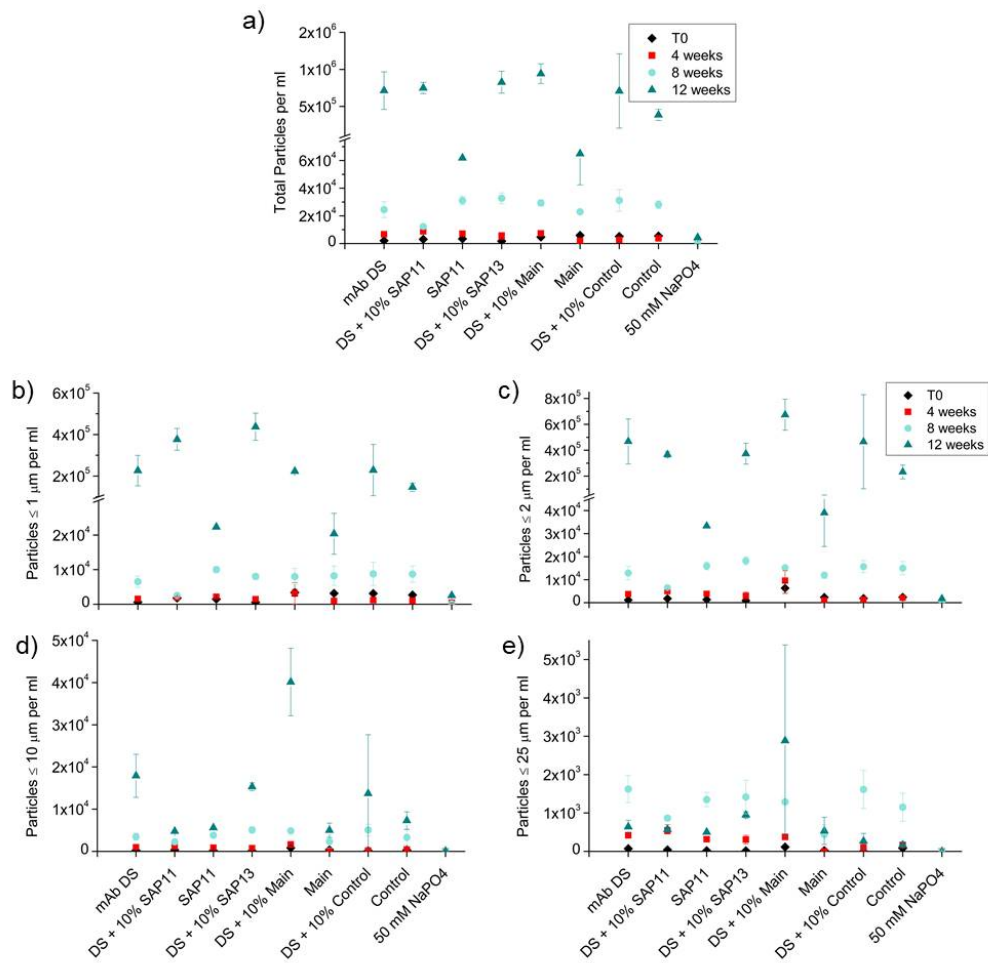


Figure 2.9: Number of particles in mAb variants and spiked DS samples stressed at 45 °C for 12 weeks a) accumulated numbers, b) particles $\geq 1 \mu\text{m}$, c) $\geq 2 \mu\text{m}$, d) $\geq 10 \mu\text{m}$, e) $\geq 25 \mu\text{m}$.

2.5 Conclusion and Outlook

In this study we could show, that aggregate formation in antibody formulations can specifically involve aggregation prone charge variants. For our model mAb, results suggested preferred aggregation of at least one prominent acidic variant with decreased conformational stability in thermal studies. At elevated temperatures this species aggregated due to interaction with unfolded species. In modeling of the native state, the acidic variant showed pronounced hydrophobicity, which increases aggregation propensity also with other species. The aggregates formed eluted as basic species in CEX and appeared to be at least in part reversible.

Results obtained during our research led us to the hypothesis of partially reversible aggregation. This pathway has to be confirmed in further investigations. Furthermore, the overall impact of the less stable, potentially aggregation prone acidic species on the whole drug substance has to be determined.

The applied thermal assays are commonly used tools to predict long term stability of proteins [28, 31]. We also conducted a stability study with the most prominent charge variants, to find out, if the different behavior of the acidic species has a general impact on product formulations. Thereby we were able to demonstrate a risk assessment of suspicious mAb charge variants with no safety issues. Under the applied conditions, none of the three investigated charge variants showed higher aggregation propensity in mAb DS. The aggregation behavior and the types of aggregates formed were similar in all samples.

For this mAb and under the applied conditions, the identified aggregation prone variant did not influence the overall DS stability. This statement can not be generalized and depends on conditions and molecule. Therefore, future work has to repeat this type of study with other therapeutic proteins. For deeper understanding, also other variants need to be separated, e.g. regarding hydrophobicity, and analogously analyzed in order to find aggregation prone species. In addition a chemical denaturation study would be beneficial to determine aggregation pathways [32]. The additional character-

ization data gained could lead to a deeper understanding of the therapeutic protein.

The knowledge about aggregation processes taking place in biopharmaceutical product is crucial to both, the manufacturer and regulatory authorities, and this work presents a first step in this direction. While common pharmaceutical monoclonal antibodies are typically stable for 2-3 years if stored refrigerated, deeper understanding of product related variants like charge variants and their removal during downstream processing might allow to enable long-term storage at elevated temperature. Alternatively, the formation of unstable variants could be prevented by appropriate stabilization measures. For more complex and less stable biopharmaceuticals such approaches could enable an increase of the shelf life.

Acknowledgments

The authors would like to thank Anna Sawadzka-Nowicka, Dr. Alfred Welzel and Dr. Stephan Böhm from Sandoz Biopharmaceutics for their valued advice. Thanks also belong to Isabel Koch for support during method development as well as to Tra Dao and Saskia Weißenhorn. Special gratitude to Jonas Binder for protein modeling.

Bibliography

- [1] M. C. Manning, D. K. Chou, B. M. Murphy, R. W. Payne, and D. S. Katayama, “Stability of protein pharmaceuticals: An update,” *Pharm. Res.*, vol. 27, no. 4, pp. 544–575, 2010.
- [2] S. Hermeling, D. J. Crommelin, H. Schellekens, and W. Jiskoot, “Structure-immunogenicity relationships of therapeutic proteins,” pp. 897–903, 2004.
- [3] Y. Yan, H. Wei, Y. Fu, S. Jusuf, M. Zeng, R. Ludwig, S. R. Krystek, G. Chen, L. Tao, and T. K. Das, “Isomerization and Oxidation in the Complementarity-Determining Regions of a Monoclonal Antibody: A Study of the Modification-Structure-Function Correlations by Hydrogen-Deuterium Exchange Mass Spectrometry,” *Anal. Chem.*, vol. 88, no. 4, pp. 2041–2050, 2016.
- [4] M. G. Dehling, “Conformational analysis of proteins of biopharmaceutical interest,” Ph.D. dissertation, Technische Universität München, 2018.
- [5] M. Cholewinski, B. Lueckel, and H. Horn, “Degradation pathways, analytical characterization and formulation strategies of a peptide and a protein. Calcitonine and human growth hormone in comparison,” *Pharm. Acta Helv.*, vol. 71, no. 6, pp. 405–419, 1996.
- [6] Y. Du, A. Walsh, R. Ehrick, W. Xu, K. May, and H. Liu, “Chromatographic analysis of the acidic and basic species of recombinant monoclonal antibodies,” *MAbs*, vol. 4, no. 5, pp. 578–585, 2012.
- [7] K. Ahrer and A. Jungbauer, “Chromatographic and electrophoretic characterization of protein variants,” *J. Chromatogr. B Anal. Technol. Biomed. Life Sci.*, vol. 841, no. 1-2, pp. 110–122, 2006.
- [8] S. Yadav, T. M. Laue, D. S. Kalonia, S. N. Singh, and S. J. Shire, “The influence of charge distribution on self-association and viscosity behavior of monoclonal antibody solutions,” *Mol. Pharm.*, vol. 9, no. 4, pp. 791–802, 2012.

- [9] H.-C. Mahler, W. Friess, U. Grauschopf, and S. Kiese, "Protein aggregation: pathways, induction factors and analysis." *J. Pharm. Sci.*, vol. 98, no. 9, pp. 2909–34, 2009.
- [10] D. Roberts, R. Keeling, M. Tracka, C. F. Van Der Walle, S. Uddin, J. Warwicker, and R. Curtis, "The role of electrostatics in protein-protein interactions of a monoclonal antibody," *Mol. Pharm.*, vol. 11, no. 7, pp. 2475–2489, 2014.
- [11] E. Sahin, A. O. Grillo, M. D. Perkins, and C. J. Roberts, "Comparative effects of pH and ionic strength on protein-protein interactions, unfolding, and aggregation for IgG1 antibodies," *J. Pharm. Sci.*, vol. 99, no. 12, pp. 4830–4848, 2010.
- [12] S. N. Olsen, K. B. Andersen, T. W. Randolph, J. F. Carpenter, and P. Westh, "Role of electrostatic repulsion on colloidal stability of *Bacillus halmapalus* alpha-amylase," *Biochim. Biophys. Acta - Proteins Proteomics*, vol. 1794, no. 7, pp. 1058–1065, 2009.
- [13] E. Y. Chi, S. Krishnan, T. W. Randolph, and J. F. Carpenter, "Physical stability of proteins in aqueous solution: Mechanism and driving forces in nonnative protein aggregation," pp. 1325–1336, 2003.
- [14] J. Den Engelsman, P. Garidel, R. Smulders, H. Koll, B. Smith, S. Basarab, A. Seidl, O. Hainzl, and W. Jiskoot, "Strategies for the assessment of protein aggregates in pharmaceutical biotech product development," *Pharm. Res.*, vol. 28, no. 4, pp. 920–933, 2011.
- [15] B. Hintersteiner, N. Lingg, E. Janzek, O. Mutschlechner, H. Loibner, and A. Jungbauer, "Microheterogeneity of therapeutic monoclonal antibodies is governed by changes in the surface charge of the protein," *Biotechnol. J.*, vol. 11, no. 12, pp. 1617–1627, 2016.
- [16] Y. Y. Zhao, N. Wang, W. H. Liu, W. J. Tao, L. L. Liu, and Z. D. Shen, "Charge Variants of an Avastin Biosimilar Isolation, Characterization, In Vitro Properties and Pharmacokinetics in Rat," *PLoS One*, vol. 11, no. 3, p. e0151874, 2016.

- [17] L. A. Khawli, S. Goswami, R. Hutchinson, Z. W. Kwong, J. Yang, X. Wang, Z. Yao, A. Sreedhara, T. Cano, D. Tesar, I. Nijem, D. E. Allison, P. Y. Wong, Y. H. Kao, C. Quan, A. Joshi, R. J. Harris, and P. Motchnik, “Charge variants in IgG1: Isolation, characterization, in vitro binding properties and pharmacokinetics in rats,” *MAbs*, vol. 2, no. 6, pp. 613–624, 2010.
- [18] S. V. Sule, J. E. Fernandez, V. J. Mecozzi, Y. Kravets, W. C. Yang, P. Feng, S. Liu, L. Zang, A. D. Capili, T. B. Estey, and K. Gupta, “Assessing the Impact of Charge Variants on Stability and Viscosity of a High Concentration Antibody Formulation,” *J. Pharm. Sci.*, vol. 106, no. 12, pp. 3507–3514, 2017.
- [19] S. Fekete, A. Beck, and D. Guillarme, “Characterization of cation exchanger stationary phases applied for the separations of therapeutic monoclonal antibodies,” *J. Pharm. Biomed. Anal.*, vol. 111, pp. 169–176, 2015.
- [20] G. Ponniah, A. Kita, C. Nowak, A. Neill, Y. Kori, S. Rajendran, and H. Liu, “Characterization of the Acidic Species of a Monoclonal Antibody Using Weak Cation Exchange Chromatography and LC-MS,” *Anal. Chem.*, vol. 87, no. 17, pp. 9084–9092, sep 2015.
- [21] J. Rubin, L. Linden, W. M. Coco, A. S. Bommarius, and S. H. Behrens, “Salt-induced aggregation of a monoclonal human immunoglobulin G1,” *J. Pharm. Sci.*, vol. 102, no. 2, pp. 377–386, 2013.
- [22] K. Sankar, S. R. Krystek, S. M. Carl, T. Day, and J. K. Maier, “AggScore: Prediction of aggregation-prone regions in proteins based on the distribution of surface patches,” *Proteins Struct. Funct. Bioinforma.*, vol. 86, no. 11, pp. 1147–1156, nov 2018.
- [23] Y. Yigzaw, P. Hinckley, A. Hewig, and G. Vedantham, “Ion Exchange Chromatography of Proteins and Clearance of Aggregates,” *Curr. Pharm. Biotechnol.*, vol. 10, no. 4, pp. 421–426, 2009.

- [24] S. Gandhi, D. Ren, G. Xiao, P. Bondarenko, C. Sloey, M. S. Ricci, and S. Krishnan, “Elucidation of degradants in acidic peak of cation exchange chromatography in an IgG1 monoclonal antibody formed on long-term storage in a liquid formulation,” *Pharm. Res.*, vol. 29, no. 1, pp. 209–224, 2012.
- [25] Q. Luo, M. K. Joubert, R. Stevenson, R. R. Ketchem, L. O. Narhi, and J. Wypych, “Chemical modifications in therapeutic protein aggregates generated under different stress conditions,” *J. Biol. Chem.*, vol. 286, no. 28, pp. 25 134–25 144, 2011.
- [26] C. Lehermayr, H. C. Mahler, K. Mäder, and S. Fischer, “Assessment of net charge and protein-protein interactions of different monoclonal antibodies,” *J. Pharm. Sci.*, vol. 100, no. 7, pp. 2551–2562, 2011.
- [27] B. D. Connolly, C. Petry, S. Yadav, B. Demeule, N. Ciaccio, J. M. Moore, S. J. Shire, and Y. R. Gokarn, “Weak interactions govern the viscosity of concentrated antibody solutions: High-throughput analysis using the diffusion interaction parameter,” *Biophys. J.*, vol. 103, no. 1, pp. 69–78, 2012.
- [28] T. A. Menzen, “Temperature-Induced Unfolding, Aggregation, and Interaction of Therapeutic Monoclonal Antibodies,” Dissertation, University of Munich, 2014.
- [29] J. I. Austerberry, R. Dajani, S. Panova, D. Roberts, A. P. Golovanov, A. Pluen, C. F. van der Walle, S. Uddin, J. Warwicker, J. P. Derrick, and R. Curtis, “The effect of charge mutations on the stability and aggregation of a human single chain Fv fragment,” *Eur. J. Pharm. Biopharm.*, vol. 115, no. February, pp. 18–30, 2017.
- [30] H. Bajaj, V. K. Sharma, A. Badkar, D. Zeng, S. Nema, and D. S. Kalonia, “Protein structural conformation and not second virial coefficient relates to long-term irreversible aggregation of a monoclonal antibody and ovalbumin in solution,” *Pharm. Res.*, vol. 23, no. 6, pp. 1382–1394, 2006.

- [31] D. S. Goldberg, S. M. Bishop, A. U. Shah, and H. A. Sathish, “Formulation development of therapeutic monoclonal antibodies using high-throughput fluorescence and static light scattering techniques: Role of conformational and colloidal stability,” *J. Pharm. Sci.*, vol. 100, no. 4, pp. 1306–1315, 2011.
- [32] H. Svilenov, U. Markoja, and G. Winter, “Isothermal chemical denaturation as a complementary tool to overcome limitations of thermal differential scanning fluorimetry in predicting physical stability of protein formulations,” *Eur. J. Pharm. Biopharm.*, vol. 125, pp. 106–113, 2018.

Chapter 3

Identification of Monoclonal Antibody Variants Involved in Aggregate Formation – Part 2: Hydrophobicity Variants

The following chapter was published in the European Journal of Pharmaceutics and Biopharmaceutics 2021, Vol. 160.

Authors

Robina M. Meyer ¹, Lukas Berger ², Joerg Nerkamp ², Stefan Scheler ², Sebastian Nehring ², Wolfgang Friess ¹

¹: Ludwig-Maximilians University Munich, Germany

²: Sandoz Biopharmaceuticals, Langkampfen, Austria

Keywords

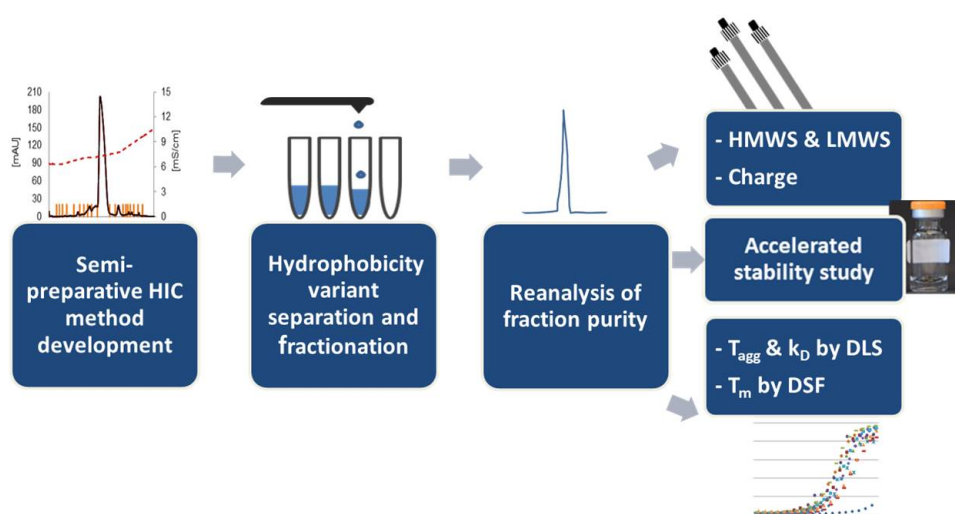
mAb hydrophobicity variants; protein aggregation; protein stability; semi-preparative HIC

3.1 Abstract

Monoclonal antibodies (mAbs) are valuable tools both in therapy and in diagnostic. Their tendency to aggregate is a serious concern. Since a mAb drug substance (DS) is composed of different variants, it is important for manufacturers to know the behavior and stability not only of the mAb as a whole, but also of the variants contained in the product.

We present a method to separate hydrophobicity variants of a mAb and subsequently analyzed these variants for stability and aggregation propensity. We identified a potentially aggregation prone hydrophilic variant which is interrelated with another previously identified aggregation prone acidic charge variant. Additionally, we assessed the risk posed by the aggregation prone variant to the DS by spiking hydrophobicity variants into DS and did not observe an enhanced aggregation propensity. Thus we present an approach to separate, characterize and analyze the criticality of aggregation prone variants in protein DS which is a step forward to further assure drug safety.

Graphical Abstract



3.2 Introduction

Hydrophobicity is defined as the repulsion between a non-polar compound and a polar environment such as water. In proteins, hydrophobic interactions of non-polar amino acids, such as phenylalanine, tryptophan or valine, play a dominant role in protein folding and structure stabilization by building an internal core [1]. The occurrence and variation of non-polar amino acids on the protein surface are characteristic for each protein [2]. The variation in hydrophobicity enables the separation of proteins based on these characteristics by hydrophobic interaction chromatography (HIC) [3, 4].

For the investigation of hydrophobicity variants, HIC was found to be an advantageous method as it maintains the structural properties of the protein due to the involvement of only weak binding interactions and the use of a predominantly polar mobile phase. [5]. In comparison, the orthogonal method of reversed phase chromatography (RPC) requires denaturing conditions, like the use of non-polar solvents, to elute the protein from the strong binding stationary phase of the column. Nevertheless, also HIC elution can involve small amounts (5-10 %) of water soluble organic solvents like acetonitrile or isopropanol in analytic scale [6] or propylene or ethylene glycol in preparative scale [7] to compete with the hydrophobic protein patterns for binding to the stationary phase and enhance elution. In either case, the ideal chromatographic conditions have to be developed individually for every protein.

Besides for purification purposes, fractionation of hydrophobicity variants of mAbs in literature is focused on the investigation of post-translational modification and degradation, including modifications like oxidized amino acids [8, 9, 10, 11], C-terminal heterogeneity [12] and deamidation [13]. Some of these publications additionally investigated the impact of these modifications in antigen binding.

These and any other modifications need to be considered with respect to aggregation propensity of the molecules. Especially a altered hydrophobicity of amino acids can favor aggregation by intermolecular interactions of hydrophobic patches on the protein surfaces. [14]. Aggregates pose a serious

3. Identification of Monoclonal Antibody Variants Involved in 52 Aggregate Formation – Part 2: Hydrophobicity Variants

quality and safety risk [15]. Thus, it is important to analyze the stability of the different protein variants, like hydrophobicity variants, ideally at an early stage of development.

In order to address this challenge, we developed a semi-preparative method for the separation of hydrophobicity variants of a mAb drug substance (DS). Several elution enhancers were tested to achieve elution while maintaining the structure of the mAb variants. Ultimately, a method was developed that enables fractionation of single hydrophobicity variants with high purity. We characterized every variant regarding size, thermal stability and self-interaction. Multiple hydrophilic variants were involved in aggregate formation. One of these variants showed decreased stability and was correlated with a potentially aggregation prone acidic charge variant that was identified in an earlier study of our group. Finally, we evaluated the criticality of aggregation prone variants by spiking them into DS which was put on stability. Aggregation propensity of the whole DS was not increased by the addition of more aggregation prone variants.

Applying our approach either at an early or later stage in development enhances the knowledge of the therapeutic protein characteristics and would increase drug safety.

Our contributions are:

- the development of a HIC method using propylene glycol to separate and collect single hydrophobicity variants on a semi-preparative scale,
- the identification of at least one potentially aggregation prone hydrophilic variant of a mAb, and
- the demonstration of correlation of this variant with an acidic charge variant previously described as potentially prone for aggregation.
- the risk assessment of hydrophobicity variants on DS stability in an accelerated stability study.

3.3 Materials and Methods

3.3.1 mAb Model Protein

The IgG1 model monoclonal antibody (mAb) was provided by Sandoz Biopharmaceuticals, Schaffhausen, Austria. It was produced in CHO cells and 55 mg/ml of the drug substance were formulated in a 50 mM sodium phosphate buffer at pH 6.2. The mAb had an extinction coefficient of $1.7 \text{ ml g}^{-1} \text{ cm}^{-1}$ at 280 nm and a isoelectric point at 8.2.

3.3.2 Separation of Hydrophobicity Variants

HIC method development and fractionation of variants was performed with a GE ÄKTA purifier FPLC system (GE Healthcare, Uppsala, Sweden) and a $4.6 \times 250 \text{ mm}$ ProPac HIC-10 column (Thermo Scientific). Method development involved potential elution enhancers L-arginine (Sigma Aldrich, Darmstadt, Germany), glycerol (Grüssing, Filsum, Germany), polyethylene glycol 6000 (PEG; Serva, Heidelberg, Germany), propylene glycol (PG; BASF, Ludwigshafen, Germany) and acetonitrile (ACN; Carl Roth, Karlsruhe, Germany). 5 % v/v of the respective elution enhancer were added to both equilibration solution (1 M ammonium acetate pH 6.2) and elution solution (0.1 M ammonium acetate pH 6.2). After injection of 13 mg/ml mAb at a flow rate of 0.7 ml/min, a linear gradient was applied and chromatograms were compared in Unicorn 5.31 Software (GE Healthcare).

The method development resulted in the following procedure for collection of hydrophobicity variants. mAb dilution of 13 mg/ml in equilibration solution (1 M ammonium acetate pH 6.2 containing 6 % propylene glycol as elution enhancer) was injected with a flow rate of 0.7 ml/min. Hydrophobicity variants were eluted with a step wise gradient from 0 to 100 % 0.1 M ammonium acetate pH 6.2, 6 % propylene glycol and fractions of 0.75 ml volume were collected in 15 ml polypropylene (PP) tubes by a Frac-920 fraction collector (GE Healthcare). Method programming and analysis were done with Unicorn 5.31 Software. The fractions of single variants from several separation cycles were pooled in order to collect sufficient volume of analyz-

able material. As control sample, all fractions collected were reunited and the same subsequent processes were applied to ensure the validity of our process. Fractions and control were concentrated in VivaSpin 20 centrifugation filter units with 30,000 Da MWCO (Sartorius Stedim Biotech, Göttingen, Germany). Prior to further analysis, the buffer was exchanged to 10 mM sodium phosphate pH 6.2. A Nanodrop 2000 photometer (Thermo Scientific, Wilmington, Delaware, USA) was used to determine the final concentrations via the extinction coefficient.

3.3.3 Analytical Hydrophobic Interaction Chromatography (HIC)

Analytical HIC was performed in accordance with the separation method to analyze the purity of each pooled hydrophobicity variant. An Agilent 1200 series HPLC system (Agilent Technologies, Santa Clara, California, USA) equipped with a 4.6×250 mm ProPac HIC-10 column (Thermo Scientific) was employed. The column was equilibrated with 1 M ammonium acetate pH 6.2 and 6 % propylene glycol. 30 μg of sample (diluted in equilibration solution) were injected at a flow rate of 0.7 ml/min and hydrophobicity variants were eluted in a step wise gradient to 100 % of elution solution 0.1 M ammonium acetate pH 6.2, 6 % propylene glycol. UV absorption at 280 nm was detected and chromatograms were analyzed with ChemStation[®]B.02.01-SR2 (Agilent Technologies) regarding retention time and area under the curve (AUC). For correction of each injection, a chromatogram of a buffer injection was subtracted.

3.3.4 Size Exclusion Chromatography (SEC)

HP-SEC was run on an Agilent 1200 series HPLC system (Agilent Technologies) equipped with a Tosoh TSKgel[®]G3000SWXL column (7.8×300 mm, Tosoh Bioscience, Stuttgart, Germany). 30 μg per sample were injected onto the column using a mobile phase of 25 mM sodium phosphate pH 6.2 with 125 mM sodium chloride at a flow rate of 0.5 ml/min. In addition, 10 μl

of a gel filtration standard (BioRad Laboratories, Hercules, CA, USA) were injected. Chromatograms were analyzed with ChemStation software version B.02.01-SR2 (Agilent Technologies) regarding retention time and AUC after UV detection at 280 nm and a buffer injection signal was subtracted as blank. Standard deviations of triplicates are depicted in error bars.

3.3.5 Ion Exchange Chromatography (IEX)

Hydrophobicity variants and controls were analyzed by high-performance cation exchange chromatography with a 3×250 mm ProPac WCX-10 column (Thermo Scientific) connected to an Agilent 1200 HPLC system (Agilent Technologies). All samples were diluted in equilibration buffer (25 mM sodium phosphate buffer pH 6.2) and $30 \mu\text{g}$ of each sample were injected onto the column with a flow rate of 1 ml/min. Elution was done by a step wise salt gradient from zero to 125 mM sodium chloride and a pH gradient from pH 6.20 to pH 6.39. The eluted samples were detected by UV absorption at 280 nm and chromatograms were corrected and processed as described above.

3.3.6 Dynamic Light Scattering (DLS)

DLS analysis was conducted with a DynaPro Plate Reader II (Wyatt Technologies, Dernbach, Germany). Samples and dilution buffer (10 mM sodium phosphate pH 6.2) were filtered with a $0.2 \mu\text{m}$ regenerated cellulose filter (Sartorius, Göttingen, Germany) prior to dilution. After dilution, each sample was centrifuged at $8\,944 \times g$ for 10 min to remove any insoluble particles and the supernatant was used for analysis. $5.5 \mu\text{l}$ per sample were transferred into 1536-well-plates (Aurora, Whitefish, MT, USA) in triplicates. At 2000 rpm the plate was centrifuged for two minutes in order to remove trapped air from the plate bottom. All wells containing samples were sealed with a drop of silicone oil and once more centrifuged at $447 \times g$ for one minute. Aggregation onset temperatures ($T_{\text{agg onset}}$) were measured with a temperature ramp from $25 \text{ }^\circ\text{C}$ to $70 \text{ }^\circ\text{C}$ and at $0.143 \text{ }^\circ\text{C}/\text{min}$ and a concentration of 1.5 mg/ml. Diffusion interaction parameters (k_{D}) were determined by the analysis of dif-

3. Identification of Monoclonal Antibody Variants Involved in 56 Aggregate Formation – Part 2: Hydrophobicity Variants

fusion coefficients (D) at 25 °C of six protein concentrations between 1 mg/ml and 4 mg/ml. Five acquisitions and an acquisition time of 5s were applied for each well. The instrument was controlled and data was acquired with Dynamics 7.6 software (Wyatt Technologies). The standard deviation (SD) of triplicates was depicted in error bars. The diffusion interaction parameter was calculated as linear fit of D and the protein concentration to obtain the diffusion coefficient at infinite dilution (D_0). After the normalization of D by D_0 , the slope of the linear fit corresponds to the interaction parameter k_D [16]. Assumptions on self-interaction were based on a linear correlation of k_D and the second osmotic virial coefficient A_2 [17]. A k_D of -6.29 ml/g is the point of sign reversal, where the corresponding thermodynamic interaction parameter A_2^* changes from net attraction to net repulsion [18].

3.3.7 Differential Scanning Fluorimetry (nanoDSF)

Thermal unfolding was analyzed as the increase of intrinsic fluorescence intensity. Triplicates of each sample were filled in standard nanoDSF™ grade capillaries. Samples were excited at 280 nm and fluorescence was detected at 330 and 350 nm. The ratio of 350 / 330 nm was used for data analysis. Measurements were performed with the Prometheus NT.48 (NanoTemper Technologies, Munich, Germany). Standard deviations were depicted in error bars. The temperature was ramped at 1 °C/min from 25 to 80 °C. Aggregation was detected in terms of reflection intensity referred to as scattering.

Protein melting temperatures (T_m) were determined from the maximum of the first derivative of the thermal unfolding curve with the software PR. ThermControl V2.1 (NanoTemper).

Forced degradation studies were performed at isothermal 67 °C for 12 h. For analysis, the scattering onset in dependence on time was determined with the PR.TimeControl software V1.0.2 (NanoTemper Technologies, Munich, Germany).

An accelerated stability study was set up with triplicates of hydrophobicity variants in sealed high sensitivity grade nanoDSF capillaries. The

capillaries were stored at 45 °C for a time range of 5 months and removed for isothermal measurement at 25 °C weekly or every second week . Fluorescence signals were analyzed with the PR.ThermControl software V2.1 (NanoTemper) and plotted against time.

3.3.8 Accelerated Stability Study and Spiking Procedures

The hydrophobicity variants, control (Ctr), buffer and DS were sterile filtered with a 0.22 μm polyethersulfone filter (VWR International, Radnor, PA). Sample duplicates were diluted with buffer to a concentration of 1.5 mg/ml and filled into pre-sterilized DIN2R glass type I vials (MGlass AG, Germany). Hydrophobicity variants were added to sterile and filtrated DS formulation to a concentration of 10 % (v/v) to obtain spiked samples of 1.5 mg/ml. The vials with a total fill volume of 0.5 ml were crimped with rubber stoppers (West Pharmaceutical Services, USA) and stored at 45 °C until the time point of analysis.

3.3.9 Visual Inspection

The presence of visible particles was assessed in accordance with Ph.Eur. chapter 2.9.20. Each vial was gently swirled and examined for at least 5 s in front of a white plate as well as in front of a black plate. The observation of particles and turbidity was recorded.

3.3.10 Ultraviolet Absorption Spectroscopy at 320nm

Turbidity measurements were performed with an Agilent 8453 UV-Vis Spectrophotometer (Agilent Technologies, Santa Clara, California, USA) and a Quartz SUPRASIL® Type ultramicro cuvette (Hellma Analytics, Müllheim, Germany) with a path length of 10 mm. 70 μl of sample were analyzed at 320 nm wavelength. TURB 4000 NTU Formazin (Sigma-Aldrich) was used as nephelometric standard in seven dilutions to calibrate the spectropho-

tometer. The results are presented in nephelometric turbidity units (NTU), correspondingly. Error bars show the standard deviation (SD).

3.3.11 Fluorescence spectroscopy

Intrinsic fluorescence emission was measured with a FLUOstar Omega Star plate reader (BMG Labtech, Ortenberg, Germany). 35 μ l of each vial were filled in a 384-well plate (Corning Life Science, Tewksbury, MA, USA) with transparent flat bottom. The samples were excited at 280 nm and fluorescence intensity was detected as the ratio of fluorescence at 350 to 330 nm. Error bars indicate SD.

3.3.12 Subvisible Particle Counting

Subvisible particles were conducted with the FlowCam 8100 (Fluid Imaging Technologies, Scarborough, ME, USA). Protein samples were diluted 1:1 with formulation buffer. 150 μ l sample were analyzed with 10 \times magnification at 0.150 ml/min flow rate and 29 frames per second frame rate. A segmentation threshold of 13.0 for dark pixels and 10.0 for light pixels was applied. Highly purified water (HPW) was used to rinse the flow cell after each measurement. Sub-visible particles bigger than or equal to 1, 2, 10, and 25 μ m were evaluated with VisualSpreadsheet software Version 4.7.6 (Fluid Imaging Technologies) and are presented as counts per mL with SD.

3.3.13 Multi-Angle Light Scattering Coupled Size Exclusion Chromatography (SEC-MALS)

SEC-MALS measurements were performed with a Dionex UltiMate 3000 HPLC system (Thermo Fisher Scientific, CA, USA) coupled to an UltiMate 3000 VWD multiple wavelength detector (Thermo Fisher Scientific) and a DAWN HELEOS multiangle light scattering (MALS) detector (Wyatt Technology, Santa Barbara, USA). Sample elution was monitored at 280 nm. 30 μ g per sample were injected onto a Tosoh TSKgel G3000SWXL column (7.8 \times 300 mm, Tosoh Bioscience, Stuttgart, Germany). 25 mM sodium

phosphate pH 6.2 with 125 mM sodium chloride was used as mobile phase at a flow rate of 0.5 ml/min. Chromatograms were acquired and analyzed using the Chromeleon CDS Software Version 7.2.7.10369 (Thermo Scientific). A buffer injection signal was subtracted as blank. Error bars indicate standard deviations. MALS data collection and processing were performed using the ASTRA software, Version 7.1 (Wyatt Technology).

3.4 Results and Discussion

3.4.1 HIC Method Development

The first approach to screen for hydrophobicity variants of the mAb was a method involving acetonitrile as an elution enhancer (adapted from Valliere-Douglass et al. [9]). The chromatogram showed seven variants different from the main species (Figure 3.1). Despite of the already low amount of acetonitrile of 5 % in the mobile phase, the organic solvent may still negatively impact on protein structure and stability [19, 20]. In order to ensure reliable results in subsequent analyses, it is important to maintain the characteristics of the mAb hydrophobicity variants.

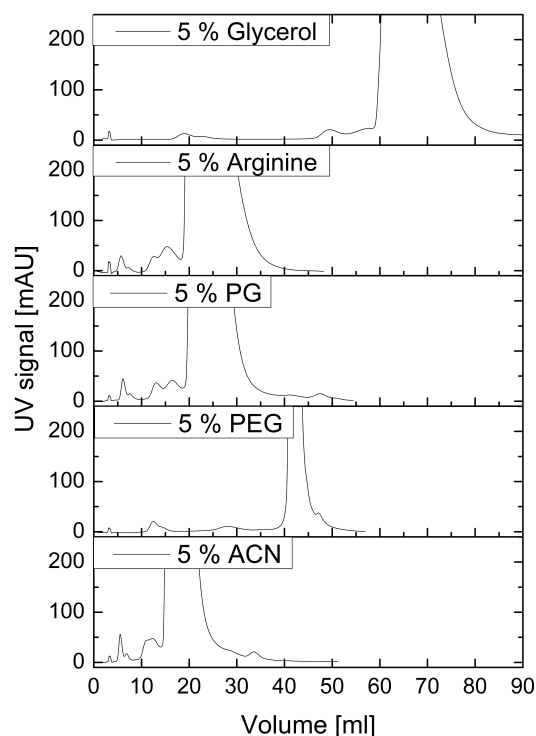


Figure 3.1: Chromatograms of semi-preparative HIC method development. Comparison of the elution enhancers glycerol, arginine, propylene glycol, polyethylene glycol and acetonitrile.

We consequently evaluated four additives described in literature with respect to their protein stabilizing effects and ability to competitively bind to hydrophobic surfaces on the column. Arginine [21, 22], glycerol [23] and polyethylene glycol (PEG) [24, 25] resolved less peaks than the reference HIC method with acetonitrile. Furthermore, the concentration of glycerol was too low as expressed in the late elution of the main species. An increase of glycerol to 8.5 % was expected to decrease the elution time. However, this concentration caused an unfavorable increase in viscosity of the mobile phase and, thereby, high back-pressure from the column. Unlike the other candidates, the use of propylene glycol [26, 27] resulted in the same amount of peaks as with acetonitrile and provided the best resolution of peaks (Figure 3.1). Thus, propylene glycol was chosen for hydrophobicity variant separation. The ideal content of propylene glycol for resolution was determined to be at 6 % v/v.

3.4.2 mAb Hydrophobicity Variant Separation and Fractionation

The semi-preparative HIC chromatogram yielded four hydrophilic variants (H+) and three hydrophobic variants (H-)(Figure 3.2). During elution, the conductivity gradient was adjusted in several steps to reduce the merging of peaks, but not all variants could be baseline separated from each other.

Reanalysis of the collected and concentrated fractions by analytical chromatography confirmed high purity of most of the fractionated variants, except for the hydrophobic variant H-3, which appeared to consist predominantly of main species (Table 4.1). In addition, the total peak area of the H-3 sample was decreased by more than 50 % compared to other injections. This could indicate either that H-3 consists of aggregates that build up to insoluble variants during sample processing, or that it might be an artifact instead of a hydrophobicity variant.

The hydrophilic fraction H+4 contained high amounts of neighboring peaks, namely main species and H+3. This might be caused by redistribution of H+4 to the observed mixture, or by merging of the neighboring

3. Identification of Monoclonal Antibody Variants Involved in Aggregate Formation – Part 2: Hydrophobicity Variants

62

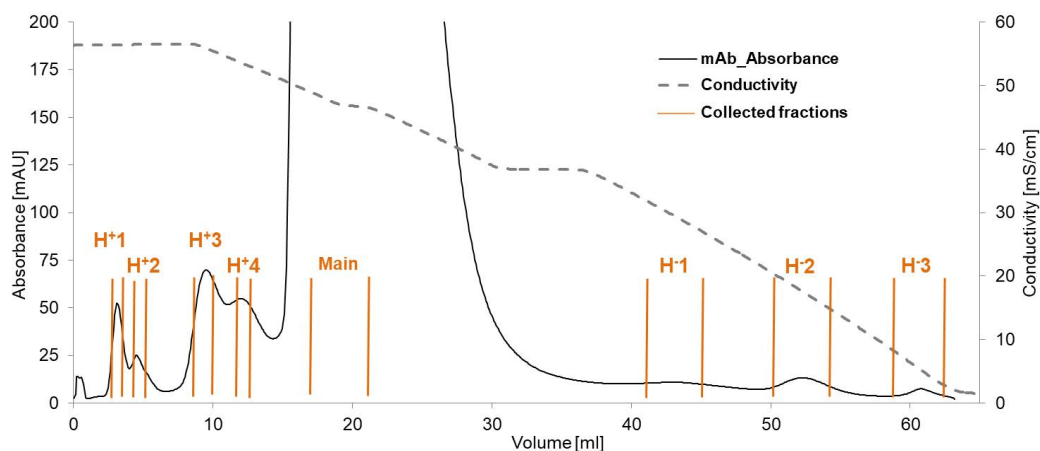


Figure 3.2: Semi-preparative HIC chromatogram of mAb hydrophobicity variant separation with 6 % of PG in mobile phases for equilibration and elution.

peaks into this fraction. We consider the latter cause to be more likely, as minor impurities of other variants were generally caused by the presence of neighboring peaks.

Thus, despite the generally low amounts of the hydrophobicity variants next to the main species, we were able to collect variant enriched fractions. The achieved concentrations were sufficient for subsequent analysis.

3.4.3 Aggregate and Degradation Product Content of the Fractions

SEC of the hydrophobicity variants showed high amounts of aggregates in hydrophilic variants (Figure 3.3). This was an interesting observation, since in HIC aggregates usually elute after monomeric and intact variants due to stronger interaction with the resin [28, 9]. This was the case in hydrophobic variant H-3. Here, size calculation with the help of a size standard revealed the presence of multimeric species. This result underlines the hypothesis of a substantial high molecular weight species content in H-3 leading to reduced recovery in the variant purity check described above.

Peak Name	Peak Area (%)	Purity (%)	Contains
H+1	0.5	87	9 % H+2
H+2	0.4	77	6 % Main 11 % H+1
H+3	1.7	84	6 % H+2 6 % H+4
H+4	1.4	39	30 % Main 29 % H+3
Main	94.6	97	
H-1	0.8	61	35 % Main
H-2	0.7	60	23 % Main 11 % H-1
H-3	0.2	1	72 % Main 8 % H-1
Control	100	n.d.	

Table 3.1: Area and purity of collected mAb hydrophobicity variants. n.d. = not determined.

In addition to 39 % of aggregates, H+2 also contained 48 % of fragments. The control, which underwent the same sample processing steps as all variants, contained 99 % monomer, like the mAb DS. Thus, the sample processing did not lead to enhanced aggregation. Based on the protein size standard, the high molecular weight species in H+1 and H+2 predominantly consist of dimers. Although hydrophobic interactions play a key role in aggregation [29, 30], these results indicate an involvement of hydrophilic variants in aggregate formation.

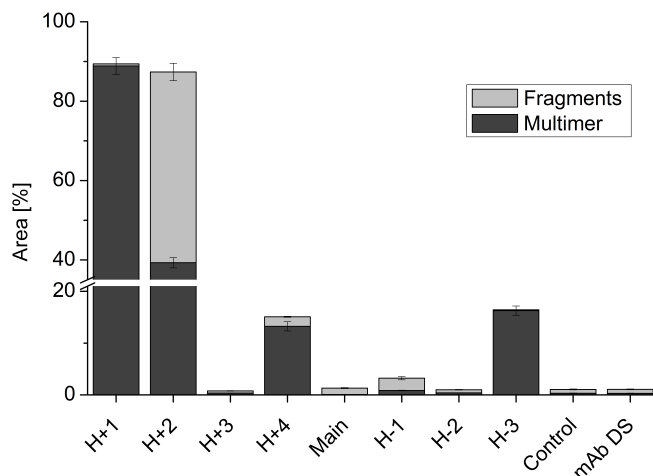


Figure 3.3: SEC results of separated mAb hydrophobicity variants.

3.4.4 Conformational Stability and Self-Interaction Propensity of mAb Hydrophobicity Variants

The thermal stability was assessed to compare unfolding and aggregation behavior of the variants. T_{agg} onset did not differ between the hydrophobicity variants except for hydrophilic variant H+3, which showed slightly decreased T_{agg} onset compared to the control and DS and a more pronounced decrease compared to main species (Figure 3.4a).

nanoDSF measurements were performed as orthogonal method to T_{agg} determination by DLS. The increase in fluorescence of H+3 at distinctly lower temperatures compared to all other variants indicated earlier unfolding of this variant (Figure 3.4b). Additionally, the increase in scattering due to the formation of aggregates was observed at slightly lower temperatures than in other fractions (Figure 3.4c). The aggregation onset temperature of H+3 determined by DSF was higher compared to DLS, most likely due to different heating ramp rates. T_m of H+1, H+2 and H+4 did not differ from DS or the control. This observation might base on the increased amounts of aggregate found in the respective variants. The reduced monomer content could reduce the effect on T_m .

A forced degradation study at 67 °C was set up to further investigate the

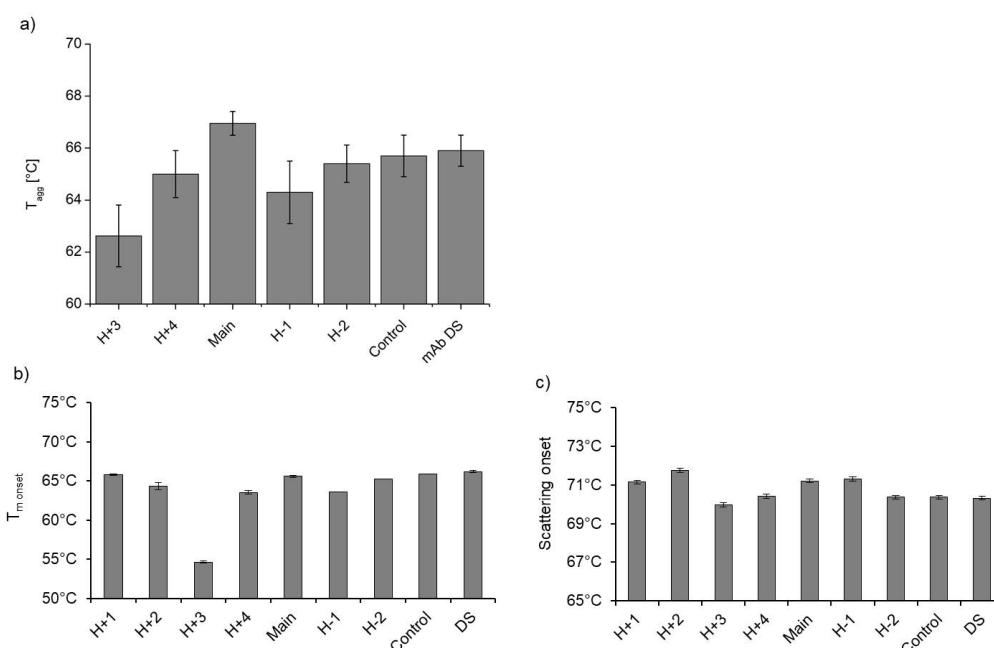


Figure 3.4: Thermal stability data including SD of mAb hydrophobicity variants with a) T_{agg} onset by DLS, b) T_m onset by DSF and c) T_{agg} onset temperature by DSF.

thermal stability of hydrophobicity variants. At the chosen temperature the variants may already be unfolded. However, despite of the potential structural destabilization, we were not able to see aggregate formation in terms of scattering at 65 °C within 12 hours. H+3 was the first variant to start aggregation during this isothermal measurement and, thereby, indicated decreased stability (Figure 3.5a). During storage at 45 °C over 21 weeks, hydrophilic variant H+3, together with H-1, showed earlier and ongoing increase in fluorescence compared to other variants (Figure 3.5b). Overall, H+3 is the least stable variant although it has the lowest aggregate content in unstressed sample.

The self-interaction data has to be interpreted with care, because of the increased amounts of aggregates of variant H+4, which could compromise the results. For the same reason, H+1 and H+2, which contained 40 % or more high molecular weight species, were not included in the measurement. The interpretation of k_D values in correlation to A_{22} according to Lehermayr and

3. Identification of Monoclonal Antibody Variants Involved in Aggregate Formation – Part 2: Hydrophobicity Variants

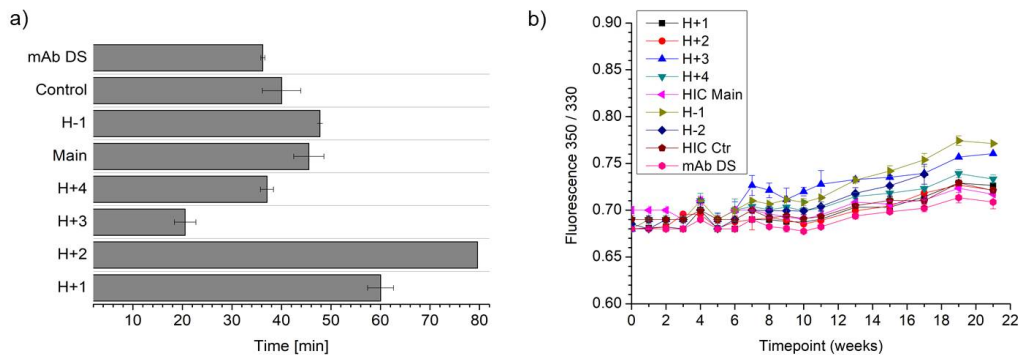


Figure 3.5: nanoDSF measurements of hydrophobicity variants a) in forced degradation study at 67 °C and b) in stability study in capillaries at 45 °C.

Menzen revealed that, hydrophilic variants showed slightly more repulsion compared to the control, while hydrophobic variants showed rather attractive forces (Figure 3.6) [17, 18]. These results were in accordance with other studies that described hydrophobic variants as a driving force in protein aggregation [29, 31, 32].

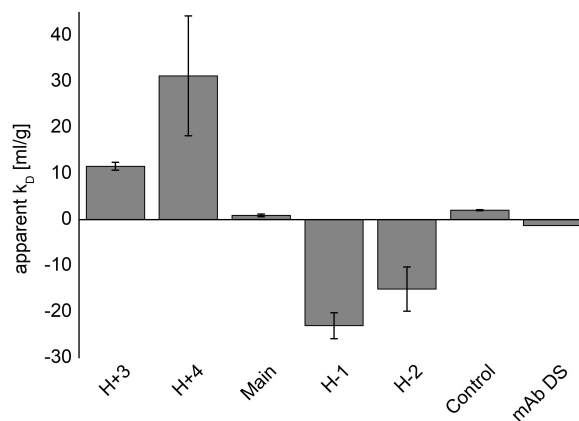


Figure 3.6: Apparent k_D values and SD of mAb hydrophobicity variants at 25 °C.

3.4.5 Correlation with Charge Variants

The hydrophobicity variants were further characterized by IEX to compare our findings with a previous study, where we separated and analyzed charge variants of the same model mAb and found 13 acidic and 8 basic variants [33]. The analysis of charge variants present in the HIC fractions showed that hydrophilic variants mainly contained acidic variants. Charged variants could differ in electrostatic repulsion at the same pH which could explain the difference in apparent k_D of hydrophilic fraction H+4 despite of its high aggregate content. The short ranged hydrophobic interactions are more prominent at high protein concentrations, while electrostatic interactions have a higher contribution in protein interaction under conditions of low mAb concentrations as used in this study [30].

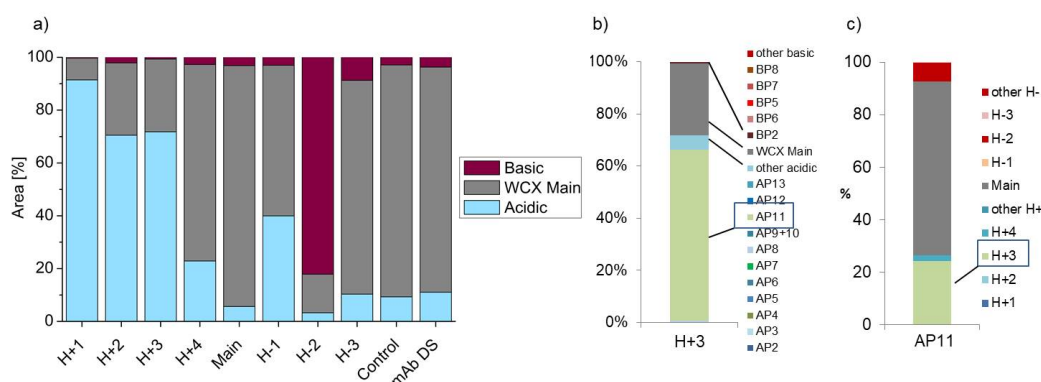


Figure 3.7: a) General charge variants content in hydrophobicity variants determined by IEX, b) Specific charge variants of our previous study found in H+3 by IEX. AP = acidic peak; BP = basic peak., c) Charge variant of our previous study with high H+3 content analyzed in HIC.

H+3 consisted of approximately $\frac{1}{3}$ main species and $\frac{2}{3}$ acidic variants, almost exclusively AP11 (Figure 3.7). A previous study of our group demonstrated, that the charge variant AP11 behaved likewise different and was suspected to be aggregation prone. A vice versa analysis of AP11 revealed that it contained high amounts, approximately 25 %, of the hydrophilic variant H+3. This shows an interrelationship between the hydrophilic and hydrophobic variants and underlines the instability of both variants.

3. Identification of Monoclonal Antibody Variants Involved in Aggregate Formation – Part 2: Hydrophobicity Variants

Furthermore, these observations underline our previous hypothesis of acidic variants to be involved in aggregate formation. In order to further characterize these potentially aggregation prone variants, which can be separated by HIC and IEX, the combination of both approaches in mixed mode chromatography (MMC) would be useful. Using this method could identify if the aggregation prone variants are one variant, which is both, more hydrophilic and more acidic than the main variant.

3.4.6 Accelerated Stability Study

The criticality of three hydrophilic variants was studied by spiking them into DS which was placed on a stability study at 45 °C for 12 weeks. Other hydrophobicity variants were not included due to the limited amounts available after fraction collection.

The presence of irreversible particles can visually be observed by cloudiness and floating substance in the vial [34]. The visual appearance was ranked according to Figure 3.8. Samples spiked in hydrophobicity variants followed the trend of the main species and the control samples.

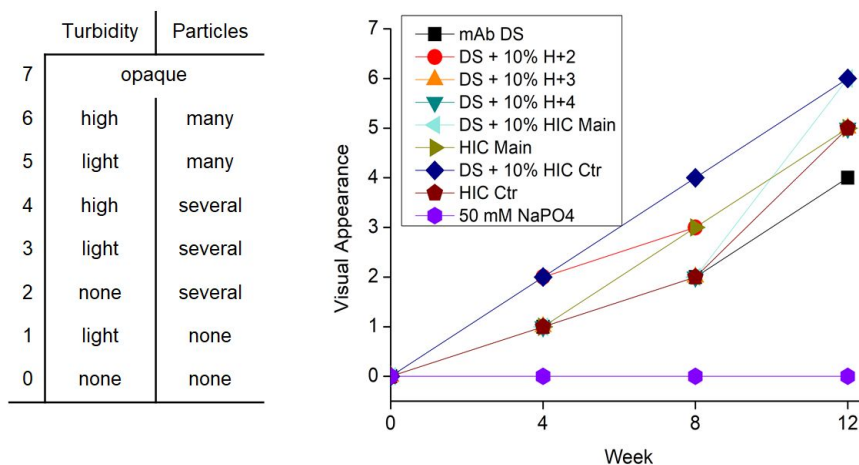


Figure 3.8: Visual appearance of mAb DS spiked with hydrophobicity variants stored at 45 °C for 12 weeks.

The visual observations were underlined by measurements of turbidity which increased after 12 weeks (Figure 3.9a). Overall, the hydrophobicity

variants did not have any impact on the DS stability.

Analysis of the conformational stability in terms of change in fluorescence did not indicate any effect of the hydrophobic variants as well. (Figure 3.9b).

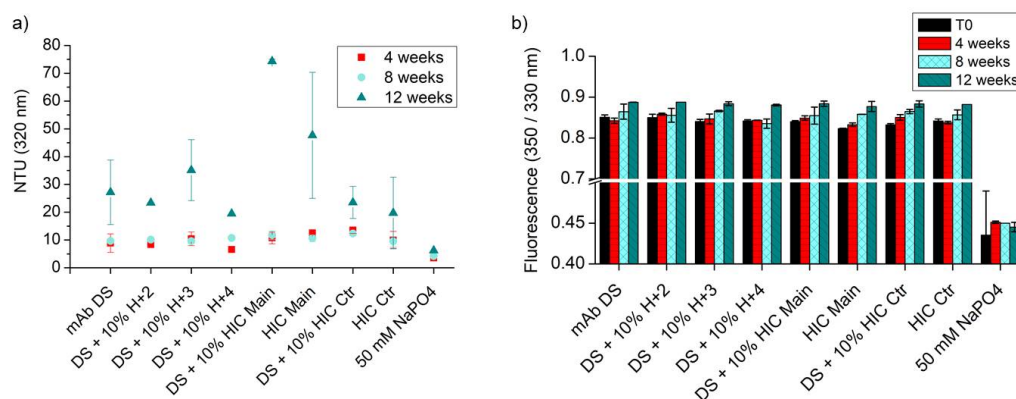


Figure 3.9: a) Turbidity at 320 nm. b) Fluorescence at 350/330 nm of mAb DS spiked with hydrophobicity variants.

Formation of soluble aggregates (HMWS) and fragments was monitored by SEC-MALS analysis. Over 4 weeks at 45 °C, the monomer content decreased to an average of 88 % without an effect of the spiking of hydrophobicity variants (Figure 3.10a).

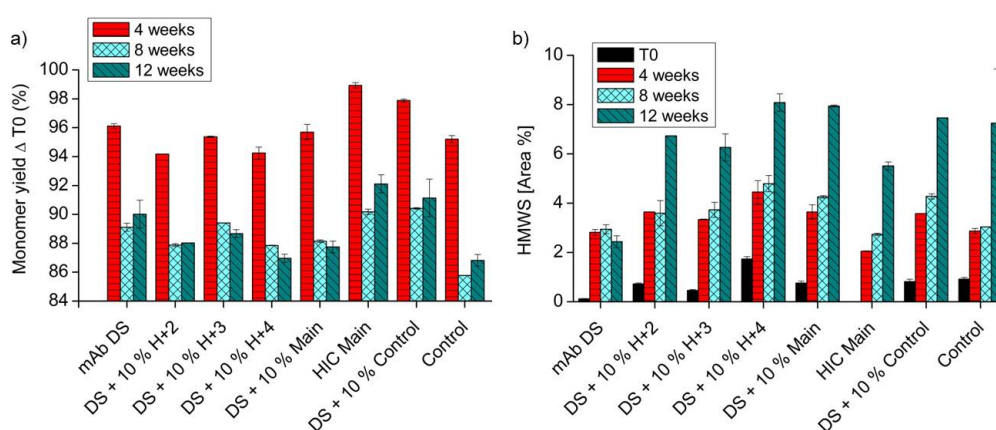


Figure 3.10: SEC data of mAb DS spiked with hydrophobicity variants and stressed at 45 °C for 12 weeks of a) monomer yield compared to T0 b) amount of aggregates per time point.

3. Identification of Monoclonal Antibody Variants Involved in Aggregate Formation – Part 2: Hydrophobicity Variants

Only the DS spiked with hydrophilic variant H+4 and the main species showed a slightly increased aggregate content (Figure 3.10b). No additional aggregate formation was triggered by spiking H+3 into DS. The molecular weight of the aggregates revealed that they mainly consisted of dimers. The formation of dimers was also observed in a previous temperature stress experiment with mAb DS. Those dimers were characterized as non-covalent. Therefore, the dimers formed during stability study were most likely also of non-covalent nature. Peaks of multimeric aggregates were observed after 12 weeks. Corresponding to aggregate and monomer content, the amount of fragments did not differ between the samples.

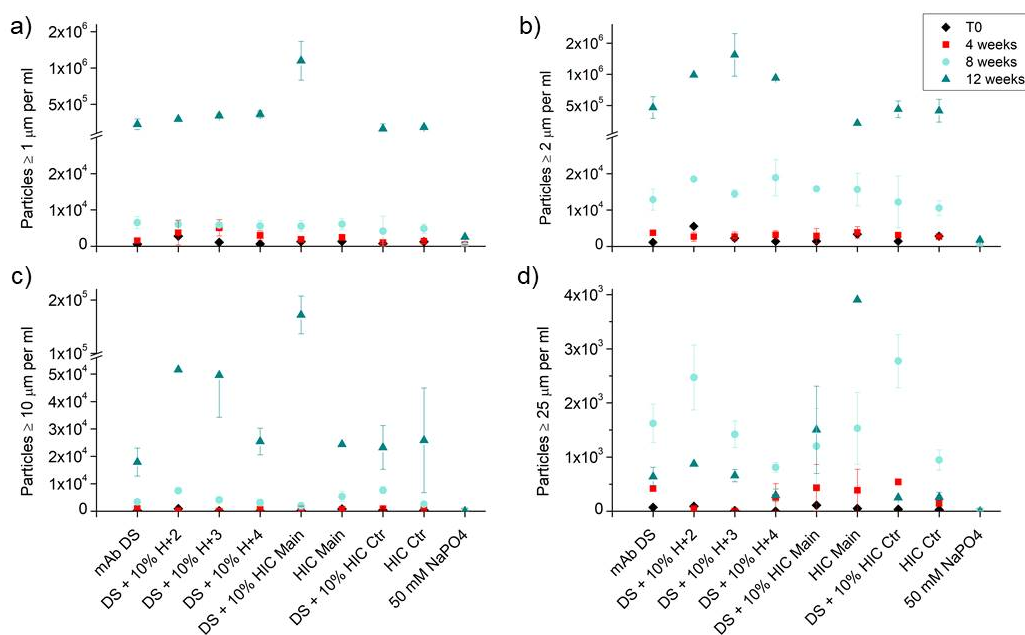


Figure 3.11: Sub-visible particles found in mAb DS spiked with hydrophobicity variants and stored at 45 °C for 12 weeks a) particles $\geq 1 \mu\text{m}$, b) $\geq 2 \mu\text{m}$, c) $\geq 10 \mu\text{m}$, d) $\geq 25 \mu\text{m}$.

Additionally, sub-visible particles were analyzed to characterize the insoluble aggregate content in number and size. The observation of sub-visible particles is important as they are widely discussed as the most immunologic form of particles [35, 36]. After 8 and 12 weeks a marked increase in total number of particles was observed, mostly attributed to particles be-

tween 1 and 2 μm (Figure 3.11b). The constant monomer yield in SEC at these time points in combination with the increase of the amount of particles point towards agglomeration of soluble aggregates assembling into insoluble particles. Particles of $\leq 25 \mu\text{m}$ decrease in number between 8 weeks and 12 weeks (Figure 3.11d), potentially forming the bigger particles noticed in visual inspection after 12 weeks.

Both particle and turbidity measurements indicate a more pronounced aggregation of DS spiked with main species, which cannot be explained, as in contrast, the respective values for pure HIC main species were within the range of HIC control and DS.

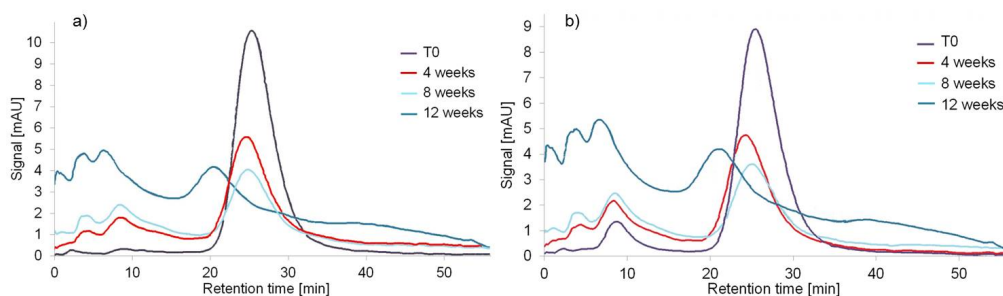


Figure 3.12: Analytical HIC chromatograms of a) mAb DS and b) DS spiked with H+3 stored at 45 °C for 12 weeks.

An additional HIC analysis of the stored samples demonstrated an increase in hydrophobicity variants upon storage without any differences between the different test samples as shown in Figure 3.12 exemplarily for DS and DS spiked with H+3. The increase was mainly caused by the formation of hydrophilic species.

In the course of the stability study, the amount of hydrophobicity variants increased at the expense of main species. This change indicating chemical changes due to the applied temperature stress may hide the specific interactions of the aggregation prone variants with the DS. The aggregation prone variants can degrade to other variants or interact with degradation products built during temperature stress, making them less interactive. Earlier time points or lower storage temperature might be indicated to show differences in physical behavior before prominent chemical changes occur. This could

3. Identification of Monoclonal Antibody Variants Involved in 72 Aggregate Formation – Part 2: Hydrophobicity Variants

improve the evaluation of the aggregation propensity of the less stable hydrophilic variant H+3. Overall, under the applied storage conditions, none of the three hydrophilic variants investigated in this stability study had an impact on the aggregation behavior of the DS.

3.5 Conclusion and Outlook

We developed a HIC method that enabled us to fractionate single hydrophobicity variants of a mAb DS under structure maintaining conditions. We found elevated levels of higher molecular weight species in three of four hydrophilic variants. The fourth hydrophilic variant, H+3, showed decreased conformational stability and correlated with an also unstable, potentially aggregation prone charge variant. Out of three hydrophobic variants, one variants contained increased amounts of aggregates resulting in reduced recovery.

A stability test of DS spiked with three hydrophilic variants revealed no increase in aggregation propensity at the storage conditions of 45 °C for 12 weeks. Therefore, the risk posed by the potentially aggregation prone variants is considered to be limited. Over the storage time, chemical changes occurred and possibly interfered with interactions between the variants and native species. Furthermore, a stability study in different formulation conditions may render a different outcome.

Considering the seen correlation between charge and hydrophobicity variants, the use of a mixed mode chromatography could combine both separation modes in one approach. This would be of interest in a future work. Furthermore, MMC provides the possibility to separate variants more distinctly from aggregates [37].

Our separation and characterization approach as well as the criticality assessment may be useful to better understand the behavior of different drug substance lots or biosimilars, to justify purification methods and potentially to remove critical variants to enhance safety of the drug product.

Acknowledgments

The authors would like to express their gratitude to Anna Sawadzka-Nowicka, Dr. Alfred Welzel and Dr. Stephan Böhm from Sandoz Biopharmaceutics for their valued advice and support.

Bibliography

- [1] P. L. Privalov and S. J. Gill, “Stability of Protein Structure and Hydrophobic Interaction,” *Adv. Protein Chem.*, vol. 39, no. C, pp. 191–234, 1988.
- [2] I. Klotz, “Comparison of molecular structures of proteins: helix content, distribution of apolar residues,” *Arch. Biochem. Biophys.*, vol. 138, pp. 704–706, 1970.
- [3] J. L. Ochoa, “Hydrophobic (interaction) chromatography,” pp. 1–15, 1978.
- [4] J. Queiroz, C. Tomaz, and J. Cabral, “Hydrophobic interaction chromatography of proteins,” *J. Biotechnol.*, vol. 87, no. 2, pp. 143–159, 2001.
- [5] J. L. Fausnaugh, L. A. Kennedy, and F. E. Regnier, “Comparison of hydrophobic-interaction and reversed-phase chromatography of proteins,” *J. Chromatogr. A*, vol. 317, no. C, pp. 141–155, 1984.
- [6] S. Fekete, J.-L. Veuthey, A. Beck, and D. Guillaume, “Hydrophobic interaction chromatography for the characterization of monoclonal antibodies and related products,” *J. Pharm. Biomed. Anal.*, 2016.
- [7] J. T. McCue, “Theory and Use of Hydrophobic Interaction Chromatography in Protein Purification Applications,” in *Guid. to Protein Purif.*, 2nd ed., M. P. D. Richard R. Burgess, Ed. Academic Press, 2009, ch. 25, pp. 405–414.
- [8] F. J. Shen, M. Y. Kwong, R. G. Keck, and R. J. Harris, “The application of tert-butylhydroperoxide oxidation to study sites of potential methionine oxidation in a recombinant antibody,” *Tech. Protein Chem.*, vol. 7, no. C, pp. 275–284, 1996.
- [9] J. Valliere-Douglass, A. Wallace, and A. Balland, “Separation of populations of antibody variants by fine tuning of hydrophobic-interaction

- chromatography operating conditions.” *J. Chromatogr. A*, vol. 1214, no. 1-2, pp. 81–9, 2008.
- [10] D. Boyd, T. Kaschak, and B. Yan, “HIC resolution of an IgG1 with an oxidized Trp in a complementarity determining region.” *J. Chromatogr. B. Analyt. Technol. Biomed. Life Sci.*, vol. 879, no. 13-14, pp. 955–60, 2011.
- [11] T. McSherry, J. McSherry, P. Ozaeta, K. Longenecker, C. Ramsay, J. Fishpaugh, and S. Allen, “Cysteinylation of a monoclonal antibody leads to its inactivation.” *MAbs*, vol. 8, no. 4, pp. 718–25, 2016.
- [12] J. Valliere-Douglass, L. Jones, D. Shpektor, P. Kodama, A. Wallace, A. Balland, R. Bailey, and Y. Zhang, “Separation and characterization of an IgG2 antibody containing a cyclic imide in CDR1 of light chain by hydrophobic interaction chromatography and mass spectrometry,” *Anal. Chem.*, vol. 80, no. 9, pp. 3168–3174, 2008.
- [13] D. Ouellette, C. Chumsae, A. Clabbers, C. Radziejewski, and I. Correia, “Comparison of the in vitro and in vivo stability of a succinimide intermediate observed on a therapeutic IgG1 molecule.” *MAbs*, vol. 5, no. 3, pp. 432–44, 2013.
- [14] H. Liu, G. Caza-Bulsecu, D. Faldu, C. Chumsae, and J. Sun, “Heterogeneity of monoclonal antibodies,” pp. 2426–2447, 2008.
- [15] S. K. Singh, “Impact of product-related factors on immunogenicity of biotherapeutics,” *J. Pharm. Sci.*, vol. 100, no. 2, pp. 354–387, 2011.
- [16] J. Rubin, L. Linden, W. M. Coco, A. S. Bommarius, and S. H. Behrens, “Salt-induced aggregation of a monoclonal human immunoglobulin G1,” *J. Pharm. Sci.*, vol. 102, no. 2, pp. 377–386, 2013.
- [17] C. Lehermayr, H. C. Mahler, K. Mäder, and S. Fischer, “Assessment of net charge and protein-protein interactions of different monoclonal antibodies,” *J. Pharm. Sci.*, vol. 100, no. 7, pp. 2551–2562, 2011.

76 3. Identification of Monoclonal Antibody Variants Involved in Aggregate Formation – Part 2: Hydrophobicity Variants

- [18] T. A. Menzen, “Temperature-Induced Unfolding, Aggregation, and Interaction of Therapeutic Monoclonal Antibodies,” Dissertation, University of Munich, 2014.
- [19] K. Gekko, E. Ohmae, K. Kameyama, and T. Takagi, “Acetonitrile-protein interactions: Amino acid solubility and preferential solvation,” *Biochim. Biophys. Acta - Protein Struct. Mol. Enzymol.*, vol. 1387, no. 1-2, pp. 195–205, 1998.
- [20] E. L. Kovrigin and S. A. Potekhin, “On the stabilizing action of protein denaturants: Acetonitrile effect on stability of lysozyme in aqueous solutions,” *Biophys. Chem.*, vol. 83, no. 1, pp. 45–59, 2000.
- [21] T. Arakawa, K. Tsumoto, K. Nagase, and D. Ejima, “The effects of arginine on protein binding and elution in hydrophobic interaction and ion-exchange chromatography,” *Protein Expr. Purif.*, vol. 54, no. 1, pp. 110–116, 2007.
- [22] C. P. Schneider, D. Shukla, and B. L. Trout, “Arginine and the hofmeister series: The role of ion-ion interactions in protein aggregation suppression,” *J. Phys. Chem. B*, vol. 115, no. 22, pp. 7447–7458, 2011.
- [23] F. R. Mansour, L. Zhou, and N. D. Danielson, “Applications of Poly(Ethylene)Glycol (PEG) in Separation Science,” pp. 1427–1442, 2015.
- [24] X. Lu, D. Zhao, G. Ma, and Z. Su, “Polyethylene glycol increases purification and recovery, alters retention behavior in flow-through chromatography of hemoglobin,” *J. Chromatogr. A*, vol. 1059, no. 1-2, pp. 233–237, 2004.
- [25] A. Hassl and H. Aspöck, “Purification of egg yolk immunoglobulins. A two-step procedure using hydrophobic interaction chromatography and gel filtration,” *J. Immunol. Methods*, vol. 110, no. 2, pp. 225–228, 1988.

- [26] V. Vagenende, M. G. Yap, and B. L. Trout, "Mechanisms of protein stabilization and prevention of protein aggregation by glycerol," *Biochemistry*, vol. 48, no. 46, pp. 11 084–11 096, 2009.
- [27] K. Gekko and S. Koga, "The stability of protein structure in aqueous propylene glycol. Amino acid solubility and preferential solvation of protein," *Biochim. Biophys. Acta (BBA)/Protein Struct. Mol.*, vol. 786, no. 3, pp. 151–160, 1984.
- [28] S. Ghose, M. Jin, J. Liu, and J. Hickey, "Integrated Polishing Steps for Monoclonal Antibody Purification," in *Process Scale Purif. Antibodies*, 1st ed., U. Gottschalk, Ed. New York: John Wiley & Sons, 2008, ch. 14, pp. 145–167.
- [29] X. Wang, T. K. Das, S. K. Singh, and S. Kumar, "Potential aggregation prone regions in biotherapeutics: A survey of commercial monoclonal antibodies," *MAbs*, vol. 1, no. 3, pp. 254–267, may 2009.
- [30] V. Kumar, N. Dixit, L. Zhou, and W. Fraunhofer, "Impact of short range hydrophobic interactions and long range electrostatic forces on the aggregation kinetics of a monoclonal antibody and a dual-variable domain immunoglobulin at low and high concentrations," *Int. J. Pharm.*, vol. 421, no. 1, pp. 82–93, dec 2011.
- [31] P. Chanphai, L. Bekale, and H. A. Tajmir-Riahi, "Effect of hydrophobicity on protein-protein interactions," *Eur. Polym. J.*, vol. 67, pp. 224–231, 2015.
- [32] S. A. Abbas, V. K. Sharma, T. W. Patapoff, and D. S. Kalonia, "Characterization of antibody-polyol interactions by static light scattering: Implications for physical stability of protein formulations," *Int. J. Pharm.*, vol. 448, no. 2, pp. 382–389, 2013.
- [33] R. M. Meyer, L. Berger, J. Nerkamp, S. Scheler, and W. Friess, "Identification of Monoclonal Antibody Variants Involved in Aggregate Formation – Part 1 : Charge Variants," *Eur. J. Pharm. Biopharm.*, vol. 158, pp. 123–131, 2021.

**3. Identification of Monoclonal Antibody Variants Involved in
78 Aggregate Formation – Part 2: Hydrophobicity Variants**

- [34] M. C. Manning, D. K. Chou, B. M. Murphy, R. W. Payne, and D. S. Katayama, “Stability of protein pharmaceuticals: An update,” *Pharm. Res.*, vol. 27, no. 4, pp. 544–575, 2010.
- [35] J. F. Carpenter, T. W. Randolph, W. Jiskoot, D. J. Crommelin, C. R. Middaugh, G. Winter, F. A. Ying-Xin, S. Kirshner, D. Verthelyi, S. Kozlowski, K. A. Clouse, P. G. Swann, A. M. Rosenberg, and B. Cherney, “Overlooking subvisible particles in therapeutic protein products: Gaps that may compromise product quality,” *J. Pharm. Sci.*, vol. 98, no. 4, pp. 1201–1205, apr 2009.
- [36] M. Ahmadi, C. J. Bryson, E. A. Cloake, K. Welch, V. Filipe, S. Romeijn, A. Hawe, W. Jiskoot, M. P. Baker, and M. H. Fogg, “Small amounts of sub-visible aggregates enhance the immunogenic potential of monoclonal antibody therapeutics,” *Pharm. Res.*, vol. 32, no. 4, pp. 1383–1394, 2015.
- [37] P. Gagnon, “IgG Aggregate Removal by Charged-Hydrophobic Mixed Mode Chromatography,” *Curr. Pharm. Biotechnol.*, vol. 10, no. 4, pp. 434–439, 2009.

Chapter 4

Characterization and Risk Assessment of Charge Variants of Recombinant Human Growth Hormone

The following chapter was submitted for publication. The version included in this thesis is identical to the submitted article except for minor changes.

Authors

Robina M. Meyer ¹, Sofya Aleshkevich ¹, Lukas Berger ², Joerg Nerkamp ²,
Stefan Scheler ², Wolfgang Friess ¹

¹: Ludwig-Maximilians University Munich, Germany

²: Sandoz Biopharmaceuticals, Langkampfen, Austria

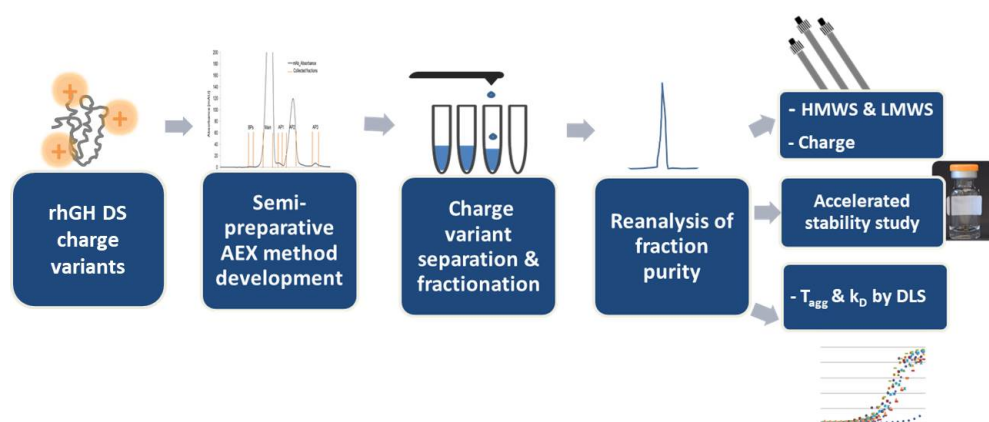
Keywords

hGH charge variants; protein aggregation; protein stability; FPLC; light scattering

4.1 Abstract

Biopharmaceutical products are subject to in depth analysis to ensure and improve their safety and efficacy. As part of this effort the stability and aggregation mechanisms of the therapeutic protein is characterized over the whole live cycle. The stability and aggregation behavior of single charge variants present in biopharmaceuticals were hardly investigated. In this study we applied a previously established methodology to assess the charge variants of the drug substance (DS) of human growth hormone (hGH). We assessed the stability and aggregation propensity of an acidic variant, which forms at a larger extend. We developed a semi-preparative method to separate and analyze the charge species. Thermal and colloidal stability of this variant was analyzed by light scattering methods and a stability testing in different buffer formulations. The acidic variant showed slightly attractive self-interaction at lower pH. Thermal stress did not result in increased aggregation propensity or decreased stability compared to the DS. Thus, the methodology enabled to assess the risk of a single protein variant within the DS of hGH. The approach can also be utilized for other protein drugs as previously shown for a monoclonal antibody.

Graphical Abstract



4.2 Introduction

Protein aggregation in biopharmaceuticals is a potential risk for product quality and safety and is closely monitored by manufacturers and regulatory authorities [1, 2]. Proteins aggregate as a result of changes in the environment during manufacturing steps, shipping and storage and while handling prior to injection [3, 4]. Several different pathways lead to a heterogeneous mix of aggregates in terms of size, structure, intermolecular bonding and reversibility [5, 6, 7]. A critical determinant in colloidal stability is the net charge on the protein surface. The protein net charge can change with single alterations in amino acid residues and the local environment of the residue, affecting the dissociation state [8]. Engineering of proteins can be applied to reduce protein aggregation by modification of the surface charge [9, 10, 11]. Charge affects protein-protein interaction and a high net charge results in repulsion of molecules, whereas a more heterogeneous distribution of opposing charges leads to attraction [12]. This interaction strongly depends on pH value and shielding by counterions in the protein solution [13]. Consequently, charge variants present in biopharmaceuticals may show differences in colloidal stability affecting the behavior of the whole DS and should be considered as a critical quality attribute [14].

Charge variants are commonly separated by gel electrophoresis, isoelectric focusing or chromatographic methods and characterized by mass spectrometry in one or multidimensional approaches [15, 16, 17, 18]. Thereby, isoforms and modifications can be identified or separated during downstream processing. Recombinant human growth hormone (rhGH) is a 22 kDa human growth hormone produced in *E.coli* [19]. Pharmacopoeias including the Ph. Eur and USP contain rhGH monographs with analysis charge variants by capillary zone electrophoresis (CZE). Corresponding electropherograms usually reveal three to five charge variants of hGH. These charge variants are dimers and cleaved rhGH forms eluting before the main peak and several deamidated forms and a Gln-18 mutant eluting after the main peak, but also include unidentified forms [20, 21].

Ion exchange chromatographic (IEX) methods for rhGH charge variant

analysis are most commonly based on anion exchange [20]. Comparable to CZE, mono- and dideamidated variants [22], a cleaved form, and dimers [23] of hGH can be separated. Despite of availability of well developed methods to detect and identify rhGH charge variants, the stability and aggregation propensity of the separated, single charge variants has not been explored.

We previously separated and characterized charge variants of a monoclonal antibody DS [24]. We identified an acidic charge variant with decreased conformational stability and increased aggregation propensity. In an accelerated stability study, this variant did not lead to an increase of aggregation and, therefore, posed limited risk to the DS. In the present study we wanted to assess, whether this approach can also be applied to a non-mAb protein with lower molecular mass. By studying rhGH, we aim to understand, whether in this case the charge variants show a different aggregation propensity, which would trigger concerns about the specifications of the DS composition.

We started with the development of a semi-preparative ion exchange chromatography to fractionate the individual charge variants. Subsequently we analyzed the separated variants for purity, aggregate content, thermal stability and self-interaction in order to identify critical variants. We found an acidic variant, that was formed predominantly during storage at 40 °C for 5 days. This variant was stable in thermal analysis but showed a higher level of self-attraction in dependence of pH.

After this initial analysis we tested the stability of the predominant acidic variant and other selected charge variants of rhGH in two different formulation buffers at elevated temperature. Furthermore, we investigated its influence on the DS by spiking the variant into DS. The stability study at elevated temperatures demonstrated, that the predominant acidic variant did not differ in aggregation propensity and did not negatively impact DS stability. The successful method transfer and the insightful characterization of the behavior of rhGH charge species prove the effectiveness of our methodology, which provides a basis for evaluation of DS composition and quality.

4.3 Materials and Methods

4.3.1 Materials

DS of rhGH was provided by Sandoz Biopharmaceuticals (Schaftenau, Austria). It was formulated at pH 7.0 in a concentration of 17 mg/ml. rhGH is a 22 kDa protein with an isoelectric point (pI) of pH 5.0 - 5.1.

4.3.2 Strong Cation Exchange Chromatography (SCX)

Analytical SCX was carried out on an Agilent 1200 series HPLC system (Agilent Technologies, Santa Clara, CA, USA) equipped with a TSKgel SP-NPR[®] column (2.5 μ m bead size; 4.6 \times 350 mm, Tosoh Bioscience, Griesheim, Germany). 20 μ g protein were injected. Elution buffer A was 20 mM sodium acetate pH 4.8 and buffer B additionally contained 125 mM sodium chloride as elution buffer. Samples were eluted by a linear gradient from 0 to 95 % buffer B at a flow rate of 1 ml/min. UV detection was performed at 280 nm. Chromatograms were analyzed with ChemStation software version B.02.01-SR2 (Agilent Technologies). For baseline correction, a chromatogram of a buffer injection was subtracted.

4.3.3 Separation of Charge Variants

rhGH DS was stressed at 40 °C for 5 days in order to increase the relative amount of charge species present. Semi-preparative charge variant fractionation of the stressed rhGH was performed with a GE ÄKTA purifier FPLC system (GE Healthcare, Uppsala, Sweden) equipped with a 9 \times 250 mm TSKgel SuperQ[®] anion exchange (AEX) column (Tosoh Bioscience). The protein DS was diluted in equilibration buffer (10 mM sodium phosphate buffer pH 8.0) to a concentration of 5 mg/ml and loaded onto the column with a flow rate of 0.8 ml/min. Charge variants were eluted with a stepwise salt gradient from 0 to 150 mM sodium chloride. 0.75 ml fractions were collected in 1.5 ml polypropylene tubes by a Frac-920 fraction collector (GE Healthcare). Method programming and evaluation were carried out with the

help of Unicorn 5.31 Software (GE Healthcare). Fractions containing single variants were pooled from several cycles to obtain sufficient material for further studies. To ensure the validity of our process, all fractions collected were reunited as control sample and were subsequently handled in the same way as the charge variant fractions. Fractions and control were concentrated in VivaSpin 20 centrifugation filter units with 5,000 Da MWCO (Sartorius Stedim Biotech, Göttingen, Germany) and buffer was exchanged to 10 mM sodium phosphate pH 7.0. The final concentrations were determined via the extinction coefficient using a Nanodrop 2000 photometer (Thermo Scientific, Wilmington, Delaware, USA).

4.3.4 Size Exclusion Chromatography (SEC)

SEC was performed on an Agilent 1200 series HPLC system (Agilent Technologies). 20 μg per vial were injected into an Acquity UPLC Protein BEH SEC[®] column (1.7 μm bead size; 4.6 \times 150 mm; Waters, Milford, MA, USA), and eluted using as mobile phase of 25 mM sodium phosphate pH 7 + 125 mM sodium chloride + 0.005 % sodium azide at a flow rate of 0.3 ml/min with UV detection at 280 nm. ChemStation software was used for chromatogram analysis (Version B.02.01-SR2, Agilent Technologies). Chromatogram baselines were corrected by subtraction of a buffer injection and the standard deviation (SD) was depicted in error bars.

4.3.5 Dynamic Light Scattering (DLS)

DLS measurements were carried out with a DynaPro Plate Reader III (Wyatt Technology, Dernbach, Germany) in a 384 well plate (Corning Life Science, Tewksbury, MA, USA). Dynamics 7.6 software (Wyatt Technologies) was used for instrument control and data acquisition. Prior and after dilution, samples were centrifuged at 10,000 rpm for 10 min to remove any insoluble particles. The supernatant was used to measure samples in duplicates. The plate was centrifuged at 2,000 rpm for two minutes in order to remove trapped air from the plate bottom. A drop of silicone oil was used to seal the wells and prevent sample evaporation.

The aggregation onset temperature (T_{agg}) was determined by ramping a 1.5 mg/ml sample from 25 to 80 °C at a rate of 0.417 °C/min with 2 s DLS acquisition time, and evaluating the hydrodynamic radius against temperature curve. Samples were analyzed in triplicates.

The diffusion interaction parameter (k_D) was derived from the diffusion coefficients (D) of seven protein concentrations between 1 mg/ml and 6 mg/ml at isothermal 25 °C in five acquisitions for 5 s. The k_D was calculated as the slope of the linear regression of D versus concentration normalized by D at infinite dilution [25]. The linear correlation of k_D and the second osmotic virial coefficient A_2 was used to make assumptions on self-interaction [26]. At a k_D of -6.29 ml/g sign reversal of the corresponding thermodynamic interaction parameter A_2^* occurs, indicating a change from net attractive to net repulsive interaction [27]. The coefficient of determination (R^2) was found above 0.9 (except for k_D values close to zero, where R^2 is close to zero) indicating high confidence of the results.

4.3.6 Static Light Scattering (SLS)

The measurement was carried out with an Optim 1000 (Avacta Analytical Ltd., Wetherby, UK) using micro-cuvette arrays. 9 μ l of each charge variant and control were analyzed at 1.5 mg/ml in 10 mM sodium phosphate pH 7 or pH 6, with or without 140 mM NaCl added. Prior to filling the cuvette, samples were centrifuged at 10,000 rpm for 10 min to remove any insoluble particles. T_{agg} was obtained from the 90° light scattering at 266 nm by ramping step wise from 25 °C to 90 °C at 0.5 °C/min. The measurements were performed in triplicates.

4.3.7 Accelerated Stability Study and Spiking Procedures

Charge variants and control, separated from rhGH DS which was stored at 40 °C for 5 days, as well as DS were sterile filtered with a 0.22 μ m polyethersulfone filter (VWR International, Radnor, PA) and diluted with

sterile filtrated buffer to 1.5 mg/ml. Additionally, these samples were added to sterile filtrated DS at a concentration of 10 % to obtain spiked samples. Pre-sterilized DIN2R glass type I vials (MGlass AG, Feldkirch, Germany) were filled with 0.5 ml, closed with 13 mm NovaPure rubber stoppers (West Pharmaceutical Services, Exton, PA, USA) and stored at 40 °C for the desired time.

4.3.8 Visual Inspection

The presence of visible particles was assessed by naked eye after gentle swirling of the vials while avoiding the formation of air bubbles. The solutions were checked for 5 s in front of a white plate. The test was repeated in front of a black plate. The occurrence of particles was recorded.

4.3.9 Ultraviolet Absorption Spectroscopy at 320nm

Turbidity measurements were performed with UV-Vis Spectrophotometer (HP/Agilent 8453, Agilent Technologies) at 320 nm wavelength. A Quartz SUPRASIL® Type ultramicro cuvette (Hellma Analytics, Muellheim, Germany) with a path length of 10 mm was used with a sample volume of 70 μ l. The instrument was calibrated with diluted TURB 4000 NTU Formazin nephelometric standard (Sigma-Aldrich, Darmstadt, Germany). Therefore, the results are presented in nephelometric turbidity units (NTU). Samples were analyzed in triplicates and normalized to rhGH DS values for each respective time point for improved comparability.

4.3.10 Sub-visible Particle Counting

A FlowCam 8100 (Fluid Imaging Technologies, Scarborough, ME, USA) was used for sub-visible particle measurements. Protein samples were diluted 1:1 with formulation buffer in triplicates. 150 μ l sample were analyzed with 10 \times magnification at 0.150 ml/min flow rate and a segmentation threshold of 13.0 for dark pixels and 10.0 for light pixels. The flow cell was rinsed with highly purified water after each measurement. Sub-visible particles in total number

and bigger than or equal to 10, and 25 nm are presented as counts per mL. Error bars indicate the standard error of the mean (SEM).

4.4 Results and Discussion

4.4.1 rhGH Charge Variant Separation and Fractionation

The analytical SCX separation of rhGH revealed only 1.2 % total amount of charge variants, including three acidic (AP) and two basic (BP) variants (Table 4.1). The two BPs were present in very low amounts and not well separated. After 5 days of storage at 40 °C, the charge variants content increased without a loss in total peak area. AP2 increased distinctly to almost 25 %, sparking the interest on further analysis of this charge variant.

Table 4.1: Relative peak areas in analytical SCX and semi-preparative AEX of rhGH charge variant separation in DS and after storage for 5 days at 40 °C and purity of the collected fractions as determined by analytical SCX. n.d. = not detected.

Peak	Peak Area (%)	Peak Area (%)	Peak Area (%)	Peak Area (%)	Purity (%)
	DS (SCX)	5 days 40 °C (SCX)	DS (AEX)	5 days 40 °C (AEX)	
Basic	0.3	0.5	0.4	0.2	n.d.
Main	98.5	73.5	98.8	74.2	94.6
AP1	0.8	1.4	0.5	1.3	33.6
AP2	0.3	24.2	0.1	23.9	87.4
AP3	0.06	0.4	0.02	0.3	91.8

These findings were confirmed in semi-preparative AEX. The change of column material was necessary in order to achieve a higher column capacity for preparative separation. The semi-preparative column eluted similar peak areas as the analytical column, both, from rhGH DS and from DS stored 5 days at 40 °C (Table 4.1). The charge variant peak pattern of rhGH DS was similar to the peaks described in electropherograms of somatotropin, measured according to the CZE test method described in the Ph.Eur. [28,

20, 21]. Three acidic variants, AP1 through AP3, were collected from stored DS (Figure 4.1). The fraction of basic variants remained low. Therefore BP1 and BP2 were collected together as basic species.

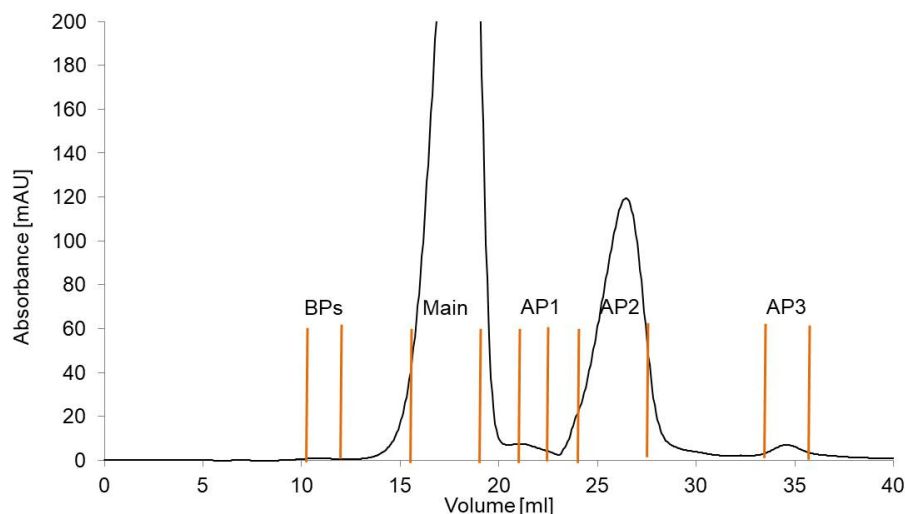


Figure 4.1: Semi-preparative AEX chromatogram of rhGH charge variant separation after storage for 5 days at 40 °C with collected fractions marked.

The purity of the collected variants was assessed via reanalysis by analytical SCX. AP2, AP3 and Main peak were collected with high purity of 87.4 %, 91.8 % and 94.6 %, respectively (Table 4.1). The purity of AP1 was compromised by the presence of main species, which was not fully separated by the AEX method (Figure 4.1). The preparative BP was not recovered by the purity check with the SCX column.

4.4.2 Aggregate and Degradation Product Content of the Fractions

5 days of storage at 40 °C had little impact on rhGH monomer content, causing only a minor increase of aggregates. The total amount of aggregates found in the charge variants in relation to their peak area was similar to the control sample, which is a pool of all fractions from AEX separation.

4. Characterization and Risk Assessment of Charge Variants of Recombinant Human Growth Hormone

Compared to the DS stored for 5 days at 40 °C both fragment and aggregate content were increased by the semi-preparative AEX separation.

Aggregation products of rhGH formed during storage are mainly non-covalent dimers [20]. The majority of aggregates was found in the BP pool, which contained more than 30 % aggregates (Figure 4.2). The described loss of recovery of BP pool may be explained by one of two hypotheses. (1) the BP pool with high aggregate content was not recovered because it did not elute from the SCX column with very low resin diameter or (2) the aggregates dissociate back into monomers as Becker et al. described for a dimeric species of rhGH with structural similarity to the monomer [29]. However, this observation was made for methods with denaturing conditions. Although the SCX was carried out under non-denaturing conditions, storage of the basic fractions at -20 °C prior to reanalysis might have impacted the dimeric aggregates.

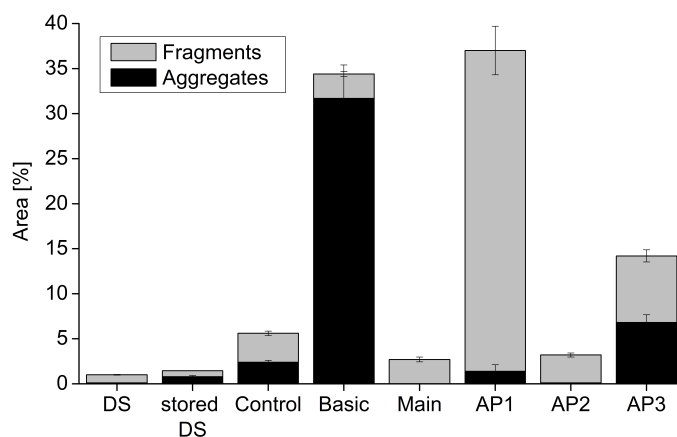


Figure 4.2: HMW and LMW content of rhGH charge variants in DS stored at 40 °C for 5 days. Error bars indicate SD.

The AP1 content increased from 0.5 % to 1.4 % after 5 days of storage at 40 °C and showed only small amounts of aggregates but a high content of fragments. This fragment content makes up to 0.5 % in relation to the total amount of stored DS. Considering the low purity of this fraction which contains more than 60 % main species, the actual share of fragments is low.

The prominent species AP2 included only low amounts of fragments, similar to the main peak, but mostly of deamidated forms of rhGH. With 9 asparagine and 13 glutamine residues, rhGH is prone for deamidation [30]. Consequently, deamidated forms of rhGH are major by-products [22]. At neutral pH, like in the DS formulation, the deamidation rate is already slightly increased. In addition to basic conditions, also elevated temperatures favor the formation of deamidated rhGH [7]. Given the strong peak area increase of AP2 after storage at 40 °C for 5 days and its monomeric character, we assume that AP2 consists of deamidated forms of rhGH.

In AP3 both aggregates and fragments were increased. This charge variant reflects chemical changes as well as deamidation. The latter, however, to a lesser extent than in AP2. The rhGH charge variants may also contain oxidized forms that are structurally similar to the main species and result from methionine oxidation [31].

4.4.3 Thermal Stability and Self-Interaction of rhGH and the AP2 Charge Variant

The thermal stability of AP2 compared to the DS stored for 5 days at 40 °C and the control was assessed in SLS and DLS measurements. The BP pool and AP1 were not included, due to a lack of material. The same applied to AP3 which was only analyzed by SLS in DS formulation buffer. In addition, the results of AP1 would have been compromised by its high main peak content. The stability was assessed in DS buffer (pH 7) and at pH 6, both with or without 140 mM sodium chloride. The lower pH was chosen in order to decrease the stability of rhGH and AP2 and to increase the aggregation propensity [32]. Sodium chloride was added to further destabilize the charge variants and shield repulsive charge interactions in order to enhance potential differences in stability.

T_{agg} determined by SLS was not significantly different for the samples based on the same buffer formulation (Figure 4.3a). T_{agg} decreased with lower pH as it was closer to the pI (5.1) of rhGH and therefore, lower protein

4. Characterization and Risk Assessment of Charge Variants of Recombinant Human Growth Hormone

net charge resulted in decreased electrostatic repulsion. The thermal stability decreased further with addition of 140 mM sodium chloride. The high concentration of sodium chloride also lowers the electrostatic repulsion, leading to increased aggregation rates [33]. In DLS analysis, the same trend was observed, with significantly higher variability in T_{agg} compared to SLS (Figure 4.3b).

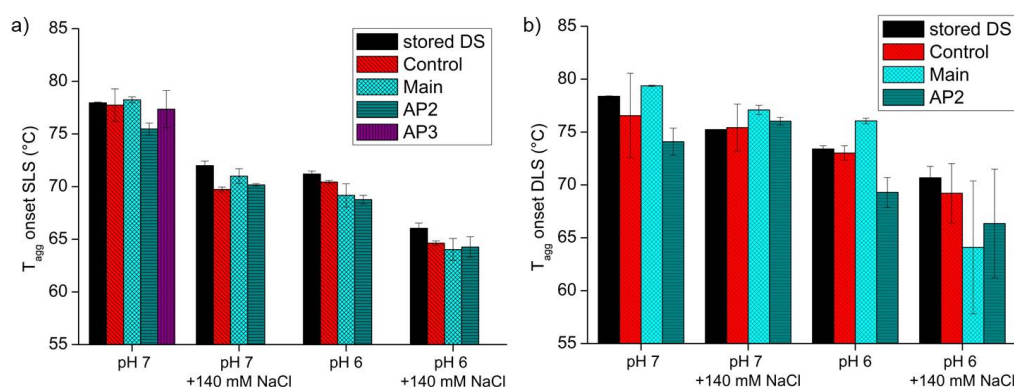


Figure 4.3: T_{agg} onset temperatures of rhGH stored at 40 °C for 5 days a) by SLS. b) by DLS. Error bars indicate SD.

Attractive and repulsive forces within the charge variants were investigated by determination of k_D in two formulations: in DS buffer at pH 7.0 and at pH 5.5. The pH of the second formulation was further decreased compared to the conditions in T_{agg} measurements in order to further decrease electrostatic repulsion. Addition of sodium chloride was omitted in order to observe protein self-interactions without salt effects.

The k_D measurement revealed repulsion of all variants at pH 7.0 (Figure 4.4). This repulsion is based on a negative net charge on the rhGH surface. Ablinger et al. reported a zeta potential around -8.5 mV at pH 7.0 and close to zero mV at pH 5.4 [34]. Correspondingly, our samples demonstrated attractive forces at pH 5.5. This result confirms the postulated decrease in electrostatic repulsion in formulations with a pH close to the pI. The strongest self-attraction was observed in AP2 at pH 5.5. In contrast, at pH 7.0, AP2 showed strong repulsive forces, more than those of the main species. Assuming that AP2 is a deamidation product, it has a slightly lower

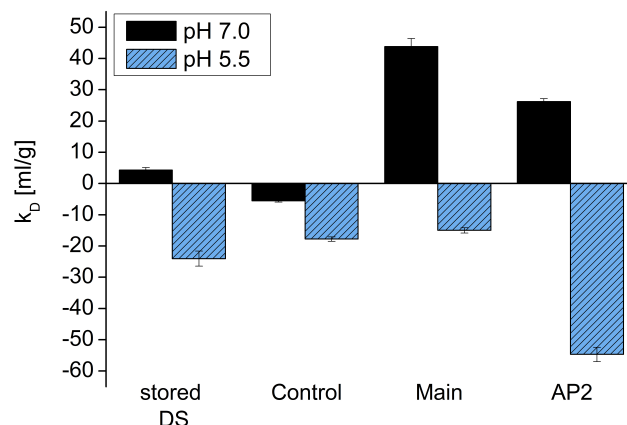


Figure 4.4: k_D of charge variants from rhGH stored at 40 °C for 5 days by DLS. Error bars indicate SD.

pI and a more negative net charge at pH 7.0. Stored DS and control showed markedly lower repulsive forces compared to the main species, potentially due to the mixture of variants present in these samples.

4.4.4 Stability Study with AP2 Charge Variant

A short term stability study for six weeks at 40 °C was set up to characterize AP2. Additional samples were generated by spiking acidic variant into fresh DS to highlight potential interactions between AP2 and other species of rhGH. Corresponding to the k_D measurement conditions, all samples were formulated in DS buffer either at pH 7.0 or at pH 5.5.

The visual inspection revealed only minimal particle formation upon storage (Supplement Table 1). In both AP2 and AP2 spiked into DS, first particles were observed after 4 weeks of storage. This was comparable to DS and control samples. Only the main species, pure and spiked into DS, appeared to be more stable. The visual observations were pH independent.

The presence of insoluble aggregates in the samples was additionally assessed in turbidity measurements. Turbidity values of both, AP2 and the

4. Characterization and Risk Assessment of Charge Variants of Recombinant Human Growth Hormone

94

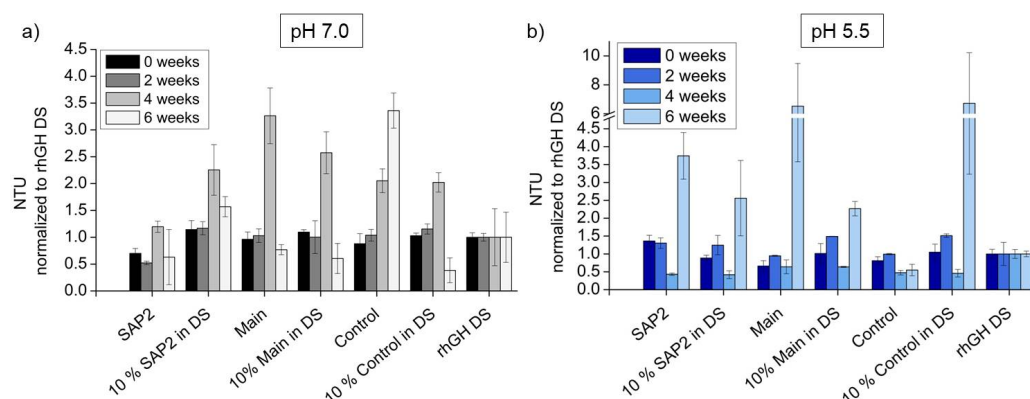


Figure 4.5: Turbidity a) in pH 7.0 and b) in pH 5.5 formulations after storage of rhGH protein variants at 40 °C for 6 weeks. The data was normalized to rhGH DS values. Error bars = SD.

spiked sample were similar to the DS and the control values (Figure 4.5a + b). The turbidity at pH 5.5 was higher than at pH 7.0, indicating increased aggregate formation at lower pH. This behavior can be explained by the pH and temperature dependence of rhGH, where more acidic conditions and higher temperatures favor the formation of aggregates [32].

SEC measurements were conducted to assess the formation of soluble particles. All samples showed an aggregate content between 1 % to 2.5 % throughout the stability study (Supplement Figure 1a + b). No differences between the samples were observed. Consequently, neither AP2 nor AP2 spiked in DS showed an enhanced propensity for self-aggregation or aggregation with other variants of rhGH.

Furthermore, the presence of sub-visible particles was investigated. Regardless of pH AP2 as pure variant was the only sample that remained low in particle count (Figure 4.6a + b). AP2 spiked in DS consistently behaved similar to other sampled spiked in DS in both formulations. Also the number of particles of $\geq 10 \mu\text{m}$ and $\geq 25 \mu\text{m}$ was not increased in and by AP2 (Supplement Figure 2). Thus, AP2 does not negatively impact sub-visible particle formation in rhGH DS.

The charge distribution within the samples was characterized by SCX. After two weeks the AP2 content in the samples (except for AP2 itself) was

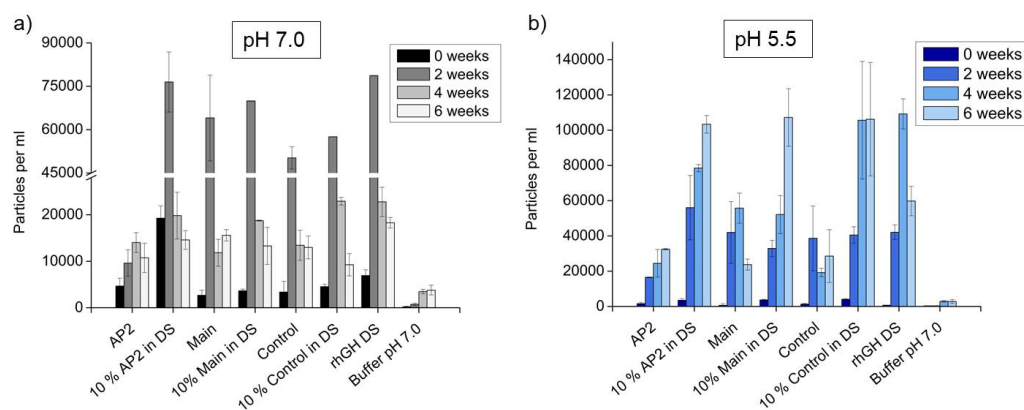


Figure 4.6: Particles observed in charge variants from rhGH stored at 40 °C for 6 weeks: a) accumulated numbers at pH 7.0, b) accumulated numbers at pH 5.5. Error bars show SEM.

1.6 to 7 fold above the initial content at pH 7.0. At pH 5.5 the AP2 content increased 1.5 to 5-fold. The main species showed the highest increase of AP2 in both formulations. Wilhelmssen et al. also described the predominant increase of the deamidated form most likely corresponding to AP2 in a stability study of somatropin solution at 4 °C [35]. After four weeks of storage, the new acidic peaks were observed due to temperature induced deamidation. A distinct identification of the peaks was no longer possible. The more pronounced increase of acidic species at pH 7.0 is consistent with literature that described rhGH as prone for deamidation at neutral pH [22, 7]. After 6 weeks of storage at 40 °C, the peak pattern of all samples was more or less identical. Differences in behavior of the variants were therefore no longer to be expected.

The stability study at 40 °C for 6 weeks revealed an increase in aggregates and particles over time. However, AP2 showed no indications of decreased stability. Despite the slightly increased self-attractive forces at pH 5.5, AP2 had no bias for aggregation with itself or other variants at neither pH formulation.

4.5 Conclusion and Outlook

In our present study we aimed to characterize charge variants of rhGH in order to identify potentially aggregation prone variants. We separated single charge variants via AEX and analyzed the thermal stability and self-interaction of the variants. An acidic variant, which was predominantly formed at elevated temperatures, showed increased attractive forces in k_D measurements under acidic conditions. Despite of the increased self-interaction, the acidic variant did not tend to aggregate neither with itself, nor with other components of rhGH DS in a subsequent short term stability study. Therefore we conclude, that this variant has a similar stability and no enhanced aggregation propensity compared to the other charge variants. The single charge variants pose no risk to the aggregation propensity in rhGH DS.

Thus, we successfully transferred our study design for charge variant investigation from a mAb to a lower molecular weight protein. The methodology appears to be applicable across different biopharmaceuticals to gain in depth knowledge on the behavior of single charge variants.

Our study was limited by the yield of variants. An up-scaling of the charge variant collection would be beneficial in order to gain variant material for further analyses of interest, for example, to investigate the pI, the chemical denaturation behavior or the folding state of the variants. Furthermore, a broad range study with our methodology to investigate the charge variants of multiple different proteins would be of interest which would help to identify patterns in aggregation behavior of charge variants.

Bibliography

- [1] C. J. Roberts, “Protein aggregation and its impact on product quality,” *Curr. Opin. Biotechnol.*, vol. 30, pp. 211–217, 2014.
- [2] J. Den Engelsman, P. Garidel, R. Smulders, H. Koll, B. Smith, S. Bas-sarab, A. Seidl, O. Hainzl, and W. Jiskoot, “Strategies for the assessment of protein aggregates in pharmaceutical biotech product development,” *Pharm. Res.*, vol. 28, no. 4, pp. 920–933, 2011.
- [3] S. Hermeling, D. J. Crommelin, H. Schellekens, and W. Jiskoot, “Structure-immunogenicity relationships of therapeutic proteins,” pp. 897–903, 2004.
- [4] A. H. Fradkin, J. F. Carpenter, and T. W. Randolph, “Immunogenicity of aggregates of recombinant human growth hormone in mouse models,” *J. Pharm. Sci.*, vol. 98, no. 9, pp. 3247–3264, 2009.
- [5] H.-C. Mahler, W. Friess, U. Grauschopf, and S. Kiese, “Protein aggregation: pathways, induction factors and analysis.” *J. Pharm. Sci.*, vol. 98, no. 9, pp. 2909–34, 2009.
- [6] D. Roberts, R. Keeling, M. Tracka, C. F. Van Der Walle, S. Uddin, J. Warwicker, and R. Curtis, “The role of electrostatics in protein-protein interactions of a monoclonal antibody,” *Mol. Pharm.*, vol. 11, no. 7, pp. 2475–2489, 2014.
- [7] M. C. Manning, D. K. Chou, B. M. Murphy, R. W. Payne, and D. S. Katayama, “Stability of protein pharmaceuticals: An update,” *Pharm. Res.*, vol. 27, no. 4, pp. 544–575, 2010.
- [8] M. Calamai, N. Taddei, M. Stefani, G. Ramponi, and F. Chiti, “Relative Influence of Hydrophobicity and Net Charge in the Aggregation of Two Homologous Proteins,” *Biochemistry*, vol. 42, no. 51, pp. 15 078–15 083, 2003.

- [9] S. S. Strickler, A. V. Gribenko, A. V. Gribenko, T. R. Keiffer, J. Tomlinson, T. Reihle, V. V. Loladze, and G. I. Makhatadze, "Protein stability and surface electrostatics: A charged relationship," *Biochemistry*, vol. 45, no. 9, pp. 2761–2766, 2006.
- [10] K. Broersen, M. Weijers, J. de Groot, R. J. Hamer, and D. Jongh, "Effect of Protein Charge on the Generation of Aggregation-Prone Conformers," *Biomacromolecules*, vol. 8, no. 5, pp. 1648–1656, 2007.
- [11] G. Raghunathan, S. Sokalingam, N. Soundrarajan, B. Madan, G. Munussami, and S. G. Lee, "Modulation of protein stability and aggregation properties by surface charge engineering," *Mol. Biosyst.*, vol. 9, no. 9, pp. 2379–2389, 2013.
- [12] E. Y. Chi, S. Krishnan, T. W. Randolph, and J. F. Carpenter, "Physical stability of proteins in aqueous solution: Mechanism and driving forces in nonnative protein aggregation," pp. 1325–1336, 2003.
- [13] A. Karshikoff, *Non-covalent Interactions In Proteins*, 1st ed. London: Imperial College Press, 2006.
- [14] S. Chung, J. Tian, Z. Tan, J. Chen, J. Lee, M. Borys, and Z. J. Li, "Industrial bioprocessing perspectives on managing therapeutic protein charge variant profiles," pp. 1646–1665, 2018.
- [15] L. Sun, M. D. Knierman, G. Zhu, and N. J. Dovichi, "Fast top-down intact protein characterization with capillary zone electrophoresis-electrospray ionization tandem mass spectrometry," *Anal. Chem.*, vol. 85, no. 12, pp. 5989–5995, 2013.
- [16] S. Claverol, O. Burlet-Schiltz, J. E. Gairin, and B. Monsarrat, "Characterization of protein variants and post-translational modifications: ESI-MSn analyses of intact proteins eluted from polyacrylamide gels." *Mol. Cell. Proteomics*, vol. 2, no. 8, pp. 483–493, 2003.
- [17] A. Goyon, L. Dai, T. Chen, B. Wei, F. Yang, N. Andersen, R. Kopf, M. Leiss, M. Mølholm, D. Guillaume, and C. Stella, "From proof of concept

to the routine use of an automated and robust multi-dimensional liquid chromatography mass spectrometry workflow applied for the charge variant characterization of therapeutic antibodies,” *J. Chromatogr. A*, vol. 1615, p. 460740, 2020.

- [18] Y. Leblanc, V. Faid, M. A. Lauber, Q. Wang, N. Bihoreau, and G. Chevreux, “A generic method for intact and subunit level characterization of mAb charge variants by native mass spectrometry,” *J. Chromatogr. B Anal. Technol. Biomed. Life Sci.*, vol. 1133, p. 121814, 2019.
- [19] R. Stanhope, F. Sörgel, P. Gravel, Y. B. Pannatier Schuetz, M. Zabransky, and M. Muenzberg, “Bioequivalence studies of Omnitrope, the first biosimilar/rhGH follow-on protein: Two comparative phase 1 randomized studies and population pharmacokinetic analysis,” *J. Clin. Pharmacol.*, vol. 50, no. 11, pp. 1339–1348, 2010. [Online]. Available: <http://doi.wiley.com/10.1177/0091270009359005>
- [20] A. Bayol, A. Bristow, E. Charton, M. Girard, and P. Jongen, “Somatropin and its variants : structural characterization and methods of analysis,” *Pharmeuropa Bio.*, vol. 2004-1, pp. 35–45, 2004.
- [21] S. M. Storms, A. Feltus, A. R. Barker, M.-A. Joly, and M. Girard, “Determination of somatropin charged variants by capillary zone electrophoresis - optimisation, verification and implementation of the European pharmacopoeia method.” *Pharmeur. Sci. Notes*, vol. 2009, no. 1, pp. 25–36, 2009.
- [22] P. Gellerfors, B. Pavlu, K. Axelsson, C. Nyhlen, and S. Johansson, “Separation and identification of growth hormone variants with high performance liquid chromatography techniques,” in *Acta Paediatr. Scand. Suppl.*, vol. 79, no. 370. John Wiley & Sons, Ltd, oct 1990, pp. 93–100.
- [23] R. L. Patience and L. H. Rees, “Comparison of reversed-phase and anion-exchange high-performance liquid chromatography for the analysis of human growth hormones,” *J. Chromatogr. A*, vol. 352, no. C, pp. 241–253, 1986.

- [24] R. M. Meyer, L. Berger, J. Nerkamp, S. Scheler, and W. Friess, "Identification of Monoclonal Antibody Variants Involved in Aggregate Formation – Part 1 : Charge Variants," *Eur. J. Pharm. Biopharm.*, vol. 158, pp. 123–131, 2021.
- [25] J. Rubin, L. Linden, W. M. Coco, A. S. Bommarius, and S. H. Behrens, "Salt-induced aggregation of a monoclonal human immunoglobulin G1," *J. Pharm. Sci.*, vol. 102, no. 2, pp. 377–386, 2013.
- [26] C. Lehermayr, H. C. Mahler, K. Mäder, and S. Fischer, "Assessment of net charge and protein-protein interactions of different monoclonal antibodies," *J. Pharm. Sci.*, vol. 100, no. 7, pp. 2551–2562, 2011.
- [27] T. A. Menzen, "Temperature-Induced Unfolding, Aggregation, and Interaction of Therapeutic Monoclonal Antibodies," Dissertation, University of Munich, 2014.
- [28] Council of Europe, "Somatropin for injection; monograph 0952," in *Eur. PHARMACOPOEIA*, 6th ed., 2008, p. 2935 ff.
- [29] G. Becker, R. Bowsher, W. Mackellar, M. Poor, P. Tackitt, and R. Riggin, "Chemical, Physical, and Biological Characterization of a Dimeric form of Biosynthetic Human Growth Hormone," *Biotechnol. Appl. Biochem.*, vol. 9, no. 6, pp. 478–487, dec 1987.
- [30] R. Pearlman and J. Y. Wang, *Stability and Characterization of Protein and Peptide Drugs: Case Histories Stability and Characterization of Human Growth Hormone*, 1993.
- [31] G. Becker, P. Tackitt, W. Bromer, D. Lefeber, and R. Riggin, "Isolation and Characterization of a Sulfoxide and a Desamido Derivative of Biosynthetic Human Growth Hormone," *Biotechnol. Appl. Biochem.*, vol. 10, no. 4, pp. 326–337, 1988.
- [32] H. Mohammadpanah, H. Rastegar, M. R. Ramazani, and M. R. Jaafari, "Effects of different buffers and pH on the stability of recombinant hu-

- man growth hormone,” *Biosci. Biotechnol. Res. Asia*, vol. 10, no. 1, pp. 193–203, 2013.
- [33] S. N. Olsen, K. B. Andersen, T. W. Randolph, J. F. Carpenter, and P. Westh, “Role of electrostatic repulsion on colloidal stability of *Bacillus halmapalus* alpha-amylase,” *Biochim. Biophys. Acta - Proteins Proteomics*, vol. 1794, no. 7, pp. 1058–1065, 2009.
- [34] E. Ablinger, S. Wegscheider, W. Keller, R. Prassl, and A. Zimmer, “Effect of protamine on the solubility and deamidation of human growth hormone,” *Int. J. Pharm.*, vol. 427, no. 2, pp. 209–216, 2012.
- [35] T. W. Wilhelmsen, V. Skibeli, and F. C. Arntzen, “Stability study of somatropin by capillary zone electrophoresis,” in *Procedia Chem.*, vol. 2, no. 1. Elsevier, jan 2010, pp. 34–45.

4. Characterization and Risk Assessment of Charge Variants of
 102 Recombinant Human Growth Hormone

Supplementary Data

Table 4.2: Visual appearance of rhGH charge variants stored at 40 °C for 6 weeks at pH 7.0 or pH 5.5. clear = no particles or turbidity observed.

		week 0	week 2	week 4	week 6
AP2	pH 7.0	clear	clear	few particles	few particles
	pH 5.5	clear	clear	few particles	few particles
10 % AP2 in DS	pH 7.0	clear	clear	few particles	few particles
	pH 5.5	clear	clear	clear	few particles
Main	pH 7.0	clear	clear	clear	clear
	pH 5.5	clear	clear	clear	clear
10 % Main in DS	pH 7.0	clear	clear	clear	clear
	pH 5.5	clear	clear	clear	clear
Control	pH 7.0	clear	clear	few particles	few particles
	pH 5.5	clear	few particles	few particles	few particles
10 % Control in DS	pH 7.0	clear	clear	few particles	few particles
	pH 5.5	clear	clear	clear	few particles
22 kDa protein DS	pH 7.0	clear	clear	few particles	few particles
	pH 5.5	clear	few particles	few particles	few particles
Buffer	pH 7.0	clear	clear	few particles	clear
	pH 5.5	clear	clear	clear	clear

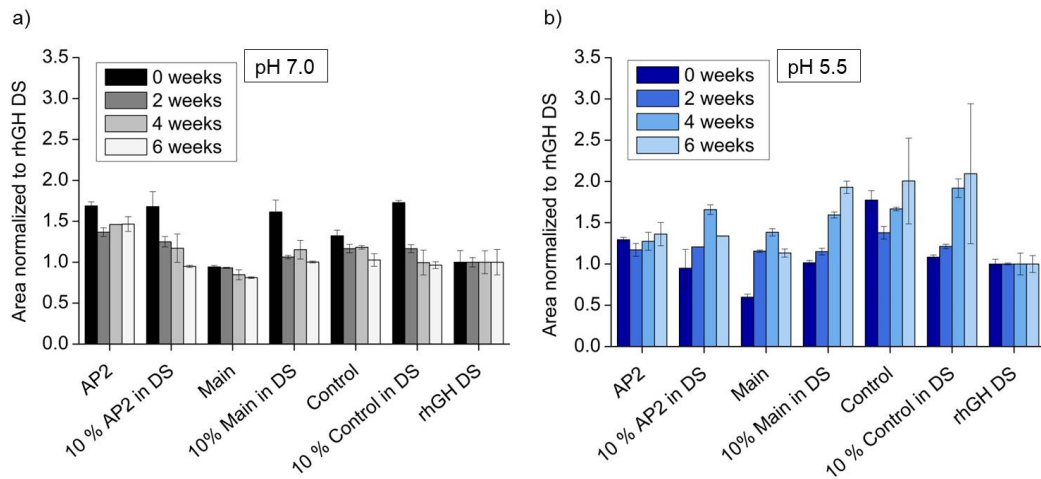


Figure 4.7: SEC of a) pH 7.0 and b) pH 5.5 formulations after storage of rhGH protein variants at 40 °C for 6 weeks. The data was normalized to rhGH DS values (= 1). Error bars = SD

4. Characterization and Risk Assessment of Charge Variants of
104 Recombinant Human Growth Hormone

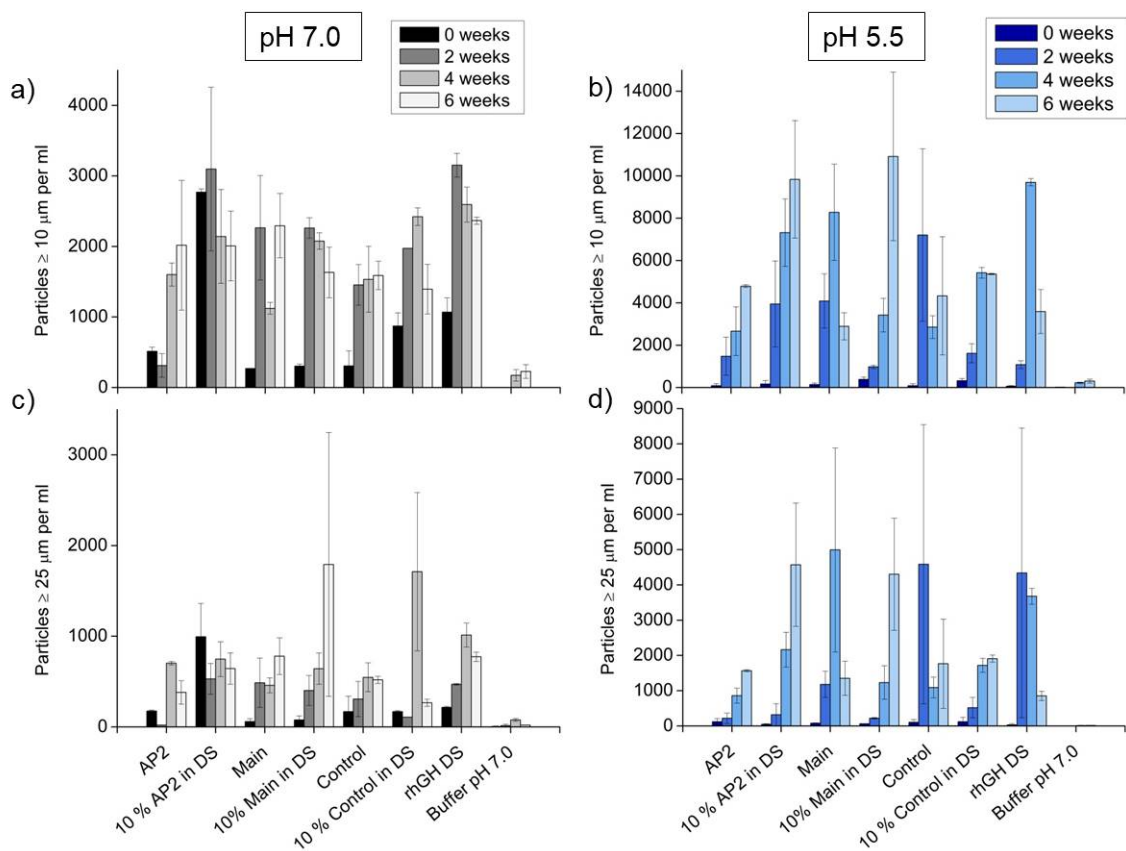


Figure 4.8: Particles observed in charge variants from rhGH stored at 40 °C for 6 weeks: a) particles $\geq 10 \mu\text{m}$ at pH 7.0, b) $\geq 10 \mu\text{m}$ at pH 5.5, c) $\geq 25 \mu\text{m}$ at pH 7.0 and d) $\geq 25 \mu\text{m}$ at pH 5.5. Error bars show SEM.

Chapter 5

I've got you covered: A first step towards a mini-chaperonin for protein variant characterization

Authors

Robina M. Meyer, Wolfgang Friess
Ludwig-Maximilians University Munich, Germany

Keywords

GroEL apical domain; mini-chaperonin; protein aggregation

5.1 Abstract

Chaperonins are proteins that ensure protein function in living organisms and prevent aggregation of proteins. Mis- and unfolded proteins are detected and repaired by the chaperonins in an active folding process. The chaperonin first

has to bind the un- or misfolded protein in a hydrophobic cavity called apical domain. We aimed to express the apical domain of GroEL, a chaperonin of e.coli, in order to detect unfolded protein variants in drug substances. This approach would offer the possibility to characterize, detect and potentially quantify mis- and unfolded variants in protein solutions or to study intrinsic unfolding in stability studies.

5.2 Introduction

While the biopharmaceutical industry is constantly searching for new or improved technical means to prevent protein aggregation and ensure protein function, living organisms have an endogenous approach: chaperonins. As a subclass of chaperons, chaperonins are oligomeric proteins with a cylindrical structure. This structure enfolds a hydrophobic cavity which can bind mis- and unfolded proteins, preventing these proteins from aggregation. Under consumption of adenosine triphosphate the falsely folded proteins are converted into their native state [1, 2]. One representative is GroEL, a 800 kDa chaperonin of e.coli. It is composed of two rings of seven 57 kDa subunits. In the center of these rings is a cavity of 45 Å in diameter [3]. Each subunit contains an apical domain which faces the cavity with strongly hydrophobic amino acids [4]. The sequence in the cavity considered to be responsible for binding hydrophobic proteins consists of isoleucine, valine, methionine, leucine, phenylalanine (IVMLF) [5]. In case of the formation of a GroEL-protein-complex the respective protein itself additionally requires a certain degree of hydrophobicity [5]. The apical domain, a 16.7 kDa fragment of GroEL consisting of the peptide residues 191-345 can be expressed as a mini-chaperonin which maintains its binding functionality [6, 7, 8, 9].

GroEL and its apical domain (GroEL-AD / mini-chaperonin) have previously been demonstrated to bind mis- and unfolded proteins in *in vitro* experiments. Naik et al. utilized the whole GroEL chaperonin as tool to screen for and quantify aggregation prone proteins [10]. They immobilized GroEL on biosensors for biolayer interferometry (BLI) and detected proteins challenged in conformational stability. They also suggested this approach

to screen for stabilizing formulations. In their experiments proteins built a complex with GroEL in dependence of the applied stress and the presence of stabilizers [11, 12]. Altamirano et al. expressed a His-tagged GroEL mini-chaperonin and attached it to column resins for refolding chromatography and were able to renature proteins and restore biological activity [8]. A similar approach was used to renature enzymes [13].

In this study, we aimed to develop an additional method for the detection of potentially aggregation prone protein variants by the detection and potentially quantification of mis- or unfolded protein variants. This could also include the surveillance of intrinsic unfolding in stability studies. Therefore, we expressed GroEL-AD with an histidine tag (His-tag). An N-terminal histidine tag was shown to not interfere with binding activity [6]. After successful expression of the mini-chaperonin, we checked the binding function as a proof of concept. Unfortunately, native gel-electrophoresis revealed that the mini-chaperonin aggregated and lost its functionality.

5.3 Materials and Methods

5.3.1 Materials

The GroEL plasmid pBB541 was a gift from Bernd Bukau (Addgene plasmid # 27394 ; <http://n2t.net/addgene:27394>). mAb DS, granulocyte colony-stimulating factor (GCSF) and recombinant human growth hormone (rhGH) were provided by Sandoz (Schaftenau, Austria).

5.3.2 Plasmid construction

The gene sequence for GroEL-AD was extracted from plasmid pBB541 and amplified by polymerase chain reaction (PCR) with forward primer 5'--CCATGGCACATCACCACCACCATCACGTGGAAGGTATGCAGTTCG-ACCGTG-3' and reverse primer 5'-TTAATTAATCATTAACGCCGCCTGCCAGTTTCG-3' (Sigma-Aldrich Life Science, Darmstadt, Germany). The primers introduced PvuII and HindIII sites flanking the PCR product coding for GroEL-AD, which enabled the ligation into a pJET1.2/blunt cloning vector (Thermo Fisher Scientific, Rockford, USA). The successful transformation and cloning of the plasmid into e.coli strain DH5 α was confirmed by sequencing (performed by the sequencing service of the LMU Biocenter, Martinsried, Germany).

The plasmid coding for GroEL-AD was once more extracted and digested with restriction enzymes PacI and NcoI (New England BioLabs, Ipswich, MA, USA), simultaneously with the promoter plasmid pET45b. pET45b was utilized to introduce a sequence coding for a N-terminal histidine tail on the apical domain. Furthermore, a lac-operon was introduced to facilitate protein expression by induction with isopropyl-D-galactopyranoside (IPTG). The new plasmid was cloned into e.coli strain BL21 for protein expression.

5.3.3 Protein expression and purification

An overnight culture of E. coli BL21 (DE3) cells coding for the His-tagged GroEL-AD was inoculated to 3% into lysogeny broth (LB) medium with

100 $\mu\text{g}/\text{ml}$ ampicillin. At an OD_{600} of 0.6-0.8 protein expression was induced by addition of 1 μM or 1 mM IPTG (Sigma, St. Louis, MI, USA) followed by incubation for 5 hours. Cells were harvested by centrifugation and purified either by small scale protein purification with HisPur™ Cobalt Purification Kit (Thermo Fisher Scientific, Rockford, USA) or up-scaled using an Äkta purifier (Cytiva, Marlborough, MA, USA) equipped with a Protino Ni-NTA column (Macherey-Nagel, Düren, Germany). In both procedures, cells were resuspended in NPI-10 buffer (50 mM sodium phosphate, 300 mM sodium chloride and 10 mM imidazole, pH 8) and lysed with 10 mg/ml lysozyme, 250 Units/ml benzoase nuclease and 250 units/ml Pierce Universal Nuclease. The lysate was loaded onto the column equilibrated with NPI-20 buffer (50 mM sodium phosphate, 1 M sodium chloride and 20 mM imidazole, pH 8), followed by three wash steps with NPI-20 buffer. The mini-chaperonin was eluted in two steps with NPI-500 buffer (50 mM sodium phosphate, 300 mM sodium chloride and 500 mM imidazole, pH 8). Buffer was exchanged to PBS.

GroEL-AD was analyzed by sodium dodecyl sulfate-polyacrylamide gel electrophoresis (SDS-PAGE) and native PAGE (both gels from BioRad, Hercules, CA, USA), both with subsequent western blotting. A 6x-His tag monoclonal antibody coupled to horse radish peroxidase (Thermo Fisher Scientific) was utilized for identification of the His-tagged mini-chaperonin. Quantification was performed via Bradford assay (BioRad).

5.3.4 MicroScale Thermophoresis (MST)

GroEL-AD was labeled with either Monolith Protein Labeling Kit RED-NHS 2nd Generation or Monolith His-Tag Labeling Kit RED-tris-NTA 2nd Generation (NanoTemper, Munich, Germany). Presence and identity of protein after labeling was checked with Tycho NT.6 (NanoTemper). The presence of GroEL-AD was confirmed by fluorescence transition at about 58 $^{\circ}\text{C}$ [14]. The labeling induced signal intensity was pre-check with Monolith NT.115 (Nanotemper) to determine the required laser intensity for MST measurements. MST-buffer (Tris buffer, Nanotemper) with 0.005% of Tween20 was used

as measuring buffer. Ligand concentrations were between 6.7 – 67 nM for RED-NHS-labeled proteins and 107 – 1070 nM for His-Tag-labeled proteins. Ligands including mAb DS, rhGH and rhodanese were incubated in 6.25 M (50 % unfolding / denaturation of mAb after 20 hours with 6.25 M Urea) or 8.0 M Urea overnight or were stressed either at 60 °C or mechanically for 1 hour.

5.3.5 Biolayer Interferometry (BLI)

BLI measurements were conducted with a BLItz (FortéBio, CA, USA). HIS1K Biosensors (FortéBio), which utilize a anti-penta-HIS antibody were incubated in PBS with 0.005 % Tween, pH 7.4 to measure the baseline. The mini-chaperonin was loaded for 150 s at 3 μ M during the loading step. After a second baseline (30 s) the association of ligands at a concentration of 30 μ M was conducted for 300 s.

With AR2G Biosensors (FortéBio), proteins of interest were loaded on the sensor by amino reactive coupling for 300 s. The mini-chaperonin was incubated for 600 s in the association step with concentrations between 50 nM - 275 nM.

With both sensor types, steps with buffer during loading or association steps served as control. The relative response was calculated as the self-interaction signal normalized to the amount of captured mAb [15].

5.4 Results and Discussion

5.4.1 Mini-chaperonin purification, quantification and identification

The successful cloning and transformation of the sequences coding for the GroEL-AD and the 6x-His tag was confirmed by PCR analysis. After protein expression, the mini-chaperonin was purified by cobalt spin columns. This process was monitored by SDS-PAGE (Figure 5.1) with bands slightly higher than 15 kDa, reflecting the 17 kDa mini-chaperonin.

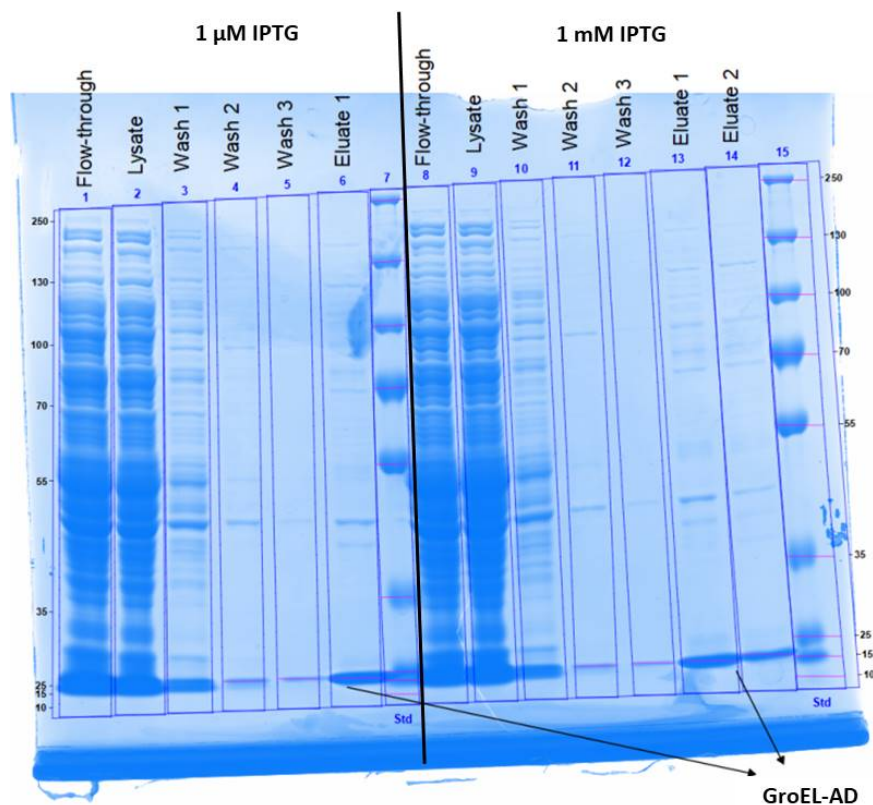


Figure 5.1: Monitoring of GroEL-AD purification by SDS PAGE stained with Coomassie blue. Left induced with 1 μ M IPTG, right with 1 mM IPTG.

The expression yielded 300 and 400 μ g/ml GroEL-AD after protein expression induction with 1 μ M or 1 mM of IPTG, respectively. Some mini-chaperonin may be trapped in inclusion bodies, that eluted as weak bands

5. I've got you covered: A first step towards a mini-chaperonin 112 for protein variant characterization

in higher size ranges [8, 16]. The purification scale-up to a Ni-NTA column yielded similar amounts of GroEL-AD. The identity of the bands that eluted at about 15 kDa was confirmed by western blotting (Figure 5.2).

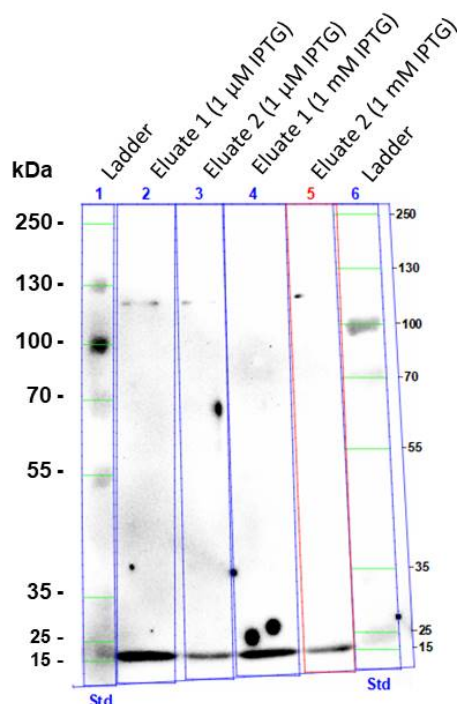


Figure 5.2: Gro-EL-AD identified by an anti-His antibody detected by chemiluminescence in western blotting.

5.4.2 Functionality of the mini-chaperonin

MST measurements were performed to investigate the functionality of the expressed GroEL-AD. During the infrared laser induced temperature gradient, binding of the mini-chaperonin to ligands can be observed by the fluorescence signal of the molecule moving, that depends on molecule size, hydration shell and conformation [17, 18]. Binding of rhodanese, a mAb and rhGH which show different hydrophobicity was tested.

Little differences in the signal between buffer, the native and the partially denatured protein samples were observed (Figure 5.3). Neither measurements

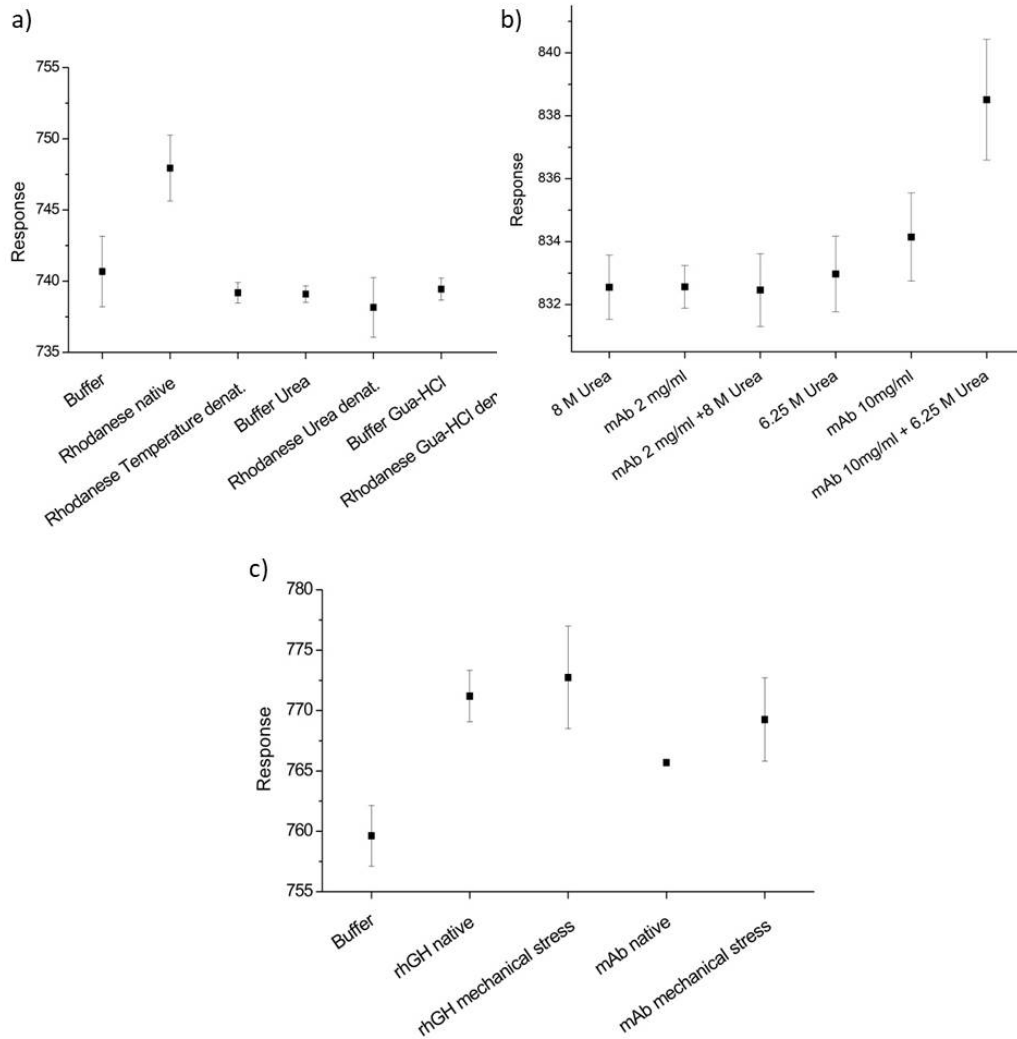


Figure 5.3: MST response of GroEL-AD labeled with NHS with ligands a) rhodanese denatured by temperature or chemical stress b) mAb chemically denatured and c) rhGH and mAb mechanically stressed.

5. I've got you covered: A first step towards a mini-chaperonin for protein variant characterization

with His-labeled GroEL-AD, nor with NHS-labeled ligands gave specific signal results. Only for rhodanese, which is known to bind well to GroEL, a low signal was observed [19, 20]. Surprisingly, heat denatured rhodanese did not bind to the mini-chaperonin (Figure 5.3a). Also mAb at high concentration of 10 mg/ml, partially denatured in urea, did not show a clear response depended on the presence of GroEL-AD compared to untreated mAb of the same concentration (Figure 5.3b). An increase of protein concentrations may result in more clear binding events, however, it would decrease the mobility of the labeled protein. Thus, GroEL-AD binding could not be detected by MST.

Additionally, BLI measurements were conducted looking for GroE-AD binding. Different buffers, protein and GroEL-AD concentrations were tested. The biosensors could be successfully loaded with either mini-chaperonin or partially denatured protein. The subsequent incubation in partially denatured protein or mini-chaperonin, respectively, did not result in any specific association of protein, confirming the MST results.

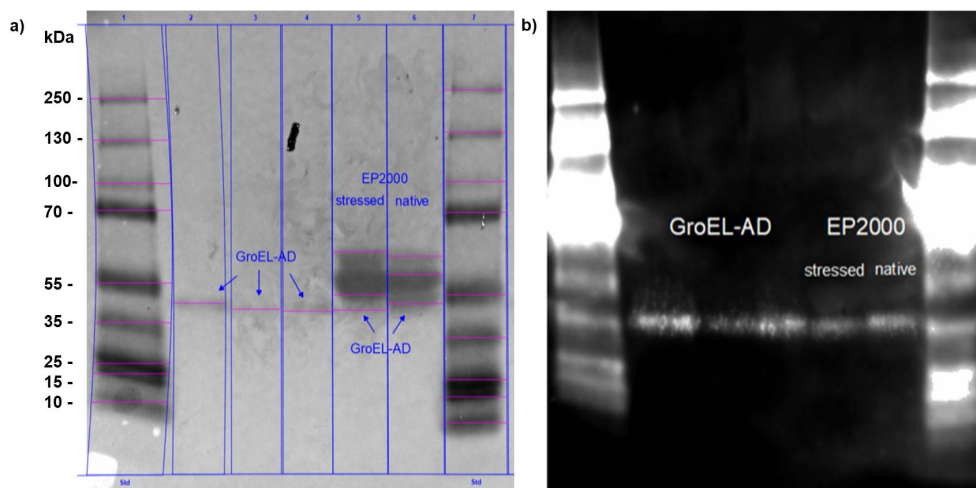


Figure 5.4: Western Blot with native PAGE of GroEL-AD displayed as a) chemiluminescence and b) inverted.

A final check of potential binding of the mini-chaperonin to protein was performed by a native PAGE with subsequent western blotting. The mini-chaperonin band was found at about 40 kDa, suggesting a multimerization

of the GroEL apical domain. The multimeric size was confirmed in dynamic light scattering.

Thus, the lack of binding of the mini-chaperonin to the two therapeutic proteins rhGH and mAb, as well as the control rhodanese, unfolded by different means, was most likely caused by the multimerization of the mini-chaperonin. The observed GroEL-AD association has not been described in literature up to now. Further investigations are necessary to achieve a stable, monomeric mini-chaperonin, specifically the expression of a more stable chaperonin fragment.

5.5 Conclusion and Outlook

We cloned and transformed a plasmid coding for the mini-chaperonin GroEL-AD and successfully expressed the protein in e.coli DH5 cells. The mini-chaperonin was purified and the identity of the resulting protein was confirmed by size and His-tag presence.

Both, in MST and in BLI measurements, no specific binding of GroEL-AD with native and unfolded rhGH, mAb, and rhodanese, which come with different hydrophobic patterns, was observed. Due to multimerization, the binding function of the apical domain was hindered. Further investigation of the structure of the mini-chaperonin could give answers on the cause for the multimerization and may provide guidance for the expression of a more stable, less self-interacting mini-chaperonin.

Acknowledgments

Special gratitude belongs to Aditi Mehta for support during this project. Amid Gupta and NanoTemper are acknowledged for advice and the provision of material and measurement time at the NanoTemper lab. The authors also thank Mathias Stotz, Manajit Hayer-Hartl and Franz-Ulrich Hartl for their valued advice.

Bibliography

- [1] Z. Lin and E. Eisensteine, “Nucleotide binding-promoted conformational changes release a nonnative polypeptide from the Escherichia coli chaperonin GroEL,” *Proc. Natl. Acad. Sci. U. S. A.*, vol. 93, no. 5, pp. 1977–1981, 1996.
- [2] K. J. Ellis and F. Hartl, “Protein folding in the cell: competing models of chaperonin function,” *FASEB J.*, vol. 10, no. 1, pp. 20–26, 1996.
- [3] K. Braig, Z. Otwinowski, R. Hegde, D. C. Boisvert, A. Joachimiak, A. L. Horwich, and P. B. Sigler, “The crystal structure of the bacterial chaperonin GroEL at 2.8 Å,” *Nature*, vol. 371, no. 6498, pp. 578–586, oct 1994.
- [4] W. A. Fenton and A. L. Horwich, “GroEL-mediated protein folding,” *Protein Sci.*, vol. 6, pp. 743–760, 1997.
- [5] T. K. Chaudhuri and P. Gupta, “Factors governing the substrate recognition by GroEL chaperone: A sequence correlation approach,” *Cell Stress Chaperones*, vol. 10, no. 1, pp. 24–36, 2005.
- [6] R. Zahn, A. M. Buckle, S. Perrett, C. M. Johnson, F. J. Corrales, R. Golbik, and A. R. Fersht, “Chaperone activity and structure of monomeric polypeptide binding domains of GroEL,” *Proc. Natl. Acad. Sci.*, vol. 93, no. 26, pp. 15 024–15 029, dec 1996. [Online]. Available: <http://www.pnas.org/cgi/doi/10.1073/pnas.93.26.15024>
- [7] A. M. Buckle, R. Zahn, and A. R. Fersht, “A structural model for GroEL-polypeptide recognition,” *Proc. Natl. Acad. Sci.*, vol. 94, no. 8, pp. 3571–3575, 1997.
- [8] M. M. Altamirano, R. Golbik, R. Zahn, A. M. Buckle, and A. R. Fersht, “Refolding chromatography with immobilized mini-chaperones,” *Proc. Natl. Acad. Sci. U. S. A.*, vol. 94, no. 8, pp. 3576–3578, 1997.

- [9] A. E. Ashcroft, A. Brinker, J. E. Coyle, F. Weber, M. Kaiser, L. Moroder, M. R. Parsons, J. Jager, U. F. Hartl, M. Hayer-Hartl, and S. E. Radford, "Structural plasticity and noncovalent substrate binding in the GroEL apical domain. A study using electrospray ionization mass spectrometry and fluorescence binding studies," *J. Biol. Chem.*, vol. 277, no. 36, pp. 33 115–33 126, 2002.
- [10] S. Naik, I. Haque, N. Degner, B. Kornilayev, G. Bomhoff, J. Hodges, A. A. Khorassani, H. Katayama, J. Morris, J. Kelly, J. Seed, and M. T. Fisher, "Identifying protein stabilizing ligands using GroEL," pp. 237–251, mar 2010.
- [11] S. Naik, O. S. Kumru, M. Cullom, S. N. Telikepalli, E. Lindboe, T. L. Roop, S. B. Joshi, D. Amin, P. Gao, C. R. Middaugh, D. B. Volkin, and M. T. Fisher, "Probing structurally altered and aggregated states of therapeutically relevant proteins using GroEL coupled to bio-layer interferometry," *Protein Sci.*, vol. 23, no. 10, pp. 1461–1478, 2014.
- [12] W. A. Lea, P. T. O'Neil, A. J. Machen, S. Naik, T. Chaudhri, W. McGinn-Straub, A. Tischer, M. T. Auton, J. R. Burns, M. R. Baldwin, K. R. Khar, J. Karanicolas, and M. T. Fisher, "Chaperonin-Based Biolayer Interferometry To Assess the Kinetic Stability of Metastable, Aggregation-Prone Proteins," *Biochemistry*, vol. 55, no. 35, pp. 4885–4908, 2016.
- [13] T. Teshima, S. Mashimo, A. Kondo, and H. Fukuda, "Affinity purification and immobilization of fusion chaperonin GroEL- (His)₆ and its utilization to mediate protein refolding," *J. Ferment. Bioeng.*, vol. 86, no. 4, pp. 357–362, 1998.
- [14] R. Golbik, R. Zahn, S. E. Harding, and A. R. Fersht, "Thermodynamic stability and folding of GroEL minichaperones 1 1Edited by P. E. Wright," *J. Mol. Biol.*, vol. 276, no. 2, pp. 505–515, feb 1998.

-
- [15] M. Domnowski, J. Jaehrling, and W. Frieß, “Assessment of Antibody Self-Interaction by Bio-Layer-Interferometry as a Tool for Early Stage Formulation Development,” *Pharm. Res.*, vol. 37, no. 2, p. 29, feb 2020.
- [16] G. L. Rosano and E. A. Ceccarelli, “Recombinant protein expression in *Escherichia coli*: Advances and challenges,” p. 172, 2014.
- [17] C. J. Wienken, P. Baaske, U. Rothbauer, D. Braun, and S. Duhr, “Protein-binding assays in biological liquids using microscale thermophoresis,” *Nat. Commun.*, vol. 1, no. 7, 2010.
- [18] T. Bartoschik, A. Gupta, B. Kern, A. Hitchcock, N. B. P. Adams, and N. Tschammer, “Quantifying the Interaction of Phosphite with ABC Transporters: MicroScale Thermophoresis and a Novel His-Tag Labeling Approach,” *Biophys. Membr. Proteins*, vol. 2168, pp. 51–62, 2021.
- [19] N. Kobayashi, S. M. Freund, J. Chatellier, R. Zahn, and A. R. Fersht, “NMR analysis of the binding of a rhodanese peptide to a minichaperone in solution,” *J. Mol. Biol.*, vol. 292, no. 1, pp. 181–190, sep 1999.
- [20] A. Natalello, R. U. Mattoo, S. Priya, S. K. Sharma, P. Goloubinoff, and S. M. Doglia, “Biophysical characterization of two different stable misfolded monomeric polypeptides that are chaperone-amenable substrates,” *J. Mol. Biol.*, vol. 425, no. 7, pp. 1158–1171, 2013.

5. I've got you covered: A first step towards a mini-chaperonin
120 for protein variant characterization

Chapter 6

Final Summary

Protein biopharmaceuticals are composed of an extremely high number of chemical variants. Even small changes in sequence or structure can cause a variant to behave differently from the naive protein. This behavior may involve increased interaction of the variant with itself or with other variants of the biopharmaceutical product. This thesis aimed for a closer examination of the main variants in protein therapeutic and, thereby, to gain a profound knowledge of the interaction behavior and the aggregation tendency of the variants.

Chapter 1 describes the origin and significance of the protein variants known in literature, with a focus on charge and hydrophobicity variants. In the further course, the impact of protein variants on stability and aggregation are introduced. Furthermore, we introduce the resulting open questions, which this thesis aims to investigate.

In order to be able to examine protein variants, they can be separated chromatographically. A semi-preparative SCX method with salt- and pH-gradient was established, to separate and enrich individual charge protein variants of a mAb DS (**Chapter 2**). The conformational and the colloidal stability of the mAb charge variants were analyzed. An acidic variant showed divergent behavior in terms of decreased conformational stability and formation of aggregates with unfolded variants. Molecular modeling of the charge

variant confirmed the increased aggregation tendency based on a more hydrophobic surface. After a subsequent stability study with the charge variants spiked into DS an elevated risk of increased aggregation on the mAb product could be excluded. Thus, the mAb charge variants did not reduce the overall mAb DS stability.

Subsequently, in **Chapter 3** we further investigated the same mAb, now with a focus on hydrophobicity variants. For the development of the semi-preparative separation method, it was particularly important to select non-denaturing conditions for the separation of the hydrophobicity variants. This was achieved by using propylene glycol as an elution enhancer. Size, thermal stability and self-interaction of the collected variants were analyzed. Among several hydrophilic variants that were involved in aggregation, one variant stood out for its additionally reduced stability. Moreover, this hydrophilic variant corresponded with the aggregation prone acidic variant described in chapter 2. Finally, the hydrophobicity variants were spiked into mAb DS and analyzed in an accelerated stability study. Also the hydrophobicity variants did not induce increased aggregation in mAb DS.

Next, the approach of charge variant investigation was transferred to rhGH (**Chapter 4**). The semi-preparative charge variant separation method was based on AEX. SEC and IEX were applied to characterize the charge variants of rhGH. The stability of the variants was assessed by DLS and SLS measurements under various buffer conditions. At elevated temperature, an acidic deamidation variant was formed in remarkably high quantity. In dependence of pH, this acidic variant showed elevated attractive self-interaction. Upon an accelerated stability study with varying pH conditions, the acidic variant was not prone for aggregation with itself or other rhGH charge variants.

Chapter 5 aimed to utilize GroEL-AD to characterize and quantify protein variants regarding their hydrophobicity. At first, the functional cavity of the chaperonin, the apical domain, was engineered and expressed in an E.coli strain. Secondly, the functionality of the obtained mini-chaperonin was tested by native PAGE, western blotting, BLI and MST. The mini-chaperonin was present as a trimer, which appears to prevent the mini-

chaperonin from attaching to hydrophobic surfaces of the protein variants. Overall, the approach is promising, but engineering and stabilization of the mini-chaperonin need to be refined.

In summary, the approach of separation and characterization of protein variants proved to be a beneficial tool to understand and classify the behavior of protein variants. It may improve the development of biopharmaceuticals by ensuring minimal risk of aggregation due to inherent variants or degradation products, which are inevitably present in protein therapeutics. By the investigation of further proteins, data can be generated in order to conclude whether behavioral patterns of variants can be transferred across proteins for aggregation risk assessment.